Martian gullies: a comprehensive review of observations, mechanisms and insights from Earth analogues

Susan J. Conway, Tjalling de Haas, Tanya N Harrison

Martian gullies: a comprehensive review of observations, mechanisms and the insights from Earth analogues

Susan J. Conway[1*]

Tjalling de Haas[2,3]

Tanya N. Harrison[4]

[1]Laboratoire de Planétologie et Géodynamique de Nantes- UMR CNRS 6112, 2 rue de la Houssinière - BP 92208, 44322 Nantes Cedex 3, France.

[2]Department of Geography, Durham University, Durham, UK

[3]Faculty of Geosciences, Universiteit Utrecht, Utrecht, The Netherlands.

[4]Arizona State University, Tempe, AZ 85287, USA

*Correspondence to: susan.conway@univ-nantes.fr

Abstract

Upon their discovery in 2000, martian gullies were hailed as the first proof of recent (<a few Ma) flowing liquid water on the surface of a dry desert planet. Many processes have been proposed to have formed martian gullies, ranging from liquid-water seepage from aquifers, melting of snow, ice and frost, to dry granular flows, potentially lubricated by CO_2. Terrestrial analogues have played a pivotal role in the conception and validation of gully-formation mechanisms. Comparison with the terrestrial landscape argues for gully formation by liquid-water debris flows originating from surface melting. However, limited knowledge of sediment transport by sublimation is a critical factor in impeding progress on the CO_2-sublimation hypothesis. We propose avenues towards resolving the debate: a) laboratory simulations targeting variables that can be measured from orbit, b) applications of landscape-evolution models, c) incorporation of the concept of sediment connectivity, d) using 3D fluid-dynamic models to link deposit morphology and flow rheology, and e) more intense exchange of techniques between terrestrial and planetary geomorphology, including quantitative and temporal approaches. Finally, we emphasize that the present may not accurately represent the past and martian gullies may have formed by a combination of processes.

1. Introduction

This review provides an overview of the research done on martian gullies since their discovery by Malin and Edgett (2000), providing the backdrop to the papers in this special issue. The review specifically highlights how the use of terrestrial analogues has provided insight into the formation mechanisms of martian gullies. The study of martian gullies has been steeped in analogy to terrestrial landforms from the very beginning – starting with their naming as "gully" (Malin and Edgett, 2000). This name was chosen in reference to their resemblance to "spur and gully" morphology on Earth, rather than referring to the terrestrial definition of gully as "a water-made cutting, usually steep-sided with a flattened floor" (Mayhew, 2015) which is "deep enough (usually >0.5 m) to interfere with, and not to be obliterated by, normal tillage operations" (https://www.soils.org/publications/soils-glossary). In making our descriptions we use terms derived from terrestrial geomorphology to describe the characteristics of martian gullies, which inevitably are rooted in the terminology used in the description of fluvial catchments and may suggest a fluvial origin. We attempt to make a reasonable balance between using process-neutral terms (which if taken to extremes are so generic as to be unhelpful) and terms that inevitably invoke a given process.

We start by providing a comprehensive review of the observational data collected on martian gullies. Following this, we summarise their proposed formation mechanisms, along with the range of Earth analogues that have been used to gain insight into martian gully formation. Within Earth analogues we include scaled physical laboratory simulations, which we argue play a similar role to flume experiments in understanding terrestrial geomorphic processes (e.g., Paola et al., 2009). We then undertake a short critical assessment of the limitations of such analogies and highlight future avenues and challenges for research as a result of this review and discussions at the second Mars gullies workshop held in London, June 2016.

2. Review of key observations of martian gullies

2.1 Morphology

Martian gullies are composite landforms that comprise an alcove, channel and depositional fan (also referred to as apron in the martian literature; Malin and Edgett, 2000). They can be up to several kilometres in length, and their length seems to be controlled by the length of the hillslope available (Hobbs et al., 2017, 2013). Alcove zones can span up to a kilometre cross-slope (Bridges and Lackner, 2006; Conway et al., 2015a; Heldmann et al., 2007; Heldmann and Mellon, 2004; Yue et al., 2014). They occur in a wide range of settings mostly in the mid-latitudes and sometimes polar regions, ranging from the walls and central peaks of impact craters to valley walls, hills, dunes, and polar pits (e.g., Balme et al., 2006; Malin and Edgett, 2000). The main requirement for their occurrence being the availability of steep slopes exceeding ~20-30° (Conway et al., 2017, 2017, e.g., 2015a; Dickson et al., 2007; Reiss et al., 2009a). Gullies can occur singularly, but they usually occur in groups and can span whole hillslopes (Figure 1: e, g-i, l). Sites with gullies number nearly 5000, and it is estimated therefore that tens of thousands of gullies exist on Mars (Harrison et al., 2009).

What follows is a generic description of gullies on Mars, placing emphasis on their most commonly observed morphological features, while also summarising the wide variation in morphology observed in martian gullies. We begin our morphologic descriptions with so called "classic" gullies, which are the most abundant (98% of the database of Harrison et al., 2015) and show the widest variation, then follow with descriptions of two uncommon, but remarkable gully-types: linear dune gullies (33 sites globally, 0.6%; Pasquon et al., 2016) and polar-pit gullies (1% of Harrison et al., 2015) (Figures 1e and 1g, respectively).

Gully-alcoves are generally theatre-shaped depressions, whose upslope extent is located at the hillcrest or mid-slope within the hillslope on which they are located. They can be incised into the bedrock, often exposing numerous metre-scale boulders, or into slope-side deposits, such as the latitude dependant mantle (LDM) or sand (e.g., Aston et al., 2011; de Haas et al., 2018, 2015a, 2013; Núñez et al., 2016b). The LDM is believed to be an ice-rich mantling unit of which the most recent layers were deposited during climate excursions, which happened in the last few millions of years (see Section 2.3). Some variations in gully source material are related to host-crater age, and lead to contrasting gully-alcove morphology (de Haas et al., 2018).

Alcoves often lead to chutes in which channels are developed, and these channels then lead onto the depositional debris fan, or apron. Here, as in the terrestrial literature, we make a distinction between "channels" and "chutes". We define channels as erosional incisions which should indicate the bankfull level of the fluid and therefore can be taken to represent a single "event" (Figure 2d). Chutes, on the other hand, are analogous to valleys in lowland geomorphology, they are erosional incisions representing the ensemble of erosional events and do not represent bankfull conditions. It should be noted, however, that incised channels cannot always be reliably identified and hence the confusion between chutes and channels in the martian gully literature, which is likely related to the rapid reworking of the martian surface. Where chutes are classified as channels, this can lead to poor application of terrestrial geomorphologic laws developed for channels. Channels extend from within the alcove and onto/across the depositional zone. It has been stated in the literature that gully channels become narrower in downslope direction (Hartmann et al., 2003), but in fact it is usually the incised chutes that narrow downslope. In many cases the upper part of martian gullies lacks a true alcove as described above – the upper escarpment, or break in slope is missing. Such gullies are usually characterised by a source area where many small channels emerge gradually from rocky hillslopes and come together to form a single chute (Figures 2e, f). Gilmore and Phillips (2002) initially reported the origin of gully-channels at outcropping bedrock layers. However, with higher resolution images in many cases it can be seen that the channels originate (often as barely distinguishable rills) above the bedrock layer (Dickson and Head, 2009) (Figure 2f).

Downslope of the alcoves, at the point where deposition dominates over erosion due to lower gradients, a depositional fan is present. These can be wide cone-shaped deposits of sediments, which originate at the apex where the chute intersects with the hillslope (e.g., Figures 1j, 1m, 2b). Similar to alluvial fans on Earth, these deposits "fan out" from the apex in planview and have a convex cross-slope curvature. Such gully-fans are often dissected by entrenched, steep-walled, channels. Both primary and secondary channels (the latter being abandoned, formerly active, channel systems), can often be identified on gully-fan surfaces (Figure 2c). The fans of adjacent gullies can merge downslope forming a bajada, a continuous deposit at the foot of the hillslope. Additionally, many other gullies lack wide, fan-shaped deposits, but have more restricted deposits, which are longer in the downslope direction than they are wide. These deposits can be digitate in shape, or indistinctly blend into the surrounding terrain.

Figure 2

Polar-pit gullies (Figure 1g) are notable not only for their high-latitude location, but they also have a distinctive morphology and morphometry. This type of gully is only found in south polar pits, which form the only steep topography at latitudes poleward of 60°S (Conway et al., 2017). These pits are believed to be formed by collapse of the terrain induced by sub-glacial volcanism (Ghatan and Head III, 2002). The gullies incised into the walls of these polar pits are characterised by regularly-spaced rounded alcoves which often reach the top of the slope and when they do, on their inner slopes are comprised of metre to decametre-scale rounded boulders. The base of the alcove sometimes leads

into a chute and the deposits more often than not form a bajada of continuous fan-deposits. Channels are slightly sinuous and lead out onto the fan, where sometimes other channel segments can also be seen. Many studies, however, do not distinguish these gullies from classic gullies elsewhere on Mars (e.g., Auld and Dixon, 2016).

Linear dune gullies (Fig. 1e) are the most uncommon and distinctive subtype of martian gullies. They are only found on dark sandy slopes, either dune slip-faces or sand-covered slopes in the southern hemisphere (Figures 1a, e, f) (Pasquon et al., 2016). They are dominated by a long parallel-sided leveed channel, which varies little in width along its length. This channel either directly follows the hillslope gradient, or possesses some considerable sinuosity (Pasquon et al., 2016). The alcove is rarely wider than the channel and is often comprised of poorly expressed tributary rills. The channel terminates downslope abruptly and the "apron" is simply comprised of the bounding levee, although in some cases the channel is perched (an erosional landform within the depositional landform) (Jouannic et al., 2015). Channel terminations can be in form of pit-chains, or can be surrounded by pits. The longest examples are found on the extraordinary Russell Crater megadune (Gardin et al., 2010; Jouannic et al., 2017; Reiss et al., 2010a; Reiss and Jaumann, 2003), which rises to 500 m in height (Gardin et al., 2010). As for classic gullies their length seems to be limited by the size of the hillslope available. They often occur alongside gullies with a "classic" morphology (Figures 1a, e, f) and there are some cases where intermediate forms can be found.

Typically gully alcove slopes on Mars exceed 20° (Conway et al., 2015a; Dickson et al., 2007; Heldmann et al., 2007; Heldmann and Mellon, 2004), while gully-fan slopes range from 5° to 25° (Conway et al., 2015a, Gulick et al., 2018; Kolb et al., 2010), with channels spanning the whole range of slopes. Conway et al. (2015b) found that gullies whose alcoves extend up to and erode into the bedrock of a crater wall tend to have the steepest alcove and apron slopes (>23° and >20° respectively). Polar-pit gullies are distinctive as they tend to have lower alcove and debris apron slopes (<25° and <12°, respectively) compared to the population as a whole. Pasquon et al. (2016) reported alcove slopes for linear gullies of 14-25° and mean slopes of 9-17° along the whole profile, which are consistent with the general population of martian gullies.

As with any classification system, there are forms that do not fit neatly into the descriptions provided above. In the most generic sense martian gullies are a form of gravity-driven mass wasting system, where material is removed from the top and transported towards the base of the hillslope. However, they are distinguishable from simple fall-deposits (scree, talus or colluvium) by the presence of the transport channel and/or chute as pointed out by Malin and Edgett (2000) and the presence of a depositional fan below the dynamic angle of repose (Kokelaar et al., 2017). Hence, it has generally been acknowledged that a channel is the essential attribute for identifying a martian gully (e.g., Balme et al., 2006). Alcoves (with a spur and gully morphology) are common in bedrock escarpments across Mars and the Moon (Dickson and Head, 2009; Sharpton, 2014) (Figure 3). Hillslopes that are contiguous with those hosting well-developed gullies can themselves show morphologies that without the context of their neighbours, would not necessarily be classified as gullies (Figure 4). These slopes have poorly developed and discontinuous channels, which have limited sinuosity trending directly downslope. Such features are also found in isolation, often in the equatorial regions of Mars (Auld and Dixon, 2016; Rummel et al., 2014) (Figure 4c) and have usually been omitted from global-scale catalogues of martian gullies (e.g., Harrison et al., 2015). Treiman (2003) classified some equatorial features as gullies, such as alcoves with aprons in the calderas of the Tharsis volcanoes and the light-toned layered mounds in Candor Chasma (Figure 4a). These equatorial features have channels—a downslope trending linear depression - yet they lack the steep banks and morphological complexity of their mid-latitude counterparts and more closely resemble

terrestrial dry mass movement chutes (refer to Section 3.1), and hence have not been classified as gullies.

As discussed in more detail in the following section, gullies have small-scale morphologies indicating many episodes of deposition and erosion. In addition, relict versions of whole gully-landforms have also been reported. In order to be identifiable as relict gullies, some aspect of the channel has to be identifiable strengthened by identification of associated relict fan and/or alcove.

Figures 3 and 4

2.2 Detailed Morphology

The arrival of the HiRISE instrument in orbit around Mars in 2006 which returns 0.25-0.5 cm/pix images of the martian surface (Alfred S. McEwen et al., 2007) has allowed the morphology of martian gullies to be catalogued in great detail. Here we describe commonly observed metre- to decametre-scale features associated with the channels and depositional parts of gullies.

The chutes and channels of gullies can be highly sinuous (Figures 1e, 5a) (Arfstrom and Hartmann, 2005; Mangold et al., 2010). Many authors report both v-shaped incisions (e.g., Dickson and Head, 2009; Hobbs et al., 2013), and tributary organisation of channels/chutes (e.g., Malin and Edgett, 2000; Morgan et al., 2010). Terraced cutbacks and longitudinal bars (Figure 5c) (Schon and Head, 2009) and more rarely levees (Figure 5b) (Hugenholtz, 2008a; Johnsson et al., 2014; Lanza et al., 2010; Levy et al., 2010; Sinha et al., 2018) have also been reported as attributes of gully-channels. In systems with well-developed fans the chute and base of the alcove can become back-filled with sediment. In these sediment-choked systems channels tend to be discontinuous and braided within the confining chutes (A. S. McEwen et al., 2007), good examples of this are seen in Gasa Crater (Figure 5d). Braiding of channels is also seen on the fans and in shallow upslope tributary systems (Gallagher et al., 2011; Levy et al., 2009).

Figure 5

Digitate deposits, either as part of a fan or on their own, are often reported to characterise the terminal part of martian gullies (Dickson and Head, 2009) (Figure 6a,b). Deposits often “spill over” the sides of channels (Stewart and Nimmo, 2002), but deposits are also re-incised by channels. A distributary organisation of channels is associated with gully-deposits (A. S. McEwen et al., 2007) and metre-sized boulders can be common on their depositional surfaces (de Haas et al., 2015d; A. S. McEwen et al., 2007). Sometimes distinct depositional lobes are also observed with high relative relief (Johnsson et al., 2014; Lanza et al., 2010; Levy et al., 2010; Sinha et al., 2018) (Figure 6a). The surfaces of martian gully-fans can often be divided into segments with different ages, based on cross-cutting relationships and morphological differences between segments (de Haas et al., 2015d, 2013; Johnsson et al., 2014; Schon et al., 2009a). This observation shows that gullies form in multiple episodes, i.e. separated by enough time to have been modified by other processes, rather than in one event (Schon and Head, 2011) (Figure 6c). This assertion is also supported by the presence of terraces within gully-chutes. The surfaces of gully-fans are in many instances heavily degraded (de Haas et al., 2015d; Dickson et al., 2015), mainly by weathering and wind erosion, but also they may be covered by LDM deposits. Gully channels can be crossed by fractures within the LDM and superpose other similar fractures (Dickson et al., 2015) (Figure 6d). As a result, gully-fan surface morphology is often dominated by secondary, post-depositional, processes. Interpretation of the primary formation processes of gullies based on fan surface characteristics may be misleading for

the often long-inactive martian gullies, and interpretation of surface morphology should be approached with care (de Haas et al., 2015d).

Because the channel and associated deposits are the parts of the gully-landform that have the least relative relief it has the poorest preservation potential, making relict gullies hard to substantiate. Dickson et al. (2015) identified inverted gully channels in >500 sites poleward of 20°S. These ridges are present on pole-facing slopes between 40°S and 50°S and are likely being revealed from under the LDM. Dickson et al. (2015) further report the burial of whole gully-systems beneath LDM and present two examples of this. Many other authors report apparently infilled alcoves next to distinct or active gully-systems (e.g., Auld and Dixon, 2016; Christensen, 2003; de Haas et al., 2018; Hoffman, 2002), which they interpret as relict gully-systems.

2.3 Associated landforms

Martian gullies do not occur in isolation, but in association with, and often with superposition relationships to, a range of other morphologic features, which we briefly summarise here (in order of descending size). Of the same order of scale or larger than martian gullies are viscous flow features (Squyres, 1978) which encompass a wide range of features, of which the subtype glacier like forms (GLF) (Hubbard et al., 2011; Souness et al., 2012; Souness and Hubbard, 2012) are the most similar in scale to gullies. Martian gullies occur in the same latitude band as GLF and crater-filling VFF (Levy et al., 2014), and recent work has shown that gullies tend to be sparse where Lobate Debris Aprons (a large subtype of VFF) and GLFs are dense (Conway et al., 2017). From surface morphology and topography alone VFF are believed to be debris covered glaciers (e.g., Mangold, 2003a; Morgan et al., 2009; Squyres, 1979) and radar data have confirmed that the ice under the debris is almost pure (Plaut et al., 2009). Gullies are sometimes observed adjacent to or topographically above such features (Figures 1d & i), but rarely intersect them. Gullies only occur in ~12% of craters filled with VFF despite occupying the same latitude band. Spatulate depressions or arcuate ridges are thought to represent the end moraines of now ablated GLFs (Hartmann et al., 2014) and often occur at the foot of gully-systems (Arfstrom and Hartmann, 2005; Berman et al., 2005; de Haas et al., 2018; Head et al., 2008) (Figure 7c,e). Gully-fans superpose these arcuate ridges and sometimes form on their downslope scarps (Figure 7d).

In Utopia Planitia and the Agyre region of Mars (Pearce et al., 2011; Soare et al., 2017, 2007) gullies occur in close association with hundred-metre-scale polygonised depressions that are linked to the ablation of excess ice, so-called thermokarst or scalloped depressions (Figure 8c). Similarly Soare et al. (2014b) found that hundred-metre-scale mounds they interpreted to be caused by ice-heave (pingos) also occurred in association with gullies in the Argyre region (Figure 8d).

Figures 7 and 8

Many gullies are intimately associated with the LDM (Aston et al., 2011; de Haas et al., 2018, 2015a; Dickson et al., 2015) and dissected LDM (Milliken et al., 2003; Mustard et al., 2001). The LDM is characterised by a terrain draping unit which infills decametre to hundred-metre topographic lows and smooths the topography at high latitudes (Kreslavsky and Head, 2002). It is often associated with polygonally patterned ground at the metre to decametre scale, which is thought to be caused by thermal contraction in ice cemented soil (Levy et al., 2009; Mangold, 2005). Initially the term “pasted-on terrain” was used to refer to the polygonally patterned terrain into which gullies are incised (Christensen, 2003), but this has later been incorporated into the catch-all term of “LDM”. Although an in-depth discussion of the LDM is beyond the scope of this paper, it should be noted that: multiple generations of LDM deposits are thought to exist (e.g., Schon et al., 2009b), and

although the LDM is generally attributed to airfall deposits of ice nucleated on atmospheric aerosols (Kreslavsky and Head, 2002), some aspects of the LDM argue for ice enrichment through freeze-thaw cycling (Soare et al., 2017). Several lines of evidence (aside from the crack-morphology) have led most researchers to agree that polygonally patterned ground indicates ice-rich terrain, including: newly-formed impact craters discovered with CTX have been found by CRISM and HiRISE to have excavated subsurface water ice (Byrne et al., 2009), in-situ discovery of ice associated with polygonally patterned ground by the Phoenix lander (Mellon et al., 2009) and the spatial correlation between high ice content as inferred from the neutron spectrometer data and polygonally patterned ground (e.g., Mangold, 2005).

Not all gullies are found in association with LDM, yet a large proportion are - Levy et al. (2009) report just over 50% of gullies in their survey (all HiRISE images 30–80° north and south latitude) are associated with polygonally patterned ground. Polygonal patterns are found on the inner slopes of alcoves and chutes of gullies as well as in the terrain the gullies incise (Figure 9b). Their fan deposits superpose polygonally patterned ground and sometimes relict fan deposits show polygonisation (Figure 9c). Volume-balance arguments indicate substantial volatile loss in gully-systems incised into this type of terrain (Conway and Balme, 2014; Gulick et al., 2018), implying excess ice in the ground at these locations. The lowest latitudinal limit of gullies coincides with the edge of the dissected LDM (Milliken et al., 2003), but also the lowest latitude extension of VFF (Levy et al., 2014). Head et al. (2003) noted that the LDM superposes crater-bound VFF, yet the LDM may superpose gullies and also be dissected by gullies (Dickson et al., 2015). Hillslopes with pasted-on material or LDM are often associated with arcuate ridges at the base of the slope, but also smaller-scale landforms informally termed “washboard terrain” encompassing parallel series of across-slope trending fractures thought to represent crevasses (Arfstrom and Hartmann, 2005; Dickson et al., 2015; Hubbard et al., 2014) (Figure 9d).

Landforms intimately associated with periglacial conditions (those conducive to freeze-thaw cycling in the ground) have been reported to occur in close proximity to, or in association with, martian gullies. These landforms are generally on the metre- to decametre-scale and the frequency of their association with gullies numbers in the tens, rather than in the hundreds, as for the features mentioned above. Cross-cutting and intimate association has been reported between gullies and (1) lobate forms (including stone garlands), which are attributed to solifluction processes where the top part of the soil profile creeps downslope due to repeated thawing (Gallagher et al., 2011; Gallagher and Balme, 2011; Johnsson et al., 2012; Soare et al., 2014a) (Figure 10d), and (2) sorted stone stripes where clasts are gathered at the edge of convection cells in the soil caused by freeze-thaw cycling (Gallagher et al., 2011) (Figure 10e). Gullies are also reported to occur in close proximity to other sorted patterned grounds, including sorted stone circles and nets and rubble piles (Balme et al., 2013; Barrett et al., 2017; Gallagher et al., 2011).

Finally gullies are often found on the same slopes as recurring slope lineae (RSL) (e.g., Dundas et al., 2017a; McEwen et al., 2011; Ojha et al., 2015), which are downslope propagating dark streaks typically a few metres to tens of metres wide and hundreds of metres long (Figure 10f). They only occur on the steepest slopes and originate at rock outcrops in terrains that have high thermal inertia (interpreted to have low dust cover). Their behaviour distinguishes them from other mass wasting phenomena; they grow during the hottest times of the year, fade during the cold season and reoccur at the same (or nearly the same) place each year (Grimm et al., 2014; Stillman and Grimm, 2018). RSL generally occur superposed on gully alcoves. No change in relief is associated with RSL so they are thought to transport only small amounts of sediment (if any). Some RSL propagate over sandy fans and occasionally slumps are also found on these fans, but their relation to RSL remains unclear

(Chojnacki et al., 2016; Ojha et al., 2017). RSL are also found on steep slopes without gullies, most notably those in Valles Marineris (Chojnacki et al., 2016; McEwen et al., 2014; Stillman et al., 2017).

Figures 9 and 10

2.4 Global trends

Gullies are found on steep slopes poleward of ~30° in each hemisphere (Harrison et al., 2015) (Figure 11). Between latitudes of 30° and 40° pole-facing gullies are strongly dominant, whereas from 40° to the pole gullies are mostly equator-facing but also exist in other orientations. Gullies are found across all elevations on Mars, but are notably absent within their general latitudinal distribution from the Tharsis bulge and the Hellas basin (Dickson et al., 2007; Heldmann et al., 2007; Heldmann and Mellon, 2004). The latter is due to the absence of steep slopes and the former seems to be an effect of surface thermal inertia (Conway et al., 2017). The general paucity of gullies in the northern hemisphere can be directly attributed to the lack of steep slopes in that hemisphere (Conway et al., 2017).

Figure 11

Although their morphology varies widely (Figure 1), there seems to be no distinctly identifiable trends in gully-morphology with latitude and/or orientation (Balme et al., 2006). An obvious exception to this general rule are the polar-pit gullies. There are hints in the literature as to gullies with different degradation states having different latitudes/orientations, but this remains to be fully-substantiated. Bridges and Lackner (2006) and Heldmann et al. (2007) did note that gullies in the northern hemisphere were more degraded in appearance than those in the southern hemisphere. Morgan et al. (2010), Raack et al. (2012) and Levy et al. (2009) reported that for the southern hemisphere equator-facing gullies seemed more degraded than the pole-facing ones.

2.5 Compositional data

Harrison et al. (2015) showed that gullies are more prevalent on terrains classified as high thermal inertia, interpreted as being low dust, low albedo, with grainsizes between 60um and 3mm (Jones et al., 2014; Putzig et al., 2005). Harrison et al. (2017) found that fans associated with active gullies in Gasa Crater have higher thermal inertia than other gully fans, yet lower thermal inertia than talus slopes. The hysperspectral imaging system CRISM has been used to examine the composition of the materials in and around gullies (Allender and Stepinski, 2018, 2017; Barnouin-Jha et al., 2008; Núñez et al., 2016a) and suggested that: (1) gullies are hosted on a wide range of geological materials, (2) in some cases gullies expose underlying rock and move it downslope, (3) many other gullies show no spectral difference from their surroundings and (4) there is no systemtic association between hydrated minerals and gullies even in the new light-toned deposits near gullies. Heldmann et al. (2010) used CRISM data and also confirmed that recent light-toned deposits in Penticton Crater have no spectral differences to surrounding material. It should be noted that the lack of systematic observations of hydrated or brine spectral signals in gullies does not mean these materials are absent (Massé et al., 2014) - hydrated signatures rapidly disappear under martian conditions and a spectral signal can easily be obscured by a surface coating of millimetres of dust, which is highly-abundant and pervasive on Mars.

Fan et al. (2009) investigated the relative water content of four gully sites compared to their surrounding areas and found that the gully sites had elevated water contents by using statistical analysis of OMEGA hyperspectral data. Dickson and Head (2009) used colour HiRISE images to

identify the seasonal accumulation of frost in the alcoves and channels of two gully systems and in one case they used CRISM to confirm its composition as water ice. Vincendon (2015) reported both seasonal water ice and CO_2 ice in association with active gullies. Dundas et al. (2017b) also find from HiRISE image data that active gullies are commonly associated with seasonal ice deposits. Sometimes these ices are observed in the alcoves of generally equator-facing gullies, but the frost is located on pole-facing sections of their alcoves (Figure 12). These results are in general accordance with those obtained for surfaces on Mars in general. Carrozzo et al. (2009) observe from OMEGA data that low latitude ice condensation occurs preferentially on shadowed (i.e. pole-facing at the present day) slopes between 30°S and 30°N. Kuzmin et al. (2009) used TES thermal inertia data to map water ice at the surface and report widespread water ice condensation on the surface occurring in winter between 40-50°S and 40-50°N, particularly in the northern hemisphere which is consistent with spectral observations (Appéré et al., 2011).

Figure 12

2.6 Temporal context (age and activity)

Gullies are geologically very young landforms that formed within the last few million years. This is inferred from the conspicuous absence of superposed impact craters on gullies (e.g., Malin and Edgett, 2000), superposition relationships with polygons, dunes and transverse aeolian ridges (e.g., Malin and Edgett, 2000; Reiss et al., 2004), their occurrence in young impact craters that formed within the last few million years (Conway et al., 2018a; de Haas et al., 2018, 2015b; Johnsson et al., 2014) and the presence of secondary craters related to recent crater impacts as marker horizons on gully-lobes(Schon et al., 2009a). Geologically young gully deposits are present in both very young and very old host craters (< 1 Ma to > 1 Ga), and their size is unrelated to host-crater age (de Haas et al., 2018; Grotzinger et al., 2013). While the spatial distribution of martian gullies has been extensively studied and quantified, their temporal evolution is poorly understood. Documenting the temporal evolution of gully systems was already noted as one of the main outstanding questions and avenues for advancement regarding the understanding of martian gullies by Dickson and Head (2009), yet very few papers have addressed this topic since then. De Haas et al. (2018) show that after their formation in fresh craters, gullies may go through repeated sequences of (1) LDM deposition and reactivation and (2) glacier formation and gully removal (Conway et al., 2018a), followed by the formation of new gully systems. In general, gullies in host craters that are younger than a few Ma have not been affected by LDM or glaciation (type 1), gullies in host craters of a few Ma to a few tens of Ma have been affected by LDM but not by glaciation (type 2), and gullies in host craters of more than a few tens of Ma have been affected by both LDM and glaciation (type 3). These various types of history are reflected in the gully morphology: type 1 gullies have large alcoves with rough surfaces that cut into bedrock and extent up to the top of the crater rim (Figure 1l; 2b); type 2 gullies are similar but are visually softened by a veneer of LDM deposits (Figure 1h,k; 9a); type 3 gullies lay within the former extent of glaciers, as indicated by the presence of, for example arcuate ridges and sublimation till, and have elongated, v-shaped, alcoves that often do not extend all the way up to the crater rim (Figure 7b,e; 8b).

Repeat imaging of martian gullies has revealed that mass transport is occurring within these systems at the present-day (Diniega et al., 2010; Dundas et al., 2017b, 2015a, 2012a, 2010a; Malin et al., 2006; A. S. McEwen et al., 2007; Pasquon et al., 2016; Raack et al., 2015; Reiss et al., 2010a; Reiss and Jaumann, 2003). Activity within gullies on dark sandy substrates in the southern hemisphere is particularly remarkable with both “classic” and “linear” gully sites showing some kind of mass transport every Mars year. In this issue Pasquon et al. (2017) show that the timing and nature of the activity of the classic gullies on dark sand dunes differs from that of linear dune gullies. Classic dune gullies are generally active in local winter (Diniega et al., 2010; Pasquon et al., 2017) and their

activity is characterised by smaller metre-scale slumps into the chute/alcove and large alcove-clearing events which leave upstanding deposits on the debris fan (Pasquon et al., 2017). Linear dune gullies are active as the seasonal surface frost finally sublimates from the surface (~Ls 200°, early spring) and their activity is characterised by the elongation of channels, appearance of new pits and appearance of new channels. Linear gullies with no changes are also observed. Volume balance arguments dictate that entire linear gully systems can be produced on the order of tens of Mars years (likely slightly longer for the large systems on the Russell megadune) and classic gullies on the order of hundreds of Mars years (Pasquon et al., 2017). Hence it is likely these dune gully systems are a product of the present-climate system. It is also worth-noting that the north polar dune fields are also remarkably active, yet the timing and character of this activity differs from the southern hemisphere (Diniega et al. 2017). Here, alcove-fan systems only tens to hundreds of metres in length form on dune slip faces in autumn or early winter. Their formation seems to be linked to the first deposits of the seasonally CO_2 ice. Channels are occasionally visible at the limit of resolution, hence why these features are not usually classed as martian gullies.

Polar-pit gullies are also more active than classic gullies elsewhere (Hoffman, 2002; Raack et al., 2015). Their activity is characterised by the gradual progression of relatively dark sediment deposits over the seasonal ices during the latter part of winter. These dark deposits are visible as topographic relief once the ice has been removed. Not all polar-pit gullies are active at once, which lead Raack et al. (2015) to surmise that the process must be supply limited, rather than environment limited.

Activity in classic gullies was first documented in the form of “bright white deposits” in Mars Orbiter Camera data (Malin et al., 2006). These deposits appear on the depositional apron of the gully, have a digitate outline, no detectable relief, and no distinct source zone (Figure 13b). Since then repeat images by HiRISE have detected movements that appear both “bright” and “dark” in the red channel (Figure 13a,b) and can have various colour hues including “blue” and “yellow”. These movements include deposits with no detectable relief, but also deposits with upstanding lobate edges containing boulders (Figure 13c), evacuation of sediment infilling channels and in one case the incision of a new channel (Dundas et al., 2017b, 2015a, 2012a, 2010a) (Figure 13d). Activity is rarer in the northern hemisphere and so far none of the observed modifications have engendered any detectable alteration in relief (Dundas et al., 2017b). Source areas for these movements cannot usually be identified, although occasionally failure scars are present. Crown fractures have been identified in the alcoves of Gasa crater (Okubo et al., 2011), where the gullies are particularly active (Dundas et al., 2017b), suggesting slope instability as a trigger for movement. Because activity in classic gullies is so sporadic there are only ~40 examples where timing can be constrained to within less than 3 months and the activity tends to occur in winter during defrosting at that latitude (Dundas et al., 2017b). Whether these observations of activity in classic gullies represent the process that forms the whole gully-landform is currently under debate.

Figure 13

3. Review of proposed martian gully formation mechanisms and their terrestrial analogues

Multiple models have been put forth in an attempt to understand how geologically youthful gully features could have formed on Mars. Our view of martian gullies has improved over time since their initial discovery thanks to long-term monitoring and higher resolution data, which is reflected by the wealth of data on their morphology and spatial distribution presented above. Accordingly, the models of formation that have been put forth have evolved over time as well. Terrestrial analogy has played a key role in developing these formation models and also in testing them against

observations. It was the analogy to systems on Earth carved by liquid water that sparked the initial controversy about gully-formation as corroborated by the flurry of comments on the initial discovery paper (Doran and Forman, 2000; Hoffman, 2000; Knauth et al., 2000; Saunders and Zurek, 2000). The reason this claim was so controversial and remains so, is that our understanding of Mars' surface environment dictates that liquid water should not be thermodynamically stable – it should only be present in its gaseous or solid forms (Hecht, 2002; Richardson and Mischna, 2005). Climate models have shown liquid water could be transiently stable, but the locations where this is predicted do not match with the locations of gullies (e.g., Richardson and Mischna, 2005; Stillman et al., 2014). Authors have therefore proposed that landforms resembling terrestrial water-carved landforms could be formed on Mars by other fluids, or even without fluids – a concept termed "equifinality". One of the reasons that multiple hypotheses for formative mechanisms are conceptually viable is the steepness of the relief and the instability of surface materials under steep gradients. Hence, any appreciable applied force might be capable of causing bulk flows. It is now generally accepted that gullies are formed by a fluid, presently thought to be H_2O or CO_2. In this section we first summarise the arguments which show that gullies on Mars are not formed by a completely dry granular flow. We then go on to present the arguments made in favour of liquid-water mechanisms and the models outlining the origin for this water. Finally we outline the arguments made in favour of CO_2-based-fluids for gully formation. Each of these sections will emphasise the role that terrestrial analogues have played in developing these working hypotheses.

3.1 Dry granular flow

Treiman (2003) proposed entirely dry flow as the agent behind martian gully formation based on the difficulty of sustaining liquid water under recent climate conditions. He explained the leveed channel morphology of martian gullies with reference to the terrestrial analogues of pyroclastic flows and dry snow avalanches, as examples of natural dry granular flows (Figure 14a,b). However, McClung and Shaerer (2006) note that "dry snow avalanches tend to travel in straight lines rather than being deflected by topography, such as gullies". Observations of snow avalanches by Kochel and Trop (2008) as Mars analogues in the Wrangell Mountains in Alaska also point to some differences: avalanches have very straight, wide channels, with broad levees, the terminal deposit is often square-lobate showing no digitate break-offs. These landforms are similar in morphology to those produced by dry granular flow in experiments (e.g., Félix and Thomas, 2004; Kokelaar et al., 2014) (Figure 14c-e) and numerical modelling (Gueugneau et al., 2017).There is also disagreement in terrestrial literature as to whether dry granular flow models are even valid for snow avalanches, which almost inevitably involve some phase-changes (e.g., Gauer et al., 2008; Hutter et al., 2005; Naaim et al., 2003; Platzer et al., 2007) and wet snow avalanches can behave like and have a similar morphology to debris flows (Bartelt et al., 2012)(covered in the next section). The same is true for pyroclastic flows, which are fluidised by hot pressurised gas in the pore space (either trapped on catastrophic collapse of the ash column and/or continually produced from the hot volatile volcanic products) (e.g., Mellors et al., 1988; Siebert et al., 1987; Sparks and Wilson, 1976). We will come back to the pyroclastic analogy within our discussion concerning the fluidisation by CO_2 gas evolved by sublimation (Section 3.3.3).

Figure 14

Shinbrot et al. (2004) also supported a dry granular flow model based on the fact that both martian gullies and dry mass movement features on terrestrial sand dune slip faces (Figure 14g-i) both have leveed channels (e.g., Sutton et al., 2013a). Shinbrot (2004; 2007) used a spinning disc to simulate the lower cohesion induced by lower gravity and generated features with wide, shallow channels and gentle lateral levees (Figure 14). However, other authors have found that martian gullies in the detail are morphologically distinct from dry features on Earth and dry mass movement features

elsewhere on Mars (Figure 3), as detailed below. Martian gullies show evidence for flows that divert around an obstacle and re-integrate after passing it (i.e., braided), which requires a certain flow thickness, viscosity and fluidity which according to our present knowledge is not achievable in dry flows even under low gravity (Brusnikin et al., 2016). Dry granular flows do not behave in this manner unless they are sufficiently thick and fine-grained such that Van der Waals forces are many orders of magnitude larger than intergranular friction and grain weight (Campbell, 1990; Derjaguin et al., 1975; Johnson et al., 1971). Conway and Balme (2016) compared the morphometries of the catchments of martian gullies to dry mass wasting features on Earth (talus slopes), on the Moon and ungullied crater walls on Mars and found that martian gullies were statistically dissimilar from these nominally "dry" landforms. The runout of dry granular flows should not extend very far beyond slopes greater than the dynamic angle of repose (~20°; Kleinhans et al., 2011; Pouliquen, 1999) which has been confirmed to be the case for dry avalanches on the Moon (Kokelaar et al., 2017) yet the majority of martian gully-fans are shallower than this. Conway et al., 2015a, measured a median slope of 14° for 67 gully-fans and Kolb et al. (2010) concluded 72% of the 76 fans they studied were likely emplaced by fluidised flows. It should be noted that Pelletier et al. (2008) and Kolb et al. (2010) found that the new bright deposits reported by Malin et al. (2006) in Penticton and Hale craters occur on steep enough slopes to be attributed to dry granular flows. The general consensus among the Mars gully community today is that gullies do not form via an entirely dry granular flow mechanism, although dry mass movement processes could occur within pre-existing gullies today (Harrison et al., 2015). Dry granular flows remain a reasonable mechanism for spur and gully landforms, which often lack channels/chutes.

3.2 Liquid water gullies

Martian gullies are similar to terrestrial analogue landforms carved by water on a number of levels, which has lead researchers to propose a number of water-related flow processes for their genesis. It should be noted that the ubiquity of precipitation involvement, directly or indirectly, in such analogues makes extrapolation to Mars somewhat questionable. In the first part of this section we discuss the arguments that have been made in favour of each of these water-based flow processes in light of their terrestrial analogues (Section 3.2.1). Whether or not similar landforms can be produced by other non-water flow processes will be discussed in Section 3.3. Following this we discuss the possible origins of this water along with their terrestrial analogues (Sections 3.2.2 to 3.2.5).

3.2.1 Fluvial flow, debris flow, slushflow, brines and other exotic fluids

The involvement of water in the formation of martian gullies has from the start been driven by their similarity to terrestrial water-generated landforms. On Earth the two main flow processes responsible for the downslope transport of sediment are fluvial flows and debris flows. When we refer to fluvial flows we mean flows in which the sediment concentration is sufficiently low that the fluid behaves like a Newtonian fluid and sediment entrainment solely occurs via shear stress exerted on the bed by the fluid – generically referred to as the stream power law (e.g., Hack, 1957; Sklar and Dietrich, 1998; Whipple and Tucker, 1999). Debris flows on the other hand are flows where the sediment to water ratio, typically ~20-60% water by volume (Costa, 1984; Iverson, 1997; Pierson, 2005), is sufficiently high that the rheology of the fluid changes and it behaves more like a bingham plastic, or a viscous fluid (e.g., Ancey, 2007; Iverson, 2014, 1997). Steep first order catchments on Earth are often dominated by debris flow processes, which leave an identifiable morphological fingerprint on the landscape (Jackson et al., 1987; Lague and Davy, 2003; Mao et al., 2009). Slushflow is a special kind of debris flow where some of the clastic material is replaced by ice (André, 1990; Decaulne and Saemundsson, 2006; Nyberg, 1989; Rapp, 1960). In the most general sense brines can replace water in both fluvial flows and debris flows, so could also be a component of the sediment transport in martian gullies. In addition there is a range of more "exotic" processes that

cannot occur on Earth have been revealed in scaled-physical models in the laboratory, which could be active in martian gullies. In the following sections we will discuss these different sediment transport processes, how they have been applied to martian gullies and the relevant terrestrial analogues.

Fluvial flow

Once produced, liquid water has been shown by multiple authors to have a residency time of up to a few hours on the martian surface under the temperature and pressure conditions of both the present and the geologically recent past (e.g., Carr, 1983; Haberle et al., 2001; Hecht, 2002; Heldmann, 2005; McKay and Davis, 1991). This duration combined with the evidence for multiple events required to form martian gullies leaves plenty of scope for water to form martian gullies.

There are uncountable numbers of erosion-deposition systems on Earth that comprise the generic elements of a source alcove, a transportation channel and depositional apron/fan, especially if no scale or slope constraints are imposed. In searching for kilometre-scale systems in which only 1st or 2nd order catchments are developed as for martian gullies it becomes clear that in many cases the depositional part of any given terrestrial system has been removed by other parts of the hydraulic system (located in the sea, or a lake, or eroded by a trunk river). This fact alone indicates that martian gully systems are water-starved compared to those on Earth and do not form part of a larger connected hydraulic system.

Terrestrial gullies formed by fluvial flow comparable in scale and structure to those on Mars have been reported from a wide variety of sites with a large range of climatic settings (Table 1), ranging from cold or hot deserts to relatively humid mountain environments. In addition to the planview similarity between fluviatile terrestrial gullies and martian gullies, authors have noted similarity in catchment properties (Conway and Balme, 2016), long-profiles (Conway et al., 2015b; Hobbs et al., 2017; Yue et al., 2014), cross-sectional properties (Yue et al., 2014), fan-slopes, channel organisation and channel features such as streamlining, terracing and braiding (Gallagher et al., 2011; Kumar et al., 2010; Reiss et al., 2011). Note, however, that features such as terraces are also common on terrestrial debris-flow fans (Figure 15e-h).

Figure 15

Following from these similarities several authors have used terrestrial inspired fluvial erosion models to infer the discharge and therefore the amount of water required to form gullies (Heldmann et al., 2005; Hobbs et al., 2014; Parsons and Nimmo, 2010). These models are based on knowledge obtained via field or experimental data on Earth in fluvial fluid flows with low sediment content and link channel geometries to flow discharge.

Debris flow

Debris flow analogue sites for martian gullies are dominantly located in arid, periglacial, or glacial climates. Many authors have noted the key characteristics (Figure 16): (1) lateral levees (2) lobate or digitate deposits and (3) poorly-sorted gravel or coarser sized sediments as deposits (Costard et al., 2007a; Hartmann et al., 2003; Kochel and Trop, 2008; Reiss et al., 2009a), which are attributes often seen in martian gullies. Heldmann et al. (2010) drew an analogy between mudflows in the Atacama and the new light-toned deposits on Mars (Malin et al., 2006). They found the higher albedo mudflow was a smooth deposit, with 90% fines compared to 78% fines in the surrounding material and that the deposit and surrounding material were spectrally indistinguishable – thus a viable hypothesis for the origin of the light-toned martian gully-deposits. In contrast, the Atacama debris

flows described by Oyarzun et al. (2003) have very marked topographic effects and form an elevated digitate fan deposit and a channel with lateral levees, similar to those described in glacial and periglacial environments.

Figure 16

Multiple types of morphometric analyses which reference terrestrial data have already been applied to martian gullies, and they imply predominant gully-formation by debris flows. They include, slope-area relations (Conway et al., 2011b; Lanza et al., 2010), gully width-depth relations (Yue et al., 2014), channel sinuosity (Mangold et al., 2010), the short length of gullies (Heldmann et al., 2005) and the often steep depositional slopes of the fans (>15°) (e.g., Conway et al., 2015a; Dickson et al., 2007; Heldmann and Mellon, 2004; Lanza et al., 2010; Levy et al., 2010). These analyses are in contrast to many analyses of surficial morphology suggesting a formation by fluvial flows (e.g., Heldmann and Mellon, 2004; Reiss et al., 2011, 2009a). All these studies make strong references to Earth analogues in order to define the morphometric properties distinctive to debris flows. The fact that martian gullies bear resemblance to terrestrial systems carved by fluvial flows and by debris flows is not surprising, because firstly systems on Earth (and likely Mars) are polygenetic and secondly, as detailed below primary formation processes can be masked by secondary ones.

Terrestrial studies inform us that effectiveness of secondary modification depends on the ratio between the characteristic time scales to build morphology by primary deposition and to modify morphology by secondary processes (de Haas et al., 2014). Alluvial fans whereon the return periods of primary geomorphic activity are low and/or whereon secondary processes are highly effective are therefore most susceptible to secondary modification. In extremely dry environments where rates of geomorphic activity are low, such as in terrestrial deserts and on Mars, surfaces are often modified by secondary processes. Secondary modification of alluvial fan surfaces can result from multiple processes, such as wind erosion, fluvial erosion and weathering (Blair and McPherson, 2009, 1994; de Haas et al., 2015d, 2015b, 2014, 2013). Which of these processes dominate secondary reworking differs between sites. On Earth, for example, de Haas et al. (2014) describe a debris-flow fan in the Atacama desert with a surface that has primarily been reworked by weathering and fluvial runoff. This fan is relatively wind-sheltered, however, and many other fan surfaces in terrestrial deserts are heavily modified by wind (e.g., Anderson and Anderson, 1990; Blair and McPherson, 2009; de Haas et al., 2015d, 2014; Morgan et al., 2014). Inactive parts of alluvial fans in the high-arctic, periglacial, environment of Svalbard are also prone to secondary modification (de Haas et al., 2015c). Here, secondary reworking mainly results from snow avalanches, weathering and periglacial conditions in the topsoil resulting in the formation of patterned ground, solifluction lobes and hummocks on inactive fan surfaces. The origin of long-inactive and modified fans can be determined by sedimentological analysis of stratigraphic exposures, because reworking is superficial and barely recorded in the subsurface (Blair and McPherson, 2009, 1994; de Haas et al., 2014). Wind scour can be an aid in revealing such stratigraphic relationships.

Figure 17

Similar to terrestrial fan systems, the morphological signatures of the primary processes forming martian gullies may thus have been removed and/or masked by secondary processes (Figure 17). High-resolution HiRISE images (~0.25 m/pix) enable the recognition of large boulders and large-scale stratigraphic layering in sedimentary outcrops on Mars, and thereby sedimentological subsurface analyses. Sedimentological analysis of outcrops in gully-fans in 51 HiRISE images widely distributed over the southern mid-latitudes shows that the sedimentology visible in incised sections of many

gullies is consistent with debris-flow sedimentology as observed on Earth (de Haas et al., 2015d). The great majority (96%) of outcrop exposures in gully-fans fed by catchments which mainly comprise bedrock and thus host boulders, contain sedimentological evidence for debris-flow formation. These exposures contain many randomly distributed large boulders (>1 m) suspended in a finer matrix and in some cases lens-shaped and truncated layering. This may explain the long-lasting discrepancy between morphometric analyses that imply gully formation by debris flows (e.g., Conway et al., 2011b; Lanza et al., 2010; Mangold et al., 2010) and frequent observations of fan surfaces lacking clear debris-flow morphology, suggesting formation by fluvial flows (e.g., Dickson and Head, 2009; Levy et al., 2010; Reiss et al., 2011).

In a similar fashion as for fluvial flows, authors have used terrestrial relationships between channel geometries and discharge/flow velocity for debris flow dynamics to infer the water content and associated reservoir-size for martian gullies (Jouannic et al., 2012; Levy et al., 2010; Mangold et al., 2010; Miyamoto et al., 2004). Further, by using terrestrial knowledge of the size-frequency and sediment concentrations of debris flows not only can the water-reservoir be estimated, but also the timing and cadence of gully-activity (de Haas et al., 2015b).

Slushflows and other exotic fluids

Both slushflows and icy debris flows have been proposed for martian gullies inspired by their observation on Earth (Auld and Dixon, 2017; Kochel and Trop, 2008) (Figure 18). Icy debris flows have the same morphological attributes as debris flows, but some of the transported solids are ice – this leads to a small amount of deflation of the deposits post-deposition (Kochel and Trop, 2008). The deposits of such flows are similar to those of wet snow avalanches (Figure 18), but for wet snow avalanches the only remaining morphology is a low concentration clasts (Decaulne et al., 2013; e.g., Decaulne and Sæmundsson, 2010; Laute and Beylich, 2013) (Figure 18h) that through repeated action can result in a recognisable avalanche debris cone (de Haas et al., 2015c) (Figure 18g). On Earth these cones are built by a combination of processes (Luckman, 1992; Stoffel et al., 2006), so the contribution of avalanches to the sediment budget can be hard to ascertain. Slushflows are somewhat similar to debris flows in that they contain a low amount of liquid water compared to solids, however those solids are not just sediments but relatively large quantities of snow and ice (> 70%). This leads to a number of differences with debris flows, they can initiate on slopes as low as 10° (Elder and Kattelmann, 1993) (Figure 18a), and although they can have lateral levees, the deposits tend to be chaotic with no clearly defined downslope boundary (Larocque et al., 2001). Like debris flows they can occur in a hillslope or torrent-fan system (Figure 18b). Physical scale experiments under terrestrial atmospheric conditions have been performed by Auld and Dixon (2017), and showing that slushflow could account for some of the erosional and depositional features of martian gullies. Auld and Dixon (2017) allowed a mixture of liquid and ice to run over an erodible sediment bed, so the concentration of sediment approaches that for an icy debris flow, rather than a slushflow which has a lower sediment concentration and less topographic relief than an icy debris flow.

For icy debris flows, avalanches and slushflows, there should be substantial ice content within the deposited debris. This high volatile content could account for some of the features of martian gullies, including the slope-orthogonal fractures (Figures 6d and 9d) and the presence of thermal contraction polygons on the debris fans (Figure 9c). However, ice exposed at the surface of Mars would also sublimate and therefore martian gully-fans should also show signs of sublimation, including disruption of surface textures, pitting and possibly collapse-structures, which are not systematically observed.

Figure 18 and 19

Scaled physical models have been used to explore the effects of the martian atmospheric pressure on the sediment transport capacity of liquid water. Martian surface air pressure and temperature are generally below the triple point of water and this means water is transient and unstable – often termed metastable (Hecht, 2002) and therefore boils. Frozen soil conditions lead to reduced infiltration, which can lead to both overland flow and debris flow processes at much lower discharge than if the soil was above freezing (Conway et al., 2011a; Gabet, 2000; Jouannic et al., 2015; Védie et al., 2008) (Figure 19a-c). Laboratory simulation experiments have shown that boiling leads to three processes that are not experienced by water flows on Earth (Herny et al., 2018; Massé et al., 2016; Raack et al., 2017): grain saltation at the flow boundary, granular avalanches triggered by the saltation and gas production and finally sediment levitation (Figure 19d). All three processes can act together to lead to much more efficient sediment transport than the equivalent for stable water and no terrestrial field analogues exist for these sediment transport mechanisms.

Depressed freezing temperatures

The potential influence of brines on the morphology of water-eroded features has not been addressed in great detail via terrestrial analogy. In their studies of the Antarctic Dry Valleys Marchant and Head (2007) noted that the water flowing in streams could be saline, but did not remark on any influence this had on the morphology of the system compared systems developed with non-saline water. Similarly Harris et al. (2007), Lyons et al. (2005) and in arctic Canada Pollard et al. (1999) noted springs were forming channels with saline waters yet did not make a full morphological analogy to martian gullies or a comparison to pure water springs. Levy et al. (2011) did study the morphology of saline water tracks in the Antarctic Dry Valley, but noted their relief was weak. Salts are not the only mechanism through which the freezing point of water can be depressed. Water inside the pore space of sediments can exist in a supercooled state (Kereszturi and Appéré, 2014; Kereszturi and Rivera-Valentin, 2012; K. J. Kossacki and Markiewicz, 2004; Oyarzun et al., 2003). Water in a porous medium can have freezing points as low as 233 K (-40°C) (Cahn et al., 1992; Maruyama et al., 1992) without excessive salinity due to the presence of a kinetic barrier, preventing crystallization in pore spaces where the kinetic energy is considerably lowered (Morishige and Kawano, 2000). However, to our knowledge no cases have been reported terrestrially where such interstitial water can trigger downslope sediment flows. Highly concentrated acidic water, such as that suggested by results from the MER-A and B rovers, can also result in a freezing point much lower than that of pure water (e.g., Squyres et al., 2006). Using a scaled-physical model Benison et al. (2008) examined the sediment transport capacity of acidic solutions and found that because these solutions were more dense and viscous than pure water they carved deeper and narrower channels yet still produced generically gully-like features. They noted that these solutions could also form isolated pits in the sediment bed.

In principle, the sediment erosion and, transport processes caused by a brine should have similar mechanisms to those caused by pure water, as long as the brine is sufficiently dilute to remain in the Newtonian regime. A similar argument can be made for debris flow processes occurring with brines. However, landscape-scale features with high solute concentrations are limited to hot springs on Earth (e.g., Fouke et al., 2000) and to a lesser extent rare overland flow events in deserts where salt has had time to accumulate at the surface (e.g., Callow, 2011). The effect of brines on geomorphic processes has to our knowledge not been isolated. An expectation from terrestrial geomorphology is that because we have a good knowledge of the physical processes that govern erosion and deposition by water that account for fluid viscosity, fluid and particle densities and gravitational acceleration, it should be relatively simple to transfer this knowledge to brines and then to other worlds (Grotzinger et al., 2013; Julien, 2010). Although recent low gravity work has started to throw doubt on this expectation (Kuhn, 2014).

3.2.2 Release of water at high to moderate obliquity

The bottom-up and top-down gully-formation mechanisms described in following Sections (3.2.4-3.2.6) share a common final water release mechanism: freeze and thaw under the different climate conditions experienced at high to moderate orbital obliquity on Mars. Mars has an axial tilt which has a much greater amplitude of oscillation than that of the Earth (23°±10° in the last 5Ma compared to 23°±1 for the Earth, Figure 20), due to the lack of a large stabilising Moon (Laskar et al., 2004; Laskar and Robutel, 1993). Variations in axial tilt on the Earth are a component of "Milankovitch cycles" that are known to strongly influence climate, including mean annual surface temperatures and volatile distribution (Berger, 1988). Mars' stronger variation in axial tilt is therefore assumed to have a commensurately stronger influence on its climate (Forget et al., 2006; Head et al., 2003), with Head et al. (2008) making a direct comparison to glacial-interglacial cycles on Earth. At higher orbital obliquity the polar caps receive more insolation in summer and can be completely destabilised, redistributing their volatiles via the atmosphere to the lower latitudes, resulting in a more vigorous atmospheric circulation, higher atmospheric pressure and humidity (e.g., Dickson, 2014; Madeleine et al., 2014). These changes in atmospheric conditions bring Mars' surface much closer to the triple point making freeze-thaw cycling and transient liquid water more likely (e.g., Costard et al., 2002; Richardson and Mischna, 2005).

Figure 20

This mechanism enables authors to reconcile the observations that mid-latitude gullies are dominantly pole-facing and that higher latitude gullies have a weaker equator-facing preference, as these are the places where insolation conditions are expected to favour melt. Costard et al. (2002) initially invoked orbital obliquities of 45° or more (which last occurred more than 5 Ma ago) to account for these trends. The Costard model finds that the only locations on Mars that would experience daily mean temperatures higher than the melting point for ice (273 K) are the mid to high latitudes on pole-facing slopes, where gullies are indeed observed. However, the Costard model does not predict the observed onset of equator-facing gullies poleward of 40° latitude (Conway et al., 2017). More recent studies have shown that more moderate obliquities of 30-35° which occurred in the last hundreds of thousands of years can provide good matches to these orientation observations (Conway et al., 2018b; Williams et al., 2009), but invoke much shallower melting conditions.

3.2.3 Release of groundwater from aquifers

The shallow aquifer hypothesis was first proposed by Malin and Edgett (2000), and then expanded upon by Mellon and Phillips (2001) and Goldspiel and Squyres, (2011). This model involves an aquifer confined by an impermeable rock layer and dry overlying regolith (to provide thermal insulation) lying upslope from a ridge. At a point close enough to the surface toward the ridge where ground ice is stable, an ice plug forms. Obliquity-induced freeze-thaw cycles lead to increased fluid pressure within the aquifer, eventually fracturing the ice plug and allowing water from the aquifer to burst out of the side of the slope and run downhill, forming a gully. Goldspiel and Squyres, (2011) concluded this model could only function if the aquifer were briney, or had high permeability (like that of gravel) or high initial temperature (high geothermal heat flux).

Another flavour of this model was proposed by Gaidos (2001) where a deep aquifer is confined by an impermeable rock layer on the bottom and the cryosphere (Clifford, 1993) on the top. Decreasing heat flow in the subsurface leads to expansion of the cryosphere, pressurizing the confined aquifer to the point of fracturing the cryosphere. The liquid water from the aquifer then travels upward through the fractures due to increased pore pressure until low vertical stresses or failure of the surrounding rock occur, at which point the water begins moving laterally and a sill of liquid water

forms. If the sills reach the surface on a slope, the water is expelled and gullies form. Hartmann et al. (2003) proposed a shallow aquifer formed by localized geothermal melting of ground ice. Debris flows would then triggered either by direct rapid release of water to the surface or by saturation-induced failure. The fact that water travels along impermeable layers in the subsurface and exits at cliff faces in Iceland (Decaulne et al., 2005; Hartmann et al., 2003), and gully-like forms were located downslope was used as a direct support for their hypothesis.

Grasby et al. (2014) reported on landforms resembling martian gullies (alcove-channel-apron) being formed by springs fed by a sub-permafrost groundwater circulation system in the Canadian high arctic (Figure 21). This goes one step further than other authors who used terrestrial analogues to demonstrate that springs can bring water to the surface in environments considered as analogous to Mars in the high artic and Antarctica (Andersen et al., 2002; Harris et al., 2007; Heldmann et al., 2005; Lyons et al., 2005) and did not attempt to draw a morphological analogy. Coleman et al. (2009) used a scaled physical model to simulate gullies formed by emergence of water from an underground aquifer. Their experiments were performed in sand under terrestrial temperature and pressure and they concluded that gully-like landforms could be produced by aquifer flow at the base of a cliff.

Figure 21

Observations of gullies occurring at rock outcrops and at consistent heights below local highs (e.g., Gilmore and Phillips, 2002; Heldmann and Mellon, 2004; Marquez et al., 2005) used as support for the aquifer hypothesis have since been shown to be an artefact of imaging quality, or far from systematic (with the majority of gully systems extending to the highest local elevation). The shallow aquifer model cannot easily account for the occurrence of gullies on isolated central peaks and massifs (e.g., Balme et al., 2006) and recharge mechanisms are problematic without invoking a deep-cryosphere connection. However, invoking a deep-cyrosphere creates the additional problem that seeps should also be observed on surfaces other than steep hillslopes. Neither the Mars Advanced Radar for Subsurface and Ionosphere Sounding (MARSIS) nor SHARAD have detected evidence for shallow aquifers on Mars (Nunes et al., 2010). Despite these difficulties, this model has recently been revived to account for the occurrence of possibly water- or brine- animated “recurring slope lineae” (Stillman et al., 2017, 2016).

Finally terrestrial analogues have also been used to argue against the groundwater hypothesis. Treiman (2003) uses terrestrial analogues to argue that the geological structure of craters is unsuitable for directing seeps to the surface – the layers dip away from the inner crater wall (Kenkmann et al., 2014). Secondly, the observation that gullies occur across a wide range of bedrock geologies which should have widely varying permeability makes a universal aquifer hypothesis unlikely. Earth, which is a similarly geologically complex planet, does not host such integrated groundwater systems.

As pointed out by Baker (2001), based on global trends in gully distribution and orientation alone it is hard to rule-out the groundwater hypothesis because the source of the water is hidden and the release mechanism is the same as that proposed for the melt-based hypotheses. Despite the many convincing arguments against this hypothesis only in situ investigation could completely rule-out aquifers as a source of water in martian gullies.

3.2.4 Melting of near-surface ground ice

A few different models of melting of near-surface ground ice to produce gullies have been proposed. In the model of Costard et al. (2002), warming of the surface at an obliquity of 45° lasts long enough for the temperature wave to penetrate far enough to melt ground ice. The meltwater then saturates the regolith and produces debris flows once critical shear stress is reached. Gilmore and Phillips (2002) on the other hand propose a model where water from melting ground ice percolates through the regolith until encountering an impermeable layer, at which point it travels laterally along the layer until it exits at the surface where the layers are exposed, such as in a crater or valley wall. However, this model suffers the structural problems raised for the aquifer models (Section 3.2.3).

Costard et al. (2007a, 2002) cited debris flows which they inferred to be produced via melting of ground ice in Greenland as terrestrial analogues in support of this hypothesis. Védie et al. (2008) and Jouannic et al. (2015, 2012) point to the formation of the active layer (defrosted upper portion of permafrost) as key in forming this kind of mass flow on martian sand dunes. Studies by Hooper and Dinwiddie (2014) and Hugenholtz (2007) in the Great Kobuk Sand Dunes Alaska and southwestern Saskatchewan, Canada and have shown that debris flows can be initiated by melting of niveo-aeolian (wind-driven snow) within sand dunes. Gallagher and Balme (2011) noted the similarity in terms of morphology and landform assemblage between retrogressive thaw on Earth (Figure 22) and gullies in the northern hemisphere of Mars. However, the wide, shallow depressions with minimal channelized flow of typical terrestrial retrogressive thaw slumps is dissimilar to most martian gullies. Yet as shown by Figure 22, such failures could be an initiation point, or component of the sediment cascade in martian gullies.

Figure 22

Terrestrial landscapes with gullies where active-layer formation is key to the morphogenesis of the component landforms have also been used to support this model of gully formation. One of the often cited case studies is Svalbard (Balme et al., 2013; Hauber et al., 2011a, 2011b; Johnsson et al., 2012; Reiss et al., 2011) where thaw is central to forming solifluction lobes, sorted patterned ground and pingos, and debris flows may be triggered by active-layer detachment (de Haas et al., 2015c). The landscape also contains debris covered glaciers and polygonally-patterned ground, which although not related to thaw attest to the ice-enrichment of the surface environment. These authors identify each of these landscape elements on Mars, where they also highlight the similar spatial arrangement and scale of the landforms. Gallagher and Balme (2011) did not draw on a specific terrestrial analogue, but referred extensively to terrestrial landscapes and the interrelation typically reported between landforms to build the case that gullies in high northern latitudes may be formed by processes analogous to retrogressive thaw slumping. Soare et al. (2017, 2014a, 2014b, 2007) have used landscapes in the Tuktoyaktuk peninsula, northern Canada, to argue that martian gullies are an element of a landscape resulting from freeze-thaw cycling, which also includes, high-centred polygons, pingos and thermokarst depressions (Figure 23).

Figure 23

In order for this hypothesis to be valid melting needs to be possible in the top metres of the ground on Mars. Modelling by Mellon and Phillips (2001) showed that the depth of the 273 K isotherm is always above the depth of any near-surface ground ice that might exist at these latitudes, under both present-day conditions and under past conditions at high obliquity. Similarly Kreslavsky et al. (2008) examined the orbital conditions which would permit an active-layer to form and concluded that these conditions last occurred >5 Ma, hence do not provide a good explanation for martian

gullies. Further, Mellon and Phillips (2001) also found that temperatures high enough to melt ice would only be attained if the ice were composed of 15–40% salts. Melting due to the presence of salts is also inconsistent with the latitudinal distribution of gullies, as they would be expected to form at all latitudes over a range of obliquity regimes in this case (Mellon and Phillips, 2001). If the process that initially formed gullies is responsible for the activity we observe today, the Costard et al. (2002) model cannot be invoked as gullies are active at Mars' current obliquity. Any models involving melting at or near the surface would also imply that gully activity would be expected in summer (as is the case for terrestrial snowmelt-initiated debris flows in Iceland, which peak in the summer (de Haas et al., 2015c; Decaulne and Sæmundsson, 2007; Rapp, 1986)), and the seasonal constraints of all of the new gully flows known to have formed within a single Mars year demonstrate that they are forming in autumn, winter, or very early spring (Diniega et al., 2010; Dundas et al., 2015, 2012, 2010; Harrison et al., 2009). If the present-day activity in gullies is separate from their initial formation mechanism, however, then these issues do not pose a problem for the ground-ice model as it could be valid during periods of higher obliquity.

3.2.5 Melting of snow

Melting of snow as the genesis of gullies was first proposed by Lee et al. (2002) and Hartmann et al. (2003) based on the resemblance of martian gullies to those on Devon Island and Iceland, respectively, created by snowmelt (Figure 24a,b). Christensen (2003) (later expanded by Williams et al., 2009) invoked snowmelt by proposing that gullies were created by melting of dust-covered snowpacks that formed at high to moderate obliquity (~35°), remnants of which are preserved as LDM deposits on gullied crater walls today. Head et al. (2008) also proposed a model involving surface meltwater, in which the last glaciation of Mars resulted in debris-covered glaciers forming against the poleward-facing walls and on the floors of mid-latitude craters. When the climate changed, the glaciers stopped accumulating and flowing, leaving alcoves exposed on the crater walls. Residual surface ice and snow in these alcoves then melted to form gullies. Schon et al. (2012) advocates this model based on the correlation between the calculated age of one particular gully they studied and the emplacement time of dust-ice covered mantling deposits. The presence of intimate relationship between glaciers and gullies is further supported by de Haas et al. (2018), who show that glacial activity often removes gully deposits (leaving only the crown of the gully-alcoves exposed) but that gullies subsequently rapidly form within the formerly glaciated crater wall (Conway et al., 2018a). The support and caveats of these models are the same as those discussed in the previous section on melting of ground ice.

Figure 24

Overland flow of water sourced from snow meltwater in the dry valleys of Antarctica produces many of the features associated with gullies on Mars: channel sinuosity, v-shaped incision, lateral levees (although their topographic expression is small) and fan-shaped deposits. Marchant and Head (2007), amongst others, argue that the cold dry climate of the Antarctic dry valleys makes them a particularly suitable analogue for Mars, which very few other terrestrial analogues can match. In this location, gully alcoves are observed to form traps for windblown snow and ice, otherwise known as nivation hollows (e.g., Christiansen, 1998; Dickson et al., 2007; Lee et al., 2004). Because of the aridity of the dry valleys, there are usually high concentrations of salt at the surface, which cause any water flow to be salty (Marchant and Head, 2007). The authors argue that this could also be the case on Mars and would favour gully formation via snowmelt. The assemblage of landforms found alongside gullies in the Dry Valleys, including notably polygonally-patterned ground and glacial landforms has also been used to support this environmental analogue as a process analogue to gullies and their associated landforms on Mars (Levy et al., 2009; Marchant and Head, 2007) (Figure 24c).

Védie et al. (2008) performed scaled physical experiments designed to simulate the formation of Russell Crater's linear dune gullies under ambient Earth pressure and low temperature (Figure 19). They found that snowmelt as a water-source did not produce morphologies distinct from other water sources (perched aquifer, melting of ground ice). A similar conclusion was reached by Sinha et al. (2018) who compared debris flows generated by snowmelt in the arid Himalaya to gullies with similar morphology on Mars. These studies imply that snowmelt is hard to distinguish from other near-surface sources of water by morphology alone and hence it would be difficult to detect its influence in the formation of martian gullies.

3.2.6 Melting of H_2O frost

Kossacki and Markiewicz (2004) investigated whether gullies could have formed from seasonal melting of accumulated H_2O frost under favourable pressure and wind speed conditions. In this model, H_2O frost transitions to the liquid phase after the complete removal of the overlying CO_2 frost layer (which deposits atop H_2O frost seasonally on Mars). CO_2 frost can remain on crater walls into late spring. Once insolation increases above a certain intensity (in late spring/early summer), the last CO_2 frost sublimates away, which could result in the rapid heating (and melting) of the underlying H_2O frost. The presence of salts within the water ice could aid in lowering the melting temperature and favour this process. The estimated maximum volume of liquid that could be generated by this melting is <0.2–0.55 kg/m^2 depending on latitude, which Kossacki and Markiewicz (2004) state is not enough to generate any surface flow, but could affect the cohesive properties of the surface layer of the slope. With an average water-vapour abundance of only ~10 precipitable micrometres in the current martian atmosphere (Jakosky and Barker, 1984; Jakosky and Farmer, 1982), other authors have also argued that frost accumulation and subsequent melting would likely not be significant enough to saturate the regolith to the point of slope failure, but rather the dampening would lead to increased cohesion (e.g., Dundas et al., 2015). The darkening of the surface by this dampening has been hypothesised to be the origin of RSL on Mars (McEwen et al., 2011), where downslope percolation of small amounts of water explain the gradual growth of these relatively dark features. A terrestrial analogue for this kind of water percolation was reported by Levy et al. (2011) in the form of water tracks in Antarctica. These water tracks are saline and supplied by melting snow, pore-ice and ground ice. They have also been used as analogies for martian linear gullies on dark sand dunes– where a dark halo is observed to appear at the same time as new/modified gully-tracks (Jouannic et al., 2017). Pasquon et al. (2016) termed these dark halos "RDF" or Recurrent Diffusing Flows. Jouannic et al. (2017) also use an unusual example of snowmelt on a glacier as a process analogue for the formation of new "perennial rills" within these RDF, however they leave open the question of which fluid is involved.

Recent scaled physical models under Mars pressures have revealed that the metastable nature of water on Mars means that more sediment transport could occur than might be expected from stable water (Herny et al., 2018; Massé et al., 2016; Raack et al., 2017). Therefore, the main argument against the meltwater hypothesis – that melting surface frost cannot produce enough water for surface flow – may be somewhat ameliorated if these processes are indeed active.

The argument that frosts are too thin (because of the low atmospheric humidity) to explain the size of martian gullies, has some potential counter-arguments, as follows. Water vapour abundance in the martian atmosphere is highly variable, dependent upon the time of day, season, and local conditions (e.g., Tamppari and Lemmon, 2014). Due to its low concentration in the atmosphere and its variability, modelling the distribution of water vapour in the past is challenging (e.g., Madeleine et al., 2014; Steele et al., 2017), particularly under high obliquity when the water cycle is predicted to be more intense (e.g., Haberle et al., 2003). Hence, it is challenging to make any solid statements about frost availability at martian gully sites in the past. Further, present-day measurements of

water vapour from orbit are likely unrepresentative of transient and local surface conditions, which would be sufficient to generate small amounts of melt, as argued in the RSL literature (Chojnacki et al., 2016; McEwen et al., 2014). Wind redistribution of seasonal frosts could also increase the local thicknesses of frosts, somewhat analogously to the melting of snow hypothesis discussed in the previous section. Equally the distribution of surface frosts is highly sensitive to small variations in topography, so despite the general prediction that frost should not accumulate on equator-facing slopes as they are never deeply shadowed (Schorghofer and Edgett, 2006), observations of frost are made on equator-facing slopes (Dundas et al., 2017b) (Figure 12). Terrestrial analogy dictates that only episodic optimal conditions are required and they can produce significant landscape change (Levy, 2015; Marchant and Head, 2007).

3.3 CO_2 related mechanisms

Carbon dioxide is the major constituent of the martian atmosphere and condenses onto the surface at the high latitudes every winter. Its sublimation in the spring is believed to responsible for sediment transport in the form of "spiders" (e.g., Kieffer et al., 2006; Piqueux et al., 2003a; Portyankina et al., 2010) and dark spots and flows on polar dunes(e.g., Gardin et al., 2010; Kereszturi et al., 2009; Kossacki and Markiewicz, 2014). CO_2 frost is known to extend continuously from the pole to latitudes of 50° in mid-winter (e.g., Piqueux et al., 2015) and is found on steep pole-facing slopes from latitudes from 50° to 30° (Vincendon et al., 2010b). Hence, its geographical distribution matches that of gullies and the timing of recent gully-activity in martian winter matches with its presence. The polar-pit gullies and classic dune gullies are the only examples where the tight constraint on timing leaves CO_2 as the only unambiguous candidate to account for the sediment movements observed in these systems. However, as discussed in Section 2.1, polar-pit gullies are somewhat different from the majority of gully systems, so the processes that form them may differ from those active in other gully systems.

Based on the timing of observed present-day gully activity (generally in winter coinciding with periods when CO_2-frost is on the ground), a CO_2-based process for gully formation is favoured by Diniega et al. (2010), Dundas et al. (2017b, 2015a, 2012a, 2010a), Pasquon et al. (2016) and Raack et al. (2015). A CO_2- -related process is supported by the observation of a higher level of activity in the south polar-pit gullies (Raack et al., 2015) compared to those in the mid-latitudes, as more frost is deposited on slopes at higher latitudes. South polar pits should host ~1 m of CO_2 frost accumulation in winter (Hoffman, 2002), which is significantly more than lower latitude gullies, where microns of accumulation are predicted (Vincendon et al., 2010a). However, CO_2 frost has not been detected spectroscopically at latitudes equatorward of ~34°S (Vincendon et al., 2010b), and present-day gully activity has been observed at latitudes as low as 29°S. Dundas et al. (2015) do note that CO_2 frost processes might simply be the dominant driver of activity within pre-existing gullies today, and not the process by which they initially formed.

In the following sections we will present the various CO_2-driven mechanisms of gully-formation that have been proposed. We start with liquid CO_2 which has now been rejected on the grounds of thermodynamics, but is presented here because the authors used terrestrial analogues to support their arguments. We then present mechanisms that involve the gravitational displacement of solid CO_2 with or without the evolution of CO_2 gas. Finally we detail the mechanisms that primarily involve the transport of sediment by gas evolved from CO_2 sublimation.

3.3.1 Release of liquid CO_2 from shallow aquifers

Musselwhite et al. (2001) proposed that martian gullies formed via the outbreak of liquid CO_2 from near-surface "aquifers". In this model, similar to the shallow groundwater model of Malin and Edgett

(2000) described in Section 3.2.2, liquid CO_2 builds up in an aquifer behind a dry ice "dam" that forms at the point in the subsurface where liquid CO_2 is no longer stable. Seasonal and/or obliquity cycle driven heating weakens the dry ice "dam", eventually resulting in the rapid release of liquid CO_2 to the surface. Upon reaching the surface, the CO_2 would rapidly vaporise, forming a gas-supported flow that entrained rock and ice, carving a gully as it moved downhill. The authors argue for CO_2 over H_2O as the gully-carving agent on Mars, because CO_2 is the most abundant volatile on the planet. This model was quickly dismissed due to the difficulty in both accumulating and sustaining significant amounts of either condensed CO_2 or CO_2 clathrate-hydrate in the martian crust (Stewart and Nimmo, 2002). Stewart and Nimmo (2002) state that gas-supported flows of this nature would have velocities much too high to create morphologies observed in martian gullies, and would be expected to result in forms more like terrestrial pyroclastic flows than the fluvial/debris flow forms of gullies (Stewart and Nimmo, 2002). Therefore, they used the dissimilarity of a terrestrial landform to martian gullies in order to counter the hypothesis proposed by Musselwhite et al. (2001). They particularly point to the visual dissimilarity between the deposits of the Mt. St. Helen's pyroclastic flows and the depositional fans of martian gullies (Figures 6 and 14).

3.3.2 CO_2 frost avalanches, blocks and frosted granular flow

Ishii and Sasaki (2004) proposed that avalanches of solid CO_2 frost could gradually carve gullies over time by "scratching" into the surface as chunks of frost fell during periods of sublimation (i.e., spring into summer). Frost avalanches have also been proposed as gully formation/evolution mechanisms by some authors based on HiRISE observations of frost-dust avalanches on a north polar scarp (Russell et al., 2008) and the hypothesis of Costard et al. (2007b) that "dark streaks" observed over frost in gullies are dry avalanches. However, present-day CO_2 frost avalanches on scarps of the northern polar layered deposits have not been observed to form any gully-like features (Russell et al., 2008). Because these avalanches do not involve a volatile phase their behaviour and morphology should be similar to that of dry granular flows and therefore this model has been discounted on the same grounds (see Section 3.1).

Figure 25

A different type of sublimation-induced CO_2 ice avalanching has been suggested as the formation mechanism behind linear dune gullies, such as those on the dunes in Russell Crater (Diniega et al., 2013). In this model (originally proposed by Hansen et al. (2011) for mass-movement features on the north polar erg of Mars), blocks of CO_2 ice dislodge from the top of the dune in springtime due to sublimation induced by solar heating. The blocks then travel downslope, levitating on a cushion of CO_2 gas, carving leveed linear channels. The authors use a field-simulation analogue to support their hypothesis, where the authors placed decametre-scale sublimating blocks of CO_2 ice on terrestrial dunefields (Figure 25) and produced similar narrow leveed channels (and terminal pits). These pits have also been reproduced in laboratory simulations with sublimating blocks of CO_2 ice (Mc Keown et al., 2017). As discussed in Sections 2.1 and 2.6, the peculiar morphology and precise timing of the activity of linear gullies suggests that their formation process is different from the other martian gullies, so this mechanism has not been applied to the general population of gullies.

Figure 26

Hugenholtz (2008b) proposed frosted granular flow as a gully formation mechanism on Mars based on terrestrial observations (Figure 26). Frosted granular flow is a rare type of mass movement on Earth where clasts are lubricated by thin frost coatings, facilitating downslope movement. They tend to occur in the fall and spring when the air temperature oscillates around freezing (273 K) at times of

relatively high humidity on snow-free surfaces (Hétu et al., 1994; Hétu and Gray, 2000). Hétu et al. (1994) noted four conditions required for frosted granular flow: (1) unconsolidated sediment easily mobilized downslope, (2) a slope gradient at or near the angle of repose in the source region, (3) frost accumulation on the unconsolidated grains, and (4) a trigger for mass movement (on Mars this could be, for example, rockfall (Hétu et al., 1994), point-source defrosting (Costard et al., 2007b), vapour-induced instability (Hoffman, 2002), or avalanching of CO_2 frost (Ishii and Sasaki, 2004)). Locations of repeated flows typically either follow pre-existing channels or, when diverted by obstacles, create new channels. Grains ranging in size from fine-grained sand (~0.0007 cm) to large clasts (20 cm) can be mobilized by these flows on slopes as low as ~25°; however, frosted granular flows predominantly transport gravel-sized grains (Hétu and Gray, 2000; Hugenholtz, 2008b). As for debris flows, kinetic sieving results in accumulation of large clasts at the flow margins and surface of frosted granular flows. Frosted granular flows are reported to exhibit levees, straight to sinuous channels, concave profiles, and digitate terminations (Hétu et al., 1994; Hétu and Gray, 2000), which are similar to debris flows. Seasonal H_2O frost accumulates as far north as 13°S in the winter (Vincendon et al., 2010a), and early morning frost has been observed on the ground by the Opportunity rover at 2°S (Landis, 2007), covering the entire latitude range where gullies are found in the southern hemisphere. Hugenholtz (2008b) proposes that CO_2 frost rather than water ice frost may be the lubricating mechanism for frosted granular flows on Mars. However, this seems unlikely because only thin diurnal night time CO_2 frost has been detected at latitudes lower than ~34°S (Piqueux et al., 2016; Vincendon et al., 2010b). Additionally, CO_2 frost does not accumulate in the mid- to high-latitudes in areas that are never deeply shadowed at any point in the year (Schorghofer and Edgett, 2006), and gullies are found on equator-facing slopes where CO_2 frost is not predicted to accumulate. In addition, frosted granular flow seems unlikely as a principle driver for gully formation based on their morphology. The morphology of frosted granular flow channels and deposits are very similar to that of classic granular flows described in Section 3.1 and lack the morphological complexity shown by typical martian gullies, including tributary networks, deep incisions, streamlined forms and terraces (Figures 2, 5, 6).

3.3.3 CO_2 gas-fluidized flow

Hoffman (2002) and Cedillo-Flores et al (2011) proposed that gullies in at least Mars' polar regions, such as those in the south polar pits of Sisyphi Cavi, formed by fluidization of aeolian sediment deposited atop CO_2 frost once the frost begins to sublime in springtime (Figure 27). This model requires a slope covered with CO_2 frost, which is then subsequently mantled by sediment, sand, or dust via aeolian transport from adjacent non-frosted slopes. The frost layer rapidly sublimes due to heating of the overlying lower-albedo material. This introduces instability to the slope, triggering mass movement. Mechanical heating as the material moves downslope generates more CO_2 vapour, acting as a lubricant to allow the mass to behave like a fluid and carving a channel. This model differs from that of Musselwhite et al. (2001) in that it only invokes surface CO_2 ice based on the aforementioned thermodynamic difficulty in sustaining CO_2 ground ice on Mars.

Figure 27

Recent activity within polar pit gullies coincides with periods of defrosting (Hoffman, 2002; Raack et al., 2015), which has led to the suggestion that CO_2 defrosting is capable of initiating mass movement of the underlying sediment (rather than sediment deposited atop it). Hoffman (2002) suggests that the closest terrestrial analogue to this sort of gas-fluidized flow is a density flow, and presents submarine turbidity channels for their morphological similarity to martian gullies, where the submarine landforms display sinuous channels (Figure 28) and distributary fans.

Figure 28

Following along the same lines, Pilorget and Forget (2016) propose a model where CO_2 ice condenses onto the surface in autumn, gradually forming a continuous slab. Sublimation at the base of the slab ice occurs due to differential solar heating of the underlying regolith, because the slab ice is relatively transparent to sunlight. Some of the resulting CO_2 gas diffuses into the regolith, trapped between impermeable permafrost and the overlying CO_2 slab ice. In mid-winter, CO_2 ice begins to condense in pore spaces within the upper few centimetres of the underlying regolith. Pressure builds up to a point where the CO_2 gas ruptures the overlying ice, forming jets of CO_2 gas that could destabilize the slope and cause a fluidized debris flow. This was inspired by the model of sub-slab sublimation which has been proposed for the formation of south polar spiders (Kieffer et al., 2006; Piqueux et al., 2003b). Pilorget and Forget (2016) describe this type of gas-supported flow as being akin to a terrestrial pyroclastic flow (Figure 14). They note that not every "eruption" of CO_2 gas would be expected to generate a gully, but multiple eruptions in the same place could occur due to re-condensation, leading to repeated events within an individual gully system. In fact, in the case of the Russell Crater dune gullies, their model predicts eruptions on a daily basis from L_s 150–205°, which coincides with the appearance of dark flows, but not linear gully activity (Jouannic et al., 2017; Pasquon et al., 2017). One of the prerequisites for this model is the presence of a CO_2 ice slab, which is not expected at the mid-latitude sites where the majority of active gullies are located and is not easily applicable to gullies on equator-facing slopes in the mid-latitudes, where CO_2 if present is likely to be spatially discontinuous and thin (Conway et al., 2018b; Dundas et al., 2017b).

As argued by Hoffman (2002), density currents, such as pyroclastic flows and submarine turbidity currents are the nearest analogy for sediment transport by sublimating CO_2. Numerical models have shown that pyroclastic flows on Earth behave like dense granular flows and produce a broad central linear channel with lateral levees and terminal lobes (Félix and Thomas, 2004; Mangeney et al., 2007). Terrestrial laboratory experiments of fluidization of dry material with CO_2 gas (Cedillo-Flores et al., 2008; Sylvest et al., 2018, 2016) similarly produce features morphologically similar to dry sand flows on terrestrial dunes, as the gas rapidly escapes (Figure 14). Further work is needed to ascertain whether CO_2 sublimation can produce long-lived fluidisation and therefore morphologies similar to martian gullies. It has been hypothesised that the repeated action of discrete granular flows can produce connected networks (Shelef and Hilley, 2016) and complex channel geometries as seen in martian gullies and terrestrial equivalents. As stated by Hoffman (2002) "quantitative diagnostic criteria must be developed to distinguish between the morphologies produced by subaerial flows and those of density flows".

3.4 Summary of gully formation mechanisms

Since their discovery, many processes, often based on terrestrial analogues, have been proposed by a variety of authors to understand the formation of gullies on Mars. Hypothesized geomorphic flow processes range from completely dry to various types of water- and CO_2-lubricated flows. To fully understand gully formation, these processes need to be able to account for activity in gullies at the present-day as well as during past, higher-obliquity, conditions.

At present, dry flows have been ruled out as a predominant gully-forming mechanisms, because of the typical gully-fan slopes, which are well below the dynamic angle of repose, and gully morphology that is inconsistent with dry-flow morphology. Present-day gully activity is intimately linked to CO_2-defrosting, and therefore CO_2 likely plays a role in the formation of many present-day flows. However, this process is not able to account for the distribution of the full gully population, such as gullies on equator-facing mid-latitude slopes. Liquid water should not be thermodynamically stable under current martian conditions, and therefore is unlikely to account for present-day gully activity. On the other hand, during periods of higher-obliquity in the past, climate models predict that snow and ice should have been stable down to ~30° of latitude, consistent with the global distribution of

gullies. Moreover, under these conditions snow and ice was likely able to melt, and thereby form gullies.

In short, as extensively discussed above, there is no single gully-formation mechanism that is consistent with all the observations of the full gully-population on Mars. Like on Earth, it is therefore likely that multiple processes operate within gullies, and that the predominant mechanism could change over time, under changing atmospheric conditions as a result of variations in orbital forcing.

4. The role of Earth analogues in gully-research

4.1 Earth analogues: their advantages and their limitations

A full review of the usefulness of Earth analogues in planetary science is outside the scope of this review and we refer interested readers to more detailed works on this topic (e.g., Baker, 2014). Here we discuss particular issues that have arisen repeatedly during our review of the martian gully literature. Earth analogues have been intensely used to construct working hypotheses regarding the processes and fluids that lead to gully formation on Mars. Different types of terrestrial analogy have been used and we have pulled-out these general themes, where most papers on martian gullies use one or more of these approaches:

- Plan-view morphology at the landscape-scale or feature-scale
- Three-dimensional (3D) or plan-view morphometry
- Environmental analogues
- Landscape assemblages
- Physical scale experiments
- Empirical laws from terrestrial studies

Out of these types of analogues the ones that rely on planview morphology are the most controversial, because of equifinality, whereby similar landforms can be produced by widely different processes (Chorley, 1962). A case in point is that pyroclastic flows have been interpreted to be both similar and unlike martin gullies by different authors (Sections 3.1 and 3.3.3) (Pilorget and Forget, 2016; Stewart and Nimmo, 2002; A. H. Treiman, 2003). The fact that widely different processes can result in leveed channels with lobate terminal deposits on Earth (including debris flows, lava flows, and pyroclastic flows; Figure 29), suggests that various physical processes can be responsible for a similar morphology. However, once the morphometry, upslope landforms, and landscape setting of these lobate deposits are taken into account the similarity with the alternative landform is reduced (Baker, 2017). Hence, using a combination of morphological and morphometric similarities at a range of spatial scales can establish a more robust analogy (Mutch, 1979; Zimbelman, 2001) and is an approach that has been adopted by many researchers working on martian gullies. To build a successful analogy, full similarity over a range of scales and processes is not required, i.e., not every aspect of the target landscape needs to be reproduced (e.g., climate, geology, soil, topography). In the case of martian gullies, Antarctica is the nearest environmental analogue (low temperatures and humidity; e.g., Marchant and Head, 2007), Iceland forms a better geological analogue (basalt bedrock; Hartmann et al., 2003), and impact craters form the best analogue in terms of topographic and structural setting (e.g., Osinski et al., 2006) and all of these have been used to gain fruitful insights into martian gully formation.

Figure 29

The debate over carbon dioxide as an active agent of morphological change in martian gullies highlights one of the potential limitations of Earth analogy. That is, can we successfully argue that liquid water is involved in martian gullies by using Earth analogues if we cannot provide the counter-point of landscapes created by CO_2 sublimation, or at least gas-supported flows? In this case are terrestrial analogues helpful at all, or simply misleading? Analogy (Hesse, 1966) can still be useful: although not providing definitive explanations, it does provide a source of hypotheses that move geological research into productive lines of inquiry (Gilbert, 1896). We argue that for terrestrially rare or unknown processes, further progress can be made by using numerical modelling and scaled physical models (which we consider here as a subtype of terrestrial analogy). Laboratory experiments can be used to determine if the physical processes governing sediment transport by CO_2 sublimation are indistinguishable from those driven by water as the interstitial fluid. Substantial work is required, however, to both properly understand the physics that govern these processes and then to appropriately scale up the processes observed in the laboratory to assess if they can indeed produce the landforms we observe.

Establishing a terrestrial analogue allows us to exploit the depth of knowledge on that process in order to respond to Mars-specific questions. For example, based on an analogy between fluvial and martian gullies, Parsons and Nimmo (2010) and Hobbs et al. (2014) applied empirical terrestrial relationships between discharge and fluvial channel dimensions to estimate the water required to form martian gullies. Yet, success of empirical approaches depends on whether the empirical parameters are inherently terrestrial. Recent work in low gravity parabolic flights has highlighted, for example, that the empirical drag coefficient used when estimating the settling velocity of particles in a flow, is dependent on gravity, when previously it was believed to be independent (Kuhn, 2014). Therefore, particles under martian gravity settle more quickly and have a much narrower distribution in settling velocities (for a given range of particle shapes and sizes) than would be predicted by applying the empirical settling velocity. Nevertheless applying terrestrial empirical laws can give important insights into gully formation and evolution, as long as interplanetary differences are carefully considered.

4.2 Future directions

The work reviewed in this paper shows that terrestrial analogues have played an important role in martian gully research. We consider transporting both terrestrial analogies in terms of both landscape-process interpretation, but also in terms of the methodologies used to interpret the formative environment, as a fruitful avenue that should continue to be exploited in future martian gully research. We have also identified five further avenues where we think further research could yield important insights.

Terrestrial experience tells us that separating individual landscape-forming processes from one another is disingenuous. For instance, fluvial flows can evolve into debris flows via gradual incorporation of loose debris downslope (firehose effect, or bulking; Coe et al., 2008; Godt and Coe, 2007). Erosion of bedrock is typically limited during fluvial or debris flow events in steep catchments, landslide processes are a common prerequisite for making sediment available in catchments (Benda and Dunne, 1997) and the bedrock is initially weakened by weathering (Matsuoka and Murton, 2008; Phillips, 2005). Those loose sediments are then removed by debris flow or fluvial processes, the efficiency of such sediment cascades is defined as “connectivity” (e.g., Cavalli et al., 2013). We advocate that progress can be made in martian gully research by considering the landform as a series of sediment cascades and the connectivity of the landscape as a whole system (Bennett et al., 2014; Heckmann and Schwanghart, 2013). In considering the cascade of sediments relatively little work has focussed on establishing terrestrial analogues and understanding the processes in the erosional part of martian gullies (i.e., the alcoves). A notable exception is the study by Okubo et al.

(2011) who examined the potential triggers of landslides in alcoves to supply sediment to martian gullies in Gasa crater. However, these authors did not consider the fate of the sediments post-failure. The increasing availability of high resolution digital elevation models of martian gullies is opening up the opportunity to study the connectivity and sediment cascades from source to sink using both morphological and morphometric techniques.

The increasing availability of digital elevation models of martian gullies also offers another opportunity – the possibility of employing landscape evolution models to understanding gully formation. Such an approach has been applied in the study of the degradation of martian impact craters via fluvial systems driven by rainfall (Howard, 2007). However, this approach has yet to be applied to martian gullies. Martian gullies are ripe for this application because of two recent innovations: 1) the increasing use of synthetic DEMs as a starting point for landscape evolution models (Hillier et al., 2015), allowing gullies to be simulated in undisturbed topography and 2) the recognition that landscape evolution models can be driven by stochastic discrete flow events (Shelef and Hilley, 2016), rather than flow driven by continuous variables. The use of landscape evolution models could help us to explore the age of gullies, the climate drivers and the expected sedimentary packages relevant for understanding the rock record on Mars.

Similarly, there is a wide range of advanced 2D to 3D numerical models that are used simulate dry and wet sediment-gravity flows on Earth over realistic topography (e.g., debris flows, grain flows and snow avalanches) (Christen et al., 2010, 2007; Iverson and George, 2014; Mergili et al., 2017; O'Brien et al., 1993). Such models can correct for martian gravity, and in combination with high-resolution DEMs, be used to infer the initiation and flow conditions that led to the formation of deposits on martian gully-fans. Such analyses could shed new light on the palaeoclimatic conditions leading to gully formation. Yet, despite their great potential, only Pelletier et al. (2008) used one such model, FLO-2D, to infer the volumetric water content in a recent flow deposits in a crater in the Centauri Montes region. An important application of such models would be distinguishing between fluvial, debris flow and gas supported flows based on the extent and thickness of the observed deposits.

Scaled-physical models are another area where we think that significant progress can be made in understanding the processes that form martian gullies. Lapotre et al. (2017) highlighted that natural water flows on Earth cover a narrow range of fluid densities, viscosities, and grain densities and they inevitably occur under terrestrial gravity, which means that the effects of these different parameters on flow behaviour is hard to assess from terrestrial observations alone. Laboratory experiments allow us to vary such parameters. In addition, certain physical processes can be isolated and studied in detail in order to understand the basic underlying mechanics. The relative importance of the driving variables can be assessed experimentally (in terms of rates, frequency and magnitude) and the physical equations can be used to explore the parameter space guiding future laboratory work. Gravity can be adjusted via the use of parabolic flights and has been used to study granular flows under martian gravity (Kleinhans et al., 2011), but has not yet been extended to fluidised flows. The study of sediment transport by CO_2 sublimation is in its infancy and is of particular importance for breaking the impasse between liquid water vs CO_2 for forming and modifying gullies. The potential role of brines and metastable fluids in sediment transport on Mars is also an area where significant work remains. An important area for future work will be using experiments to place limits on slope angles and grainsizes for deposition and erosion caused by different transport mechanisms, which can then be compared to slope and grainsize observations of martian gullies. Laboratory simulations exploring how volatiles such as CO_2 and water vapour interact with the martian regolith and respond to changes in surface temperatures are also needed to understand the processes involved in triggering the sediment cascades we observe in martian gullies. Laboratory studies also present the advantage of being able to study the dynamic component of sediment transport, which is severely

lacking on Mars where the gap between images can be several sols, but is usually at least several months.

The formative processes of gullies and their spatial distribution has been extensively studied and quantified (e.g., Balme et al., 2006; Dickson et al., 2007; Harrison et al., 2015; Heldmann and Mellon, 2004; Kneissl et al., 2009), while only few studies have addressed their temporal evolution (de Haas et al., 2018, 2015b; Dickson et al., 2015). Focusing on the temporal evolution of gullies is an important avenue of future research, as the dominant formative mechanism of gullies may change over time and because gullies may interact with other processes over time. Recent work by de Haas (2018, 2015b) shows that crater dating provides a promising tool for unravelling gully formation mechanisms as long as the considered temporal resolution is large enough to be resolved via crater counting.

5. Conclusions

In this review we have summarised the main hypotheses proposed for martian gully formation and the role that Earth analogues have played in conceiving and developing these hypotheses. There remains a debate in the community between the role of CO_2 and liquid water in forming gullies. Using terrestrial analogy alone, liquid water is the most plausible candidate, yet current modifications in gullies occur at times of year when surface liquid water is unlikely. Sediment transport by sublimating CO_2 lacks a terrestrial analogue, hence it is difficult to judge whether the morphology of all martian gullies could be produced by this mechanism. Knowledge from Earth tells us that landforms are not made by a single processes and that these processes can vary in space and in time. Hence, we believe that the present processes in gullies likely do not accurately represent those active in the past. An urgent effort is required to ascertain the sediment transport capacity of CO_2 supported flows on Mars and its resulting landforms to make progress.

We find that on balance terrestrial analogies are useful for understanding the complexity and interplay of processes involved in creating gullies on Mars – such insights are difficult to obtain from either remote sensing, numerical modelling, or laboratory studies alone. We emphasise that caution should be taken in applying these analogies taking into consideration the important environmental differences between Earth and Mars.

We highlight six particular areas where we think progress can be made in Mars gully research in the near future:

- Laboratory simulations using scaled-physical models, focusing specifically on exploring variables that can be observed from orbit.
- The use of landscape evolution models which are specifically adapted to recent and past martian climate.
- Application of the concept of sediment connectivity, with specific emphasis on the insights that can be gained from the erosional landforms of martian gullies with reference to Earth analogues.
- Application of advanced 2D and 3D numerical sediment-gravity flow models, to back calculate the conditions leading to observed gully deposits.
- Cross-fertilisation of concepts and methodologies used in terrestrial geomorphology to the study of martian gullies.

- Quantitative analyses of the temporal evolution of martian gullies, and the identification and exploration of terrestrial analogues representative for martian gullies during different time periods.

The activity of Martian gullies extends from the present day back to the last few million years, and they are geographically widespread. Therefore, understanding the processes that shape them has the potential to unlock the secrets of Mars' recent and past climate, hydrosphere and habitability.

6. Acknowledgements

We thank reviewers Vic Baker and Alan Howard for their constructive comments that improved this manuscript. SJC is supported by the French Space Agency CNES for her HiRISE related work and was assisted by NASA grant NNX14AO21G, whose PI is Jim McElwaine. TdH is funded by the Netherlands Organization for Scientific Research (NWO) via Rubicon grant 019.153LW.002. Geospatial support for this work provided by the Polar Geospatial Center under NSF-OPP awards 1043681 and 1559691. Thanks to Nathalie Thomas and Armelle Decaulne for supplying photographs.

7 .References cited:

Allender, E., Stepinski, T.F., 2018. Global analysis of gully composition using manual and automated exploration of CRISM imagery. Icarus 302, 319–329. https://doi.org/10.1016/j.icarus.2017.11.017

Allender, E., Stepinski, T.F., 2017. Automatic, exploratory mineralogical mapping of CRISM imagery using summary product signatures. Icarus 281, 151–161. https://doi.org/10.1016/j.icarus.2016.08.022

Ancey, C., 2007. Plasticity and geophysical flows: A review. J. Non-Newton. Fluid Mech. 142, 4–35.

Andersen, D.T., Pollard, W.H., McKay, C.P., Heldmann, J., 2002. Cold springs in permafrost on Earth and Mars. J. Geophys. Res. Planets 107, 5015.

Anderson, S.P., Anderson, R.S., 1990. Debris-flow benches: Dune-contact deposits record paleo-sand dune positions in north Panamint Valley, Inyo County, California. Geology 18, 524. https://doi.org/10.1130/0091-7613(1990)018<0524:DFBDCD>2.3.CO;2

André, M.-F., 1990. Frequency of debris flows and slush avalanches in Spitsbergen: a tentative evaluation from lichenometry. Pol. Polar Res. 11, 345–363.

Anglés, A., Li, Y., 2017. The western Qaidam Basin as a potential Martian environmental analogue: An overview. J. Geophys. Res. Planets 122, 856–888. https://doi.org/10.1002/2017JE005293

Appéré, T., Schmitt, B., Langevin, Y., Douté, S., Pommerol, A., Forget, F., Spiga, A., Gondet, B., Bibring, J.-P., 2011. Winter and spring evolution of northern seasonal deposits on Mars from OMEGA on Mars Express. J Geophys Res 116, E05001. https://doi.org/doi:10.1029/2010JE003762

Arfstrom, J., Hartmann, W.K., 2005. Martian flow features, moraine-like ridges, and gullies: Terrestrial analogs and interrelationships. Icarus 174, 321–335. https://doi.org/10.1016/j.icarus.2004.05.026

Aston, A.H., Conway, S.J., Balme, M.R., 2011. Identifying Martian gully evolution, in: Balme, M., Bargery, A.S., Gallagher, C., Gupta, S. (Eds.), Martian Geomorphology. The Geological Society of London, pp. 151–169.

Auld, K.C., Dixon, J.C., 2017. An Experimental Investigation of Martian Gully Formation: A slushflow Model. Geol. Soc. Lond. Spec. Publ. 467, doi: 10.1144/SP467.2.

Auld, K.C., Dixon, J.C., 2016. A Classification of Martian Gullies from HiRISE Imagery. Planet. Space Sci. 131, 88–101. https://doi.org/10.1016/j.pss.2016.08.002

Baker, V.R., 2017. Debates-Hypothesis testing in hydrology: Pursuing certainty versus pursuing uberty. Water Resour. Res. 53, 1770–1778. https://doi.org/10.1002/2016WR020078

Baker, V.R., 2014. Terrestrial analogs, planetary geology, and the nature of geological reasoning. Planet. Geol. Field Symp. Kitakyushu Jpn. 2011 Planet. Geol. Terr. Analogs 95, 5–10. https://doi.org/10.1016/j.pss.2012.10.008

Baker, V.R., 2001. Water and the martian landscape. Nature 412, 228–236. https://doi.org/10.1038/35084172

Balme, M., Mangold, N., Baratoux, D., Costard, F., Gosselin, M., Masson, P., Pinet, P., Neukum, G., 2006. Orientation and distribution of recent gullies in the southern hemisphere of Mars: Observations from High Resolution Stereo Camera/Mars Express (HRSC/MEX) and Mars Orbiter Camera/Mars Global Surveyor (MOC/MGS) data. J. Geophys. Res. Planets 111, doi:10.1029/2005JE002607.

Balme, M.R., Gallagher, C.J., Hauber, E., 2013. Morphological evidence for geologically young thaw of ice on Mars: A review of recent studies using high-resolution imaging data. Prog. Phys. Geogr. 37, 289–324. https://doi.org/10.1177/0309133313477123

Barnouin-Jha, O.S., McGovern, A., Buczkowski, D., Seelos, K., Seelos, F., Murchie, S.L., Ehlmann, B.L., CRISM Team, 2008. Martian gullies as seen by the Compact Reconnaissance Imaging Spectrometer for Mars (CRISM), in: American Geophysical Union, Fall Meeting 2008. p. abstract P32B-04.

1352 Barrett, A.M., Balme, M.R., Patel, M.R., Hagermann, A., 2017. Clastic patterned ground in
1353 Lomonosov crater, Mars: examining fracture controlled formation mechanisms. Icarus 295,
1354 125–139. https://doi.org/10.1016/j.icarus.2017.06.008
1355 Bartelt, P., Glover, J., Feistl, T., Bühler, Y., Buser, O., 2012. Formation of levees and en-echelon shear
1356 planes during snow avalanche run-out. J. Glaciol. 58, 980–992.
1357 https://doi.org/10.3189/2012JoG11J011
1358 Benda, L., Dunne, T., 1997. Stochastic Forcing of Sediment Supply to Channel Networks from
1359 Landsliding and Debris Flow. Water Resour. Res. 33, 2849–2863.
1360 https://doi.org/10.1029/97wr02388
1361 Benison, K.C., LaClair, D., Walker, J., 2008. Physical sedimentology experiments with sulfuric acid
1362 solutions: Implications for Mars? Earth Planet. Sci. Lett. 270, 330–337.
1363 Bennett, G.L., Molnar, P., McArdell, B.W., Burlando, P., 2014. A probabilistic sediment cascade
1364 model of sediment transfer in the Illgraben. Water Resour. Res. 50, 1225–1244.
1365 https://doi.org/10.1002/2013WR013806
1366 Berger, A., 1988. Milankovitch Theory and climate. Rev. Geophys. 26, 624–657.
1367 https://doi.org/10.1029/RG026i004p00624
1368 Berman, D.C., Hartmann, W.K., Crown, D.A., Baker, V.R., 2005. The role of arcuate ridges and gullies
1369 in the degradation of craters in the Newton Basin region of Mars. Icarus 178, 465–486.
1370 https://doi.org/10.1016/j.icarus.2005.05.011
1371 Blair, T.C., McPherson, J.G., 2009. Processes and Forms of Alluvial Fans, in: Parsons, A.J., Abrahams,
1372 A.D. (Eds.), Geomorphology of Desert Environments. Springer Netherlands, Dordrecht, pp.
1373 413–467. https://doi.org/10.1007/978-1-4020-5719-9_14
1374 Blair, T.C., McPherson, J.G., 1994. Alluvial Fan Processes and Forms, in: Abrahams, A.D., Parsons, A.J.
1375 (Eds.), Geomorphology of Desert Environments. Springer Netherlands, Dordrecht, pp. 354–
1376 402. https://doi.org/10.1007/978-94-015-8254-4_14
1377 Bridges, N.T., Lackner, C.N., 2006. Northern hemisphere Martian gullies and mantled terrain:
1378 Implications for near-surface water migration in Mars' recent past. J. Geophys. Res. Planets
1379 111, 09014. https://doi.org/10.1029/2006JE002702
1380 Brusnikin, E.S., Kreslavsky, M.A., Zubarev, A.E., Patratiy, V.D., Krasilnikov, S.S., Head, J.W.,
1381 Karachevtseva, I.P., 2016. Topographic measurements of slope streaks on Mars. Icarus 278,
1382 52–61. https://doi.org/10.1016/j.icarus.2016.06.005
1383 Byrne, S., Dundas, C.M., Kennedy, M.R., Mellon, M.T., McEwen, A.S., Cull, S.C., Daubar, I.J., Shean,
1384 D.E., Seelos, K.D., Murchie, S.L., Cantor, B.A., Arvidson, R.E., Edgett, K.S., Reufer, A., Thomas,
1385 N., Harrison, T.N., Posiolova, L. V., Seelos, F.P., 2009. Distribution of mid-latitude ground ice
1386 on Mars from new impact craters. Science 325, 1674–1676.
1387 Cahn, J.W., Dash, J.G., Haiying, F., 1992. Theory of ice premelting in monosized powders. J. Cryst.
1388 Growth 123, 101–108.
1389 Callow, J.N., 2011. Understanding patterns of vegetation degradation at meaningful scales within
1390 saline landscapes. Ecohydrology 4, 841–854. https://doi.org/10.1002/eco.190
1391 Campbell, C.S., 1990. Rapid granular flows. Annu. Rev. Fluid Mech. 22, 57–92.
1392 https://doi.org/10.1146/ annurev.fl .22.010190.000421
1393 Carr, M.H., 1983. Stability of streams and lakes on Mars. Icarus 56, 476–495.
1394 https://doi.org/10.1016/0019-1035(83)90168-9
1395 Carrozzo, F.G., Bellucci, G., Altieri, F., D'Aversa, E., Bibring, J.P., 2009. Mapping of water frost and ice
1396 at low latitudes on Mars. Icarus 203, 406–420.
1397 Cavalli, M., Trevisani, S., Comiti, F., Marchi, L., 2013. Geomorphometric assessment of spatial
1398 sediment connectivity in small Alpine catchments. Sediment Sources Source--Sink Fluxes
1399 Sediment. Budg. 188, 31–41. https://doi.org/10.1016/j.geomorph.2012.05.007
1400 Cedillo-Flores, Y., Durand-Manterola, H.J., Craddock, R.A., 2008. Martian gullies created by
1401 fluidization of dry material, in: Workshop on Martian Gullies: Theories and Tests. p. abstract
1402 8019.

Cedillo-Flores, Y., Treiman, A.H., Lasue, J., Clifford, S.M., 2011. CO2 gas fluidization in the initiation and formation of Martian polar gullies. Geophys. Res. Lett. 38. https://doi.org/10.1029/2011GL049403

Chojnacki, M., McEwen, A., Dundas, C., Ojha, L., Urso, A., Sutton, S., 2016. Geologic context of recurring slope lineae in Melas and Coprates Chasmata, Mars: GEOLOGY OF MELAS AND COPRATES RSL. J. Geophys. Res. Planets 121, 1204–1231. https://doi.org/10.1002/2015JE004991

Chorley, R.J., 1962. Geomorphology and general systems theory (Report No. 500B), Professional Paper.

Christen, M., Bartelt, P., Gruber, U., 2007. RAMMS-a Modeling System for Snow Avalanches, Debris Flows and Rockfalls based on IDL. Photogramm. Fernerkund. GEOINFORMATION 2007, 289.

Christen, M., Kowalski, J., Bartelt, P., 2010. RAMMS: Numerical simulation of dense snow avalanches in three-dimensional terrain. Cold Reg. Sci. Technol. 63, 1–14. https://doi.org/10.1016/j.coldregions.2010.04.005

Christensen, P.R., 2003. Formation of recent martian gullies through melting of extensive water-rich snow deposits. Nature 422, 45–48. https://doi.org/10.1038/nature01436

Christiansen, H.H., 1998. Nivation forms and processes in unconsolidated sediments, NE Greenland. Earth Surf. Process. Landf. 23, 751–760. https://doi.org/10.1002/(SICI)1096-9837(199808)23:8<751::AID-ESP886>3.0.CO;2-A

Clifford, S.M., 1993. A model for the hydrologic and climatic behavior of water on Mars. J. Geophys. Res.-Planets 98, 10973–11016. https://doi.org/10.1029/93je00225

Coe, J.A., Kinner, D.A., Godt, J.W., 2008. Initiation conditions for debris flows generated by runoff at Chalk Cliffs, central Colorado. Geomorphology 96, 270–297.

Conway, S.J., Balme, M.R., 2016. A novel topographic parameterization scheme indicates that martian gullies display the signature of liquid water. Earth Planet. Sci. Lett. 454, 36–45. https://doi.org/10.1016/j.epsl.2016.08.031

Conway, S.J., Balme, M.R., 2014. Decametre-thick remnant glacial ice deposits on Mars. Geophys. Res. Lett. 41, 5402–5409. https://doi.org/10.1002/2014GL060314

Conway, S.J., Balme, M.R., Kreslavsky, M.A., Murray, J.B., Towner, M.C., 2015a. The comparison of topographic long profiles of gullies on Earth to gullies on Mars: A signal of water on Mars. Icarus 253, 189–204. https://doi.org/10.1016/j.icarus.2015.03.009

Conway, S.J., Balme, M.R., Kreslavsky, M.A., Murray, J.B., Towner, M.C., 2015b. The comparison of topographic long profiles of gullies on Earth to gullies on Mars: A signal of water on Mars. Icarus 253, 189–204. https://doi.org/10.1016/j.icarus.2015.03.009

Conway, S.J., Balme, M.R., Lamb, M.P., Towner, M.C., Murray, J.B., 2011a. Enhanced runout and erosion by overland flow under subfreezing and low pressure conditions: experiments and application to Mars. Icarus 211, 443–457. https://doi.org/10.1016/j.icarus.2010.08.026

Conway, S.J., Balme, M.R., Murray, J.B., Towner, M.C., Okubo, C.H., Grindrod, P.M., 2011b. The indication of Martian gully formation processes by slope–area analysis. Geol. Soc. Lond. Spec. Publ. 356, 171–201. https://doi.org/10.1144/SP356.10

Conway, S.J., Butcher, F.E.G., de Haas, T., Deijns, A.J., Grindrod, P.M., Davis, J.M., 2018a. Glacial and gully erosion on Mars: A terrestrial perspective. Geomorphology. https://doi.org/10.1016/j.geomorph.2018.05.019

Conway, S.J., Harrison, T.N., Lewis, S.R., 2018b. Chapter 3: Martian gullies and their connection with the martian climate, in: Soare, R.J., Conway, Susan J., Clifford, S.M. (Eds.), Dynamic Mars: Recent and Current Landscape Evolution of the Red Planet. Elsevier.

Conway, S.J., Harrison, T.N., Soare, R.J., Britton, A., Steele, L., 2017. New Slope-Normalised Global Gully Density and Orientation Maps for Mars. Geol. Soc. Lond. Spec. Publ. 467, in press. https://doi.org/10.1144/SP467.3

Costa, J.E., 1984. Physical geomorphology of debris flows, in: Costa, J.E., Fleisher, P.J. (Eds.), Developments and Applications of Geomorphology. Springer-Verlag, pp. 268–317.

Costard, F., Forget, F., Jomelli, V., Mangold, N., 2007a. Debris flows in Greenland and on Mars, in: Chapman, M. (Ed.), The Geology of Mars: Evidence from Earth-Based Analogs. Cambridge University Press, Cambridge, pp. 265–278.

Costard, F., Forget, F., Mangold, N., Peulvast, J.P., 2002. Formation of recent martian debris flows by melting of near-surface ground ice at high obliquity. Science 295, 110–113. https://doi.org/10.1126/science.1066698

Costard, F., Mangold, N., Baratoux, D., Forget, F., 2007b. Current gullies activity: Dry avalanches at seasonal defrosting as seen on HiRISE images, in: Seventh International Conference on Mars. p. 3133.

de Haas, T., Conway, S.J., Butcher, F.E.G., Levy, J.S., Grindrod, P.M., Balme, M.R., Goudge, T.A., 2018. Time will tell: temporal evolution of Martian gullies and paleoclimatic implications. Geol. Soc. Lond. Spec. Publ. 467, in press. https://doi.org/10.1144/SP467.1

de Haas, T., Conway, S.J., Krautblatter, M., 2015a. Recent (Late Amazonian) enhanced backweathering rates on Mars: paracratering evidence from gully-alcoves? J. Geophys. Res. Planets 120, 2169–2189. https://doi.org/10.1002/2015JE004915

de Haas, T., Hauber, E., Conway, S.J., van Steijn, H., Johnsson, A., Kleinhans, M.G., 2015b. Earth-like aqueous debris-flow activity on Mars at high orbital obliquity in the last million years. Nat. Commun. 6. https://doi.org/10.1038/ncomms8543

de Haas, T., Hauber, E., Kleinhans, M.G., 2013. Local late Amazonian boulder breakdown and denudation rate on Mars. Geophys. Res. Lett. https://doi.org/10.1002/grl.50726

de Haas, T., Kleinhans, M.G., Carbonneau, P.E., Rubensdotter, L., Hauber, E., 2015c. Surface morphology of fans in the high-arctic periglacial environment of Svalbard: Controls and processes. Earth-Sci. Rev. https://doi.org/10.1016/j.earscirev.2015.04.004

de Haas, T., Ventra, D., Carbonneau, P., Kleinhans, M.G., 2014. Debris-flow dominance of alluvial fans masked by runoff reworking and weathering. Geomorphology 217, 165–181. https://doi.org/10.1016/j.geomorph.2014.04.028

de Haas, T., Ventra, D., Hauber, E., Conway, S.J., Kleinhans, M.G., 2015d. Sedimentological analyses of martian gullies: The subsurface as the key to the surface. Icarus 258, 92–108. https://doi.org/10.1016/j.icarus.2015.06.017

Decaulne, A., Sæmundsson, P., 2007. Spatial and temporal diversity for debris-flow meteorological control in subarctic oceanic periglacial environments in Iceland. Earth Surf. Process. Landf. 32, 1971–1983. https://doi.org/10.1002/esp

Decaulne, A., Saemundsson, P., 2006. Meteorological conditions during slush-flow release and their geomorphological impact in northwestern Iceland: A case study from the Bildudalur valley. Geogr Ann Ser -Phys Geogr 88A, 187–197.

Decaulne, A., Sæmundsson, T., Eggertsson, Ó., 2013. A multi-scale resolution of snow-avalanche activity based on geomorphological investigations at Fnjóskadalur, northern Iceland. Polar Rec. 49, 220–229. https://doi.org/10.1017/S0032247412000605

Decaulne, A., Sæmundsson, Þ., 2010. Distribution and frequency of snow-avalanche debris transfer in the distal part of colluvial cones in central north iceland. Geogr. Ann. Ser. Phys. Geogr. 92, 177–187. https://doi.org/10.1111/j.1468-0459.2010.00388.x

Decaulne, A., Saemundsson, Þ., Petursson, O., 2005. Debris flow triggered by rapid snowmelt: A case study in the Gleiðarhjalli area, Northwestern Iceland. Geogr. Ann. 87A, 487–500.

Derjaguin, B. V., Muller, V.M., Toporov, Y.P., 1975. Effect of contact deformations on the adhesion of particles. J. Colloid Interface Sci. 115, 131–143.

Dickson, J.L., 2014. GIS-based quantitative integration of global climate model simulations and geodatabases of gullies on Mars (Masters Thesis). University of Southern California.

Dickson, J.L., Head III, J.W., Levy, J.S., Morgan, G.A., Marchant, D., 2018. Gully Formation in the McMurdo Dry Valleys, Antarctica: Multiple Sources of Water, Temporal Sequence and Relative Importance in Gully Erosion and Deposition Processes. Geol. Soc. Lond. Spec. Publ. 467, in press, doi: 10.1144/SP467.4.

1505 Dickson, J.L., Head, J.W., 2009. The formation and evolution of youthful gullies on Mars: Gullies as
1506 the late-stage phase of Mars' most recent ice age. Icarus 204, 63–86.
1507 Dickson, J.L., Head, J.W., Goudge, T.A., Barbieri, L., 2015. Recent climate cycles on Mars:
1508 Stratigraphic relationships between multiple generations of gullies and the latitude
1509 dependent mantle. Icarus 252, 83–94. https://doi.org/10.1016/j.icarus.2014.12.035
1510 Dickson, J.L., Head, J.W., Kreslavsky, M., 2007. Martian gullies in the southern mid-latitudes of Mars:
1511 Evidence for climate-controlled formation of young fluvial features based upon local and
1512 global topography. Icarus 188, 315–323.
1513 Diniega, S., Byrne, S., Bridges, N.T., Dundas, C.M., McEwen, A.S., 2010. Seasonality of present-day
1514 Martian dune-gully activity. Geology 38, 1047–1050. https://doi.org/10.1130/G31287.1
1515 Diniega, S., Hansen, C.J., McElwaine, J.N., Hugenholtz, C.H., Dundas, C.M., McEwen, A.S., Bourke,
1516 M.C., 2013. A new dry hypothesis for the formation of martian linear gullies. Icarus 225,
1517 526–537. https://doi.org/10.1016/j.icarus.2013.04.006
1518 Diniega, S., Hansen, C.J., Allen, A., Grigsby, N., Li, Z., Perez, T., Chojnacki, M., 2017. Dune-slope
1519 activity due to frost and wind throughout the north polar erg, Mars. Geological Society,
1520 London, Special Publications SP467, in press, doi: 10.1144/SP467.6
1521 Doran, P.T., Forman, S.L., 2000. Ideas about the surface runoff features on Mars. Science 290, 713–
1522 714.
1523 Dundas, C.M., Diniega, S., Hansen, C.J., Byrne, S., McEwen, A.S., 2012. Seasonal activity and
1524 morphological changes in martian gullies. Icarus 220, 124–143.
1525 https://doi.org/10.1016/j.icarus.2012.04.005
1526 Dundas, C.M., Diniega, S., McEwen, A.S., 2015. Long-Term Monitoring of Martian Gully Formation
1527 and Evolution with MRO/HiRISE. Icarus 251, 244–263.
1528 https://doi.org/10.1016/j.icarus.2014.05.013
1529 Dundas, C.M., McEwen, A.S., Chojnacki, M., Milazzo, M.P., Byrne, S., McElwaine, J.N., Urso, A.,
1530 2017a. Granular flows at recurring slope lineae on Mars indicate a limited role for liquid
1531 water. Nat. Geosci. 10, 903–907. https://doi.org/10.1038/s41561-017-0012-5
1532 Dundas, C.M., McEwen, A.S., Diniega, S., Byrne, S., Martinez-Alonso, S., 2010a. New and recent gully
1533 activity on Mars as seen by HiRISE. Geophys. Res. Lett. 37.
1534 https://doi.org/10.1029/2009gl041351
1535 Dundas, C.M., McEwen, A.S., Diniega, S., Hansen, C.J., Byrne, S., McElwaine, J.N., 2017b. The
1536 Formation of Gullies on Mars Today. Geol. Soc. Lond. Spec. Publ. Martian Gullies and their
1537 Earth Analogues 467, doi: 10.1144/SP467.5
1538 Elder, K., Kattelmann, R., 1993. A low-angle slushflow in the Kirgiz Range, Kirgizstan. Permafr.
1539 Periglac. Process. 4, 301–310. https://doi.org/10.1002/ppp.3430040403
1540 Eyles, N., Daurio, L., 2015. Little Ice Age debris lobes and nivation hollows inside Ubehebe Crater,
1541 Death Valley, California: Analog for Mars craters? Geomorphology 245, 231–242.
1542 https://doi.org/10.1016/j.geomorph.2015.05.029
1543 Fan, C., Schulze-Makuch, D., Xie, H., Lu, N., 2009. Investigation of water signatures at gully-exposed
1544 sites on Mars by hyperspectral image analysis. Planet. Space Sci. 57, 93–104.
1545 Félix, G., Thomas, N., 2004. Relation between dry granular flow regimes and morphology of deposits:
1546 Formation of levées in pyroclastic deposits. Earth Planet. Sci. Lett. 221, 197–213.
1547 Forget, F., Haberle, R.M., Montmessin, F., Levrard, B., Head, J.W., 2006. Formation of Glaciers on
1548 Mars by Atmospheric Precipitation at High Obliquity. Science 311, 368–371.
1549 https://doi.org/10.1126/science.1120335
1550 Fouke, B.W., Farmer, J.D., Des Marais, D.J., Pratt, L., Sturchio, N.C., Burns, P.C., Discipulo, M.K., 2000.
1551 Depositional Facies and Aqueous-Solid Geochemistry of Travertine-Depositing Hot Springs
1552 (Angel Terrace, Mammoth Hot Springs, Yellowstone National Park, U.S.A.). J. Sediment. Res.
1553 70, 565. https://doi.org/10.1306/2DC40929-0E47-11D7-8643000102C1865D

1554 Gabet, E.J., 2000. Gopher bioturbation: field evidence for non-linear hillslope diffusion. Earth Surf.
1555 Process. Landf. 25, 1419–1428. https://doi.org/10.1002/1096-
1556 9837(200012)25:13<1419::AID-ESP148>3.0.CO;2-1
1557 Gaidos, E., 2001. Cryovolcanism and the recent flow of liquid water on Mars. Icarus 153, 218–223.
1558 https://doi.org/10.1006/icar.2001.6649
1559 Gallagher, C., Balme, M.R., Conway, S.J., Grindrod, P.M., 2011. Sorted clastic stripes, lobes and
1560 associated gullies in high-latitude craters on Mars: Landforms indicative of very recent,
1561 polycyclic ground-ice thaw and liquid flows. Icarus 211, 458–471.
1562 https://doi.org/10.1016/j.icarus.2010.09.010
1563 Gallagher, C.J., Balme, M.R., 2011. Landforms indicative of ground-ice thaw in the northern high
1564 latitudes of Mars. Geol. Soc. Lond. Spec. Publ. 356, 87–110. https://doi.org/10.1144/SP356.6
1565 Gardin, E., Allemand, P., Quantin, C., Thollot, P., 2010. Defrosting, dark flow features, and dune
1566 activity on Mars: Example in Russell crater. J Geophys Res 115, doi:10.1029/2009JE003515.
1567 https://doi.org/10.1029/2009je003515
1568 Gardner, J.V., Dartnell, P., 2002. Multibeam Mapping of the Los Angeles, California Margin (Open-
1569 File Report No. 02–162). U.S. Geological Survey.
1570 Gauer, P., Lied, K., Kristensen, K., 2008. On avalanche measurements at the Norwegian full-scale
1571 test-site Rvggfonn. Cold Reg. Sci. Technol. 51, 138–155.
1572 https://doi.org/10.1016/j.coldregions.2007.05.005
1573 Ghatan, G.J., Head III, J.W., 2002. Candidate subglacial volcanoes in the south polar region of Mars:
1574 Morphology, morphometry, and eruption conditions. J. Geophys. Res. 107.
1575 https://doi.org/10.1029/2001JE001519
1576 Gilmore, M.S., Phillips, E.L., 2002. Role of aquicludes in formation of Martian gullies. Geology 30,
1577 1107–1110.
1578 Godt, J.W., Coe, J.A., 2007. Alpine debris flows triggered by a 28 July 1999 thunderstorm in the
1579 central Front Range, Colorado. Geomorphology 84, 80–97.
1580 Grasby, S.E., Proemse, B.C., Beauchamp, B., 2014. Deep groundwater circulation through the High
1581 Arctic cryosphere forms Mars-like gullies. Geology 42, 651–654.
1582 https://doi.org/10.1130/G35599.1
1583 Grimm, R.E., Harrison, K.P., Stillman, D.E., 2014. Water budgets of martian recurring slope lineae.
1584 Icarus 233, 316–327. https://doi.org/10.1016/j.icarus.2013.11.013
1585 Grotzinger, J.P., Hayes, A.G., Lamb, M.P., McLennan, S.M., 2013. Sedimentary processes on Earth,
1586 Mars, Titan, and Venus. Comp. Climatol. Terr. Planets 1, 439–472.
1587 Gueugneau, V., Kelfoun, K., Roche, O., Chupin, L., 2017. Effects of pore pressure in pyroclastic flows:
1588 Numerical simulation and experimental validation. Geophys. Res. Lett. 44, 2194–2202.
1589 https://doi.org/10.1002/2017GL072591
1590 Gulick, G., Glines, N., Hart, S., Freeman, P., 2018. Geomorphological Analysis of Gullies on the Central
1591 Peak of Lyot Crater, Geol. Soc. Lond. Spec. Publ., Martian Gullies and their Earth Analogues
1592 467, in review
1593 Haberle, R.A., Murphy, J.R., Schaeffer, J., 2003. Orbital change experiments with a Mars general
1594 circulation model. Icarus 161, 66–89.
1595 Haberle, R.M., Mckay, C.P., Schaeffer, J., Cabrol, N.A., Grin, E.A., Zent, A.P., Quinn, R., 2001. On the
1596 possibility of liquid water on present-day Mars. J. Geophys. Res. 106, 23317–23326.
1597 https://doi.org/10.1029/2000JE001360
1598 Hack, J.T., 1957. Studies of longitudinal stream profiles in Virginia and Maryland. US Geol. Surv. Prof.
1599 Pap. 294-B, 45–97.
1600 Hansen, C.J., Bourke, M., Bridges, N.T., Byrne, S., Colon, C., Diniega, S., Dundas, C., Herkenhoff, K.,
1601 McEwen, A., Mellon, M., Portyankina, G., Thomas, N., 2011. Seasonal erosion and
1602 restoration of Mars' northern polar dunes. Science 331, 575–578.
1603 https://doi.org/10.1126/science.1197636

1604 Harris, K.J., Carey, A.E., Lyons, W.B., Welch, K.A., Fountain, A.G., 2007. Solute and isotope
1605 geochemistry of subsurface ice melt seeps in Taylor Valley, Antarctica. Geol Soc Am Bull 119,
1606 548–555.
1607 Harrison, T.N., 2016. Martian Gully Formation and Evolution: Studies From the Local to Global Scale
1608 (Ph D). Western University, London, Ontario.
1609 Harrison, T.N., Malin, M.C., Edgett, K.S., 2009. Present-day gully activity observed by the Mars
1610 Reconnaissance Orbiter (MRO) Context Camera (CTX), in: Bulletin of the American
1611 Astronomical Society, DPS Meeting #41. p. 1113.
1612 Harrison, T.N., Osinski, G.R., Tornabene, L.L., 2015. Global Documentation of Gullies With the Mars
1613 Reconnaissance Orbiter Context Camera (CTX) and Implications for Their Formation. Icarus
1614 252, 236–254. http://dx.doi.org/10.1016/j.icarus.2015.01.022
1615 Harrison, T.N., Tornabene, L.L., Osinski, G.R., Conway, S.J., 2017. Thermal inertia variations from
1616 gully and mass-wasting activity in Gasa crater, Mars. Geological Society, London, Special
1617 Publications SP467, in press, doi: 10.1144/SP467.8
1618 Hartmann, W.K., Ansan, V., Berman, D.C., Mangold, N., Forget, F., 2014. Comprehensive analysis of
1619 glaciated martian crater Greg. Icarus 228, 96–120.
1620 https://doi.org/10.1016/j.icarus.2013.09.016
1621 Hartmann, W.K., Thorsteinsson, T., Sigurdsson, F., 2003. Martian hillside gullies and Icelandic
1622 analogs. Icarus 162, 259–277. https://doi.org/10.1016/S0019-1035(02)00065-9
1623 Hauber, E., Preusker, F., Trauthan, F., Reiss, D., Carlsson, A.E., Hiesinger, H., Jaumann, R., Johansson,
1624 H.A.B., Johansson, L., Johnsson, A., McDaniel, S., Olvmo, M., Zanetti, M., 2009. Morphometry
1625 of Alluvial Fans in a Polar Desert (Svalbard, Norway): Implications for Interpreting Martian
1626 Fans. Lunar Planet. Sci. Conf. 40, 1658.
1627 Hauber, E., Reiss, D., Ulrich, M., Preusker, F., Trauthan, F., Zanetti, M., Hiesinger, H., Jaumann, R.,
1628 Johansson, L., Johnsson, A., Olvmo, M., Carlsson, E., Johansson, H.A.B., McDaniel, S., 2011a.
1629 Periglacial landscapes on Svalbard: Terrestrial analogs for cold-climate landforms on Mars.
1630 Geol. Soc. Am. Spec. Pap. 483, 177–201. https://doi.org/10.1130/2011.2483(12)
1631 Hauber, E., Reiss, D., Ulrich, M., Preusker, F., Trauthan, F., Zanetti, M., Hiesinger, H., Jaumann, R.,
1632 Johansson, L., Johnsson, A., Van Gasselt, S., Olvmo, M., 2011b. Landscape evolution in
1633 Martian mid-latitude regions: insights from analogous periglacial landforms in Svalbard.
1634 Geol. Soc. Lond. Spec. Publ. 356, 111–131. https://doi.org/10.1144/SP356.7
1635 Hauber, E., Sassenroth, C., de Vera, J.-P.P., Schmitz, N., Jaumann, R., Reiss, D., Hiesinger, H.,
1636 Johnsson, A., 2018. Debris Flows and Water Tracks in Northern Victoria Land, Continental
1637 East Antarctica: A New Terrestrial Analogue Site for Gullies and Recurrent Slope Lineae on
1638 Mars. Geol. Soc. Lond. Spec. Publ. 467, in press, doi:10.1144/SP467.12.
1639 Head, J.W., Marchant, D.R., Kreslavsky, M.A., 2008. Formation of gullies on Mars: Link to recent
1640 climate history and insolation microenvironments implicate surface water flow origin. Proc.
1641 Natl. Acad. Sci. U. S. A. 105, 13258–13263. https://doi.org/10.1073/pnas.0803760105
1642 Head, J.W., Mustard, J.F., Kreslavsky, M.A., Milliken, R.E., Marchant, D.R., 2003. Recent ice ages on
1643 Mars. Nature 426, 797–802. https://doi.org/10.1038/nature02114
1644 Hecht, M., 2002. Metastability of liquid water on Mars. Icarus 156, 373–386.
1645 https://doi.org/10.1006/icar.2001.6794
1646 Heckmann, T., Schwanghart, W., 2013. Geomorphic coupling and sediment connectivity in an alpine
1647 catchment — Exploring sediment cascades using graph theory. Geomorphology 182, 89–
1648 103. https://doi.org/10.1016/j.geomorph.2012.10.033
1649 Heldmann, J.L., 2005. Formation of Martian gullies by the action of liquid water flowing under
1650 current Martian environmental conditions. J. Geophys. Res. 110, E05004.
1651 https://doi.org/10.1029/2004JE002261
1652 Heldmann, J.L., Carlsson, E., Johansson, H., Mellon, M.T., Toon, O.B., 2007. Observations of martian
1653 gullies and constraints on potential formation mechanisms II. The northern hemisphere.
1654 Icarus 188, 324–344. https://doi.org/10.1016/j.icarus.2006.12.010

Heldmann, J.L., Conley, C., Brown, A.J., Fletcher, L., Bishop, J.L., McKay, C.P., 2010. Possible Liquid Water Origin for Atacama Desert Mudflow and Recent Gully Deposits on Mars. Icarus 206, 685–690.
Heldmann, J.L., Mellon, M.T., 2004. Observations of martian gullies and constraints on potential formation mechanisms. Icarus 168, 285–304.
Heldmann, J.L., Toon, O.B., Pollard, W.H., Mellon, M.T., Pitlick, J., McKay, C.P., Andersen, D.T., 2005. Formation of Martian gullies by the action of liquid water flowing under current Martian environmental conditions. J Geophys Res-Planets 110, doi:10.1029/2004JE002261.
Herny, C., Conway, S.J., Raack, J., Carpy, S., Patel, M.R., Colle-Banse, T., 2018. Unstable liquid water as a geomorphological agent in martian gullies: experimental investigation of the effect of boiling intensity on downslope sediment transport. Geol. Soc. Lond. Spec. Publ., Martian Gullies and their Earth Analogues 467, in press, doi:10.1144/SP467.10
Hesse, M.B., 1966. Models and Analogies in Science. University of Notre Dame Press, Notre Dame, IN.
Hétu, B., Fortin, G., Dubé, J., Boucher, D., Buffin-Bélanger, T., Gagnon, J.-P., 2017. Les conditions nivologiques et hydro-météorologiques propices au déclenchement des coulées de slush: l'exemple du Québec (Canada). Climatologie.
Hétu, B., Gray, J.T., 2000. Effects of environmental change on scree slope development throughout the postglacial period in the Chic-Choc Mountains in the northern Gaspé Peninsula, Québec. Geomorphology 335–355.
Hétu, B., Van Steijn, H., Vandelac, P., 1994. Les coulées de pierres glacées : un nouveau type de coulées de pierraille sur les talus d'éboulis. Géographie Phys. Quat. 48, 3–22. https://doi.org/10.7202/032969ar
Hétu, B., Vandelac, P., 1989. La dynamique des éboulis schisteux au cours de l'hiver, Gaspésie septentrionale, Québec. Géographie Phys. Quat. 43, 389–406.
Hillier, J.K., Sofia, G., Conway, S.J., 2015. Perspective – synthetic DEMs: A vital underpinning for the quantitative future of landform analysis? Earth Surf Dynam 3, 587–598. https://doi.org/10.5194/esurf-3-587-2015
Hobbs, S.W., Paull, D.J., Clarke, J.D.A., 2017. Testing the water hypothesis: Quantitative morphological analysis of terrestrial and martian mid-latitude gullies. Geomorphology 295, 705–721. https://doi.org/10.1016/j.geomorph.2017.08.021
Hobbs, S.W., Paull, D.J., Clarke, J.D.A., 2015. Analysis of regional gullies within Noachis Terra, Mars: A complex relationship between slope, surface material and aspect. Icarus 250, 308–331. https://doi.org/10.1016/j.icarus.2014.12.011
Hobbs, S.W., Paull, D.J., Clarke, J.D.A., 2014. A hydrological analysis of terrestrial and Martian gullies: Implications for liquid water on Mars. Geomorphology 226, 261–277. https://doi.org/10.1016/j.geomorph.2014.07.034
Hobbs, S.W., Paull, D.J., Clarke, J.D.A., 2013. The influence of slope morphology on gullies: Terrestrial gullies in Lake George as analogues for Mars. Planet. Space Sci. 81, 1–17. https://doi.org/10.1016/j.pss.2012.10.009
Hobbs, S.W., Paull, D.J., Clarke, J.D.A., Roach, I.C., 2016. Multi-agent gully processes: Evidence from the Monaro Volcanic Province, Australia and in Terra Cimmeria, Mars. Geomorphology 257, 23–46. https://doi.org/10.1016/j.geomorph.2015.12.018
Hoffman, N., 2002. Active polar gullies on Mars and the role of carbon dioxide. Astrobiology 2, 313–323. https://doi.org/10.1089/153110702762027899
Hoffman, N., 2000. Ideas about the surface runoff features on Mars. Science 290, 711–711.
Hooper, D.M., Dinwiddie, C.L., 2014. Debris flows on the Great Kobuk Sand Dunes, Alaska: Implications for analogous processes on Mars. Icarus 230, 15–28. https://doi.org/10.1016/j.icarus.2013.07.006
Howard, A.D., 2007. Simulating the development of Martian highland landscapes through the interaction of impact cratering, fluvial erosion, and variable hydrologic forcing.

Geomorphology, 38th Binghamton Geomorphology Symposium: Complexity in Geomorphology 91, 332–363. https://doi.org/10.1016/j.geomorph.2007.04.017
Hubbard, B., Milliken, R.E., Kargel, J.S., Limaye, A., Souness, C., 2011. Geomorphological characterisation and interpretation of a mid-latitude glacier-like form: Hellas Planitia, Mars. Icarus 211, 330–346. https://doi.org/10.1016/j.icarus.2010.10.021
Hubbard, B., Souness, C., Brough, S., 2014. Glacier-like forms on Mars. The Cryosphere 8, 2047–2061. https://doi.org/10.5194/tc-8-2047-2014
Hugenholtz, C.H., 2008a. Frosted granular flow: A new hypothesis for mass wasting in martian gullies. Icarus 197, 65–72. https://doi.org/10.1016/j.icarus.2008.04.010
Hugenholtz, C.H., 2008b. Frosted granular flow: A new hypothesis for mass wasting in martian gullies. Icarus 197, 65–72. https://doi.org/10.1016/j.icarus.2008.04.010
Hugenholtz, C.H., Wolfe, S.A., Moorman, B.J., 2007. Sand–water flows on cold-climate eolian dunes: environmental analogs for the eolian rock record and Martian sand dunes. J. Sediment. Res. 77, 607–614. https://doi.org/10.2110/jsr.2007.063
Hutter, K., Wang, Y., Pudasaini, S.P., 2005. The Savage-Hutter avalanche model: How far can it be pushed? Philos. Transact. A Math. Phys. Eng. Sci. 363, 1507–1528. https://doi.org/10.1098/rsta.2005.1594
Ishii, T., Sasaki, S., 2004. Formation of recent martian gullies by avalanches of CO2 frost, in: Lunar and Planetary Science XXXV. p. abstract #1556. https://doi.org/10.1029/2002JE001900.Figure
Iverson, R.M., 2014. Debris flows: behaviour and hazard assessment. Geol. Today 30, 15–20. https://doi.org/10.1111/gto.12037
Iverson, R.M., 1997. The physics of debris flows. Rev Geophys 35, 245–296.
Iverson, R.M., George, D.L., 2014. A depth-averaged debris-flow model that includes the effects of evolving dilatancy. I. Physical basis. Proc. R. Soc. Math. Phys. Eng. Sci. 470. https://doi.org/10.1098/rspa.2013.0819
Jackson, L.E., Kostaschuk, R.A., MacDonald, G.M., 1987. Identification of debris flow hazard on alluvial fans in the Canadian Rocky Mountains. Rev. Eng. Geol. 7, 115–124. https://doi.org/10.1130/REG7-p115
Jakosky, B.M., Barker, E.S., 1984. Comparison of ground-based and Viking Orbiter measurements of Martian water vapor: Variability of the seasonal cycle. Icarus 57, 322–334. https://doi.org/10.1016/0019-1035(84)90121-0
Jakosky, B.M., Farmer, C.B., 1982. The seasonal and global behavior of water vapor in the Mars atmosphere: Complete global results of the Viking atmospheric water detector experiment. J. Geophys. Res. 87, 2999–3019. https://doi.org/10.1029/JB087iB04p02999
Johnson, K.L., Kendall, K., Roberts, A.D., 1971. Surface energy and the contact of elastic solids. Proc. R. Soc. Math. Phys. Eng. Sci. 324, 301–313. https://doi.org/10.1098/rspa.1971.0141
Johnsson, A., Conway, S.J., Reiss, D., Hiesinger, H., Hauber, E., 2018. Slow periglacial mass wasting (solifluction) on Mars, in: Soare, R.J., Conway, S.J., Clifford, S.M. (Eds.), Dynamic Mars. Elsevier.
Johnsson, A., Reiss, D., Hauber, E., Hiesinger, H., Zanetti, M., 2014. Evidence for very recent melt-water and debris flow activity in gullies in a young mid-latitude crater on Mars. Icarus 235, 37–54. https://doi.org/10.1016/j.icarus.2014.03.005
Johnsson, A., Reiss, D., Hauber, E., Zanetti, M., Hiesinger, H., Johansson, L., Olvmo, M., 2012. Periglacial mass-wasting landforms on Mars suggestive of transient liquid water in the recent past: Insights from solifluction lobes on Svalbard. Icarus 218, 489–505. https://doi.org/10.1016/j.icarus.2011.12.021
Jones, E., Caprarelli, G., Mills, P.F., Doran, B., Clarke, J., 2014. An Alternative Approach to Mapping Thermophysical Units from Martian Thermal Inertia and Albedo Data Using a Combination of Unsupervised Classification Techniques. Remote Sens. 6. https://doi.org/10.3390/rs6065184

1756 Jouannic, G., Gargani, J., Conway, S.J., Costard, F., Balme, M.R., Patel, M.R., Massé, M., Marmo, C.,
1757 Jomelli, V., Ori, G.G., 2015. Laboratory simulation of debris flows over sand dunes: Insights
1758 into gully-formation (Mars). Geomorphology 231, 101–115.
1759 https://doi.org/10.1016/j.geomorph.2014.12.007
1760 Jouannic, G., Gargani, J., Conway, S.J., Costard, F., Massé, M., Bourgeois, O., Carter, J., Schmidt, F.,
1761 Marmo, C., Ori, G.G., Nachon, M., Pasquon, K., 2017. Morphological characterization of
1762 landforms produced by springtime seasonal activity on Russell dune (Mars). Geol. Soc. Lond.
1763 Spec. Publ., Martian Gullies and their Earth Analogues 467, in review.
1764 Jouannic, G., Gargani, J., Costard, F., Ori, G.G., Marmo, C., Schmidt, F., Lucas, A., 2012. Morphological
1765 and mechanical characterization of gullies in a periglacial environment: The case of the
1766 Russell crater dune (Mars). Planet. Space Sci. 71, 38–54.
1767 https://doi.org/10.1016/j.pss.2012.07.005
1768 Julien, P.Y., 2010. Erosion and sedimentation. Cambridge University Press.
1769 Kenkmann, T., Poelchau, M.H., Wulf, G., 2014. Structural geology of impact craters. J. Struct. Geol.
1770 62, 156–182. https://doi.org/10.1016/j.jsg.2014.01.015
1771 Kereszturi, A., Appéré, T., 2014. Searching for springtime zonal liquid interfacial water on Mars.
1772 Icarus 238, 66–76. https://doi.org/10.1016/j.icarus.2014.05.001
1773 Kereszturi, A., Möhlmann, D., Berczi, S., Ganti, T., Kuti, A., Sik, A., Horvath, A., 2009. Recent rheologic
1774 processes on dark polar dunes of Mars: Driven by interfacial water? Icarus 201, 492–503.
1775 Kereszturi, A., Rivera-Valentin, E.G., 2012. Locations of thin liquid water layers on present-day Mars.
1776 Icarus 221, 289–295. https://doi.org/10.1016/j.icarus.2012.08.004
1777 Kieffer, H.H., Christensen, P.R., Titus, T.N., 2006. CO2 jets formed by sublimation beneath
1778 translucent slab ice in Mars' seasonal south polar ice cap. Nature 442, 793–796.
1779 https://doi.org/10.1038/nature04945
1780 Kleinhans, M.G., Markies, H., de Vet, S.J., in 't Veld, A.C., Postema, F.N., 2011. Static and dynamic
1781 angles of repose in loose granular materials under reduced gravity. J. Geophys. Res. Planets
1782 116, doi:10.1029/2011JE003865. https://doi.org/10.1029/2011JE003865
1783 Knauth, L.P., Klonowski, S., Burt, D., 2000. Ideas about the surface runoff features on Mars. Science
1784 290, 711–712.
1785 Kneissl, T., Reiss, D., Gasselt, S. van, Neukum, G., 2009. Northern-Hemisphere Gullies on Mars --
1786 Distribution and Orientation from the Evaluation of HRSC and MOC-NA Data. Lunar Planet.
1787 Sci. Conf. 40, no. 1590.
1788 Kochel, R.C., Trop, J.M., 2008. Earth analog for high-latitude landforms and recent flows on Mars: Icy
1789 debris fans in the Wrangell Volcanic Field, Alaska. Icarus 196, 63–77.
1790 Kokelaar, B.P., Bahia, R.S., Joy, K.H., Viroulet, S., Gray, J.M.N.T., 2017. Granular avalanches on the
1791 Moon: Mass-wasting conditions, processes, and features. J. Geophys. Res. Planets 122,
1792 1893–1925. https://doi.org/10.1002/2017JE005320
1793 Kokelaar, B.P., Graham, R.L., Gray, J.M.N.T., Vallance, J.W., 2014. Fine-grained linings of leveed
1794 channels facilitate runout of granular flows. Earth Planet. Sci. Lett. 385, 172–180.
1795 https://doi.org/10.1016/j.epsl.2013.10.043
1796 Kolb, K.J., McEwen, A.S., Pelletier, J.D., 2010a. Investigating gully flow emplacement mechanisms
1797 using apex slopes. Icarus 208, 132–142.
1798 Kolb, K.J., Pelletier, J.D., McEwen, A.S., 2010. Modeling the formation of bright slope deposits
1799 associated with gullies in Hale Crater, Mars: Implications for recent liquid water. Icarus 205,
1800 113–137.
1801 Komatsu, G., Senthil Kumar, P., Goto, K., Sekine, Y., Giri, C., Matsui, T., 2014. Drainage systems of
1802 Lonar Crater, India: Contributions to Lonar Lake hydrology and crater degradation. Planet.
1803 Space Sci. 95, 45–55. https://doi.org/10.1016/j.pss.2013.05.011
1804 Kossacki, K.J., Markiewicz, W.J., 2014. Seasonal flows on dark martian slopes, thermal condition for
1805 liquescence of salts. Icarus 233, 126–130. https://doi.org/10.1016/j.icarus.2014.01.032

1806 Kossacki, K. J., Markiewicz, W.J., 2004. Seasonal melting of surface water ice condensing in martian
1807 gullies. Icarus 171, 272–283.
1808 Kossacki, Konrad J., Markiewicz, W.J., 2004. Seasonal melting of surface water ice condensing in
1809 martian gullies. Icarus 171, 272–283. https://doi.org/10.1016/j.icarus.2004.05.018
1810 Kreslavsky, M.A., Head, J.W., 2002. Mars: Nature and evolution of young latitude-dependent water-
1811 ice-rich mantle. Geophys. Res. Lett. 29, 14–1. https://doi.org/10.1029/2002GL015392
1812 Kreslavsky, M.A., Head, J.W., 2000. Kilometer-scale roughness of Mars: Results from MOLA data
1813 analysis. J. Geophys. Res. 105, 26695–26712. https://doi.org/10.1029/2000JE001259
1814 Kreslavsky, M.A., Head, J.W., Marchant, D.R., 2008. Periods of active permafrost layer formation
1815 during the geological history of Mars: Implications for circum-polar and mid-latitude surface
1816 processes. Planet. Space Sci. 56, 289–302. https://doi.org/10.1016/j.pss.2006.02.010
1817 Kuhn, N., 2014. Experiments in Reduced Gravity: Sediment Settling on Mars. Elsevier.
1818 Kumar, P.S., Head, J.W., Kring, D.A., 2010. Erosional modification and gully formation at Meteor
1819 Crater, Arizona: Insights into crater degradation processes on Mars. Icarus 208, 608–620.
1820 Kuzmin, R.O., Zabalueva, E.V., Christensen, R.R., 2009. Estimation and mapping of wintertime
1821 increase in water ice content of the martian surface soil based on seasonal thermal emission
1822 spectrometer thermal inertia variations. J. Geophys. Res. E Planets 114,
1823 doi:10.1029/2008JE003222.
1824 Lague, D., Davy, P., 2003. Constraints on the long-term colluvial erosion law by analyzing slope-area
1825 relationships at various uplift rates in the Siwaliks Hills (Nepal). J. Geophys. Res. B Solid Earth
1826 108, doi:10.1029/2002JB001893.
1827 Landis, G.A., 2007. Observation of frost at the equator of Mars by the Opportunity rover, in: 38th
1828 Annual Lunar and Planetary Science Conference. Clear Lake, TX, p. abstract 2433.
1829 Lanza, N.L., Meyer, G. a., Okubo, C.H., Newsom, H.E., Wiens, R.C., 2010. Evidence for debris flow
1830 gully formation initiated by shallow subsurface water on Mars. Icarus 205, 103–112.
1831 https://doi.org/10.1016/j.icarus.2009.04.014
1832 Lapotre, M.G.A., Lamb, M.P., McElroy, B., 2017. What sets the size of current ripples? Geology 45,
1833 243–246.
1834 Larocque, S.J., Hétu, B., Filion, L., 2001. Geomorphic and dendroecological impacts of slushflows in
1835 central gaspé peninsula (québec, canada). Geogr. Ann. Ser. Phys. Geogr. 83, 191–201.
1836 https://doi.org/10.1111/j.0435-3676.2001.00154.x
1837 Laskar, J., Correia, A.C.M., Gastineau, M., Joutel, F., Levrard, B., Robutel, P., 2004. Long term
1838 evolution and chaotic diffusion of the insolation quantities of Mars. Icarus 170, 343–364.
1839 https://doi.org/10.1016/j.icarus.2004.04.005
1840 Laskar, J., Robutel, P., 1993. The chaotic obliquity of the planets. Nature 361, 608–612.
1841 https://doi.org/10.1038/361608a0
1842 Laute, K., Beylich, A.A., 2013. Holocene hillslope development in glacially formed valley systems in
1843 Nordfjord, western Norway. Sediment Sources Source--Sink Fluxes Sediment. Budg. 188, 12–
1844 30. https://doi.org/10.1016/j.geomorph.2012.11.021
1845 Lee, P., Cockell, C.S., Marinova, M.M., McKay, C.P., J. W. Rice, J., 2001. Snow and Ice Melt Flow
1846 Features on Devon Island, Nunavut, Arctic Canada as Possible Analogs for Recent Slope Flow
1847 Features on Mars. Lunar Planet. Sci. Conf. 32, no. 1809.
1848 Lee, P., Cockell, C.S., McKay, C.P., 2004. Gullies on Mars: Origin by Snow and Ice Melting and
1849 Potential for Life Based on Possible Analogs from Devon Island, High Arctic. Lunar Planet. Sci.
1850 Conf. 35, no. 2122.
1851 Lee, P., Glass, B.J., Osinski, G.R., Parnell, J., Schutt, J.W., McKay, C.P., 2006. Gullies on Mars: Fresh
1852 Gullies in Dirty Snow, Devon Island, High Arctic, as End-Member Analogs. Lunar Planet. Sci.
1853 Conf. 37, no. 1818.
1854 Lee, P., McKay, C.P., Matthews, J., 2002. Gullies on Mars: Clues to their formation timescale from
1855 possible analogs from Devon Island, Nunavut, Arctic Canada. Lunar Planet. Sci. XXXIII
1856 abstract 2050.

1857 Levy, J., 2015. A hydrological continuum in permafrost environments: The morphological signatures
1858 of melt-driven hydrology on Earth and Mars. Geomorphology 240, 70–82.
1859 https://doi.org/10.1016/j.geomorph.2014.02.033
1860 Levy, J.S., Fassett, C.I., Head, J.W., Schwartz, C., Watters, J.L., 2014. Sequestered glacial ice
1861 contribution to the global Martian water budget: Geometric constraints on the volume of
1862 remnant, midlatitude debris-covered glaciers. J. Geophys. Res. Planets 119, 2014JE004685.
1863 https://doi.org/10.1002/2014JE004685
1864 Levy, J.S., Fountain, A.G., Gooseff, M.N., Welch, K.A., Lyons, W.B., 2011. Water tracks and
1865 permafrost in Taylor Valley, Antarctica: Extensive and shallow groundwater connectivity in a
1866 cold desert ecosystem. Geol. Soc. Am. Bull. 123, 2295–2311.
1867 Levy, J.S., Head, J.W., Dickson, J.L., Fassett, C.I., Morgan, G.A., Schon, S.C., 2010. Identification of
1868 gully debris flow deposits in Protonilus Mensae, Mars: Characterization of a water-bearing,
1869 energetic gully-forming process. Earth Planet. Sci. Lett., Mars Express after 6 Years in Orbit:
1870 Mars Geology from Three-Dimensional Mapping by the High Resolution Stereo Camera
1871 (HRSC) Experiment 294, 368–377. https://doi.org/10.1016/j.epsl.2009.08.002
1872 Levy, J.S., Head, J.W., Marchant, D.R., Dickson, J.L., Morgan, G.A., 2009. Geologically recent gully-
1873 polygon relationships on Mars: Insights from the Antarctic dry valleys on the roles of
1874 permafrost, microclimates, and water sources for surface flow. Icarus 201, 113–126.
1875 https://doi.org/10.1016/j.icarus.2008.12.043
1876 Levy, J.S., Head, J.W., Marchant, D.R., Morgan, G.A., Dickson, J.L., 2007. Gully Surface and Shallow
1877 Subsurface Structure in the South Fork of Wright Valley, Antarctic Dry Valleys: Implications
1878 for Gully Activity on Mars. Lunar Planet. Sci. Conf. 38, no. 1728.
1879 Lipman, P.W., Mullineaux, D.R., 1981. The 1980 eruptions of Mount St. Helens, Washington (Report
1880 No. 1250), Professional Paper.
1881 Luckman, B.H., 1992. Debris flows and snow avalanches landforms in the Lairig Ghru, Cairngorm
1882 Mountains, Scotland. Geogr. Ann. Ser. -Phys. Geogr. 74, 109–121.
1883 Lyons, W.B., Welch, K.A., Carey, A.E., Doran, P.T., Wall, D.H., Virginia, R.A., Fountain, A.G., Csatho,
1884 B.M., Tremper, C.M., 2005. Groundwater seeps in Taylor Valley Antarctica: an example of a
1885 subsurface melt event. Ann. Glaciol. 40, 200–206.
1886 Madeleine, J.-B., Head, J.W., Forget, F., Navarro, T., Millour, E., Spiga, A., Colaïtis, A., Määttänen, A.,
1887 Montmessin, F., Dickson, J.L., 2014. Recent Ice Ages on Mars: The role of radiatively active
1888 clouds and cloud microphysics. Geophys. Res. Lett. https://doi.org/10.1002/2014GL059861
1889 Malin, M.C., Edgett, K.S., 2000. Evidence for recent groundwater seepage and surface runoff on
1890 Mars. Science 288, 2330–2335. https://doi.org/10.1126/science.288.5475.2330
1891 Malin, M.C., Edgett, K.S., Posiolova, L. V, Mccolley, S.M., Dobrea, E.Z.N., 2006. Present-day impact
1892 cratering rate and contemporary gully activity on Mars. Science 314, 1573–1577.
1893 Mangold, N., 2005. High latitude patterned grounds on Mars: Classification, distribution and climatic
1894 control. Mars Polar Sci. III 174, 336–359. https://doi.org/10.1016/j.icarus.2004.07.030
1895 Mangold, N., 2003a. Geomorphic analysis of lobate debris aprons on Mars at Mars Orbiter Camera
1896 scale: Evidence for ice sublimation initiated by fractures. J Geophys Res 108, 8021.
1897 https://doi.org/10.1029/2002JE001885
1898 Mangold, N., 2003b. Debris flows over sand dunes on Mars: Evidence for liquid water. J. Geophys.
1899 Res. 108. https://doi.org/10.1029/2002JE001958
1900 Mangold, N., Mangeney, A., Migeon, V., Ansan, V., Lucas, A., Baratoux, D., Bouchut, F., 2010. Sinuous
1901 gullies on Mars: Frequency, distribution, and implications for flow properties. J Geophys Res
1902 115, doi:10.1029/2009je003540. https://doi.org/10.1029/2009je003540
1903 Mao, L., Cavalli, M., Comiti, F., Marchi, L., Lenzi, M.A., Arattano, M., 2009. Sediment transfer
1904 processes in two Alpine catchments of contrasting morphological settings. J. Hydrol. 364,
1905 88–98.
1906 Marchant, D.R., Head, J.W., 2007. Antarctic dry valleys: Microclimate zonation, variable geomorphic
1907 processes, and implications for assessing climate change on Mars. Icarus 192, 187–222.

1908 Marquez, A., de Pablo, M.A., Oyarzun, R., Viedma, C., 2005. Evidence of gully formation by regional
1909 groundwater flow in the Gorgonum-Newton region (Mars). Icarus 179, 398–414.
1910 Maruyama, M., Bienfait, M., Dash, J.G., Coddens, G., 1992. Interfacial melting of ice in graphite and
1911 talc powders. J. Cryst. Growth 118.
1912 Massé, M., Beck, P., Schmitt, B., Pommerol, A., McEwen, A., Chevrier, V., Brissaud, O., Séjourné, A.,
1913 2014. Spectroscopy and detectability of liquid brines on mars. Planet. Space Sci. 92, 136–
1914 149. https://doi.org/10.1016/j.pss.2014.01.018
1915 Massé, M., Conway, S.J., Gargani, J., Patel, M.R., Pasquon, K., McEwen, A.S., Carpy, S., Chevrier, V.,
1916 Balme, M.R., Ojha, L., Vincendon, M., Poulet, F., Jouannic, G., 2016. Transport processes
1917 induced by metastable boiling water under Martian surface conditions. Nat. Geosci. 9, 425–
1918 428. https://doi.org/10.1038/ngeo2706
1919 Matsuoka, N., Murton, J., 2008. Frost weathering: Recent advances and future directions. Permafr.
1920 Periglac. Process. 19, 195–210. https://doi.org/10.1002/ppp.620
1921 Mayhew, S., 2015. A dictionary of geography. Oxford University Press, USA.
1922 Mc Keown, L.E., Bourke, M.C., McElwaine, J.N., 2017. Experiments On Sublimating Carbon Dioxide
1923 Ice And Implications For Contemporary Surface Processes On Mars. Sci. Rep. 7, 14181.
1924 https://doi.org/10.1038/s41598-017-14132-2
1925 McClung, D., Schaerer, P.A., 2006. The Avalanche Handbook: 3rd Edition. The Mountaineers Books,
1926 Seattle.
1927 McEwen, A.S., Dundas, C.M., Mattson, S.S., Toigo, A.D., Ojha, L., Wray, J.J., Chojnacki, M., Byrne, S.,
1928 Murchie, S.L., Thomas, N., 2014. Recurring slope lineae in equatorial regions of Mars. Nat.
1929 Geosci 7, 53–58. https://doi.org/10.1038/ngeo2014
1930 McEwen, Alfred S., Eliason, E.M., Bergstrom, J.W., Bridges, N.T., Hansen, C.J., Delamere, W.A., Grant,
1931 J.A., Gulick, V.C., Herkenhoff, K.E., Keszthelyi, L., Kirk, R.L., Mellon, M.T., Squyres, S.W.,
1932 Thomas, N., Weitz, C.M., 2007. Mars Reconnaissance Orbiter's High Resolution Imaging
1933 Science Experiment (HiRISE). J. Geophys. Res. Planets 112, E05S02.
1934 https://doi.org/10.1029/2005JE002605
1935 McEwen, A. S., Hansen, C.J., Delamere, W.A., Eliason, E.M., Herkenhoff, K.E., Keszthelyi, L., Gulick,
1936 V.C., Kirk, R.L., Mellon, M.T., Grant, J.A., Thomas, N., Weitz, C.M., Squyres, S.W., Bridges,
1937 N.T., Murchie, S.L., Seelos, F., Seelos, K., Okubo, C.H., Milazzo, M.P., Tornabene, L.L., Jaeger,
1938 W.L., Byrne, S., Russell, P.S., Griffes, J.L., MartÃ-nez-Alonso, S., Davatzes, A., Chuang, F.C.,
1939 Thomson, B.J., Fishbaugh, K.E., Dundas, C.M., Kolb, K.J., Banks, M.E., Wray, J.J., 2007. A
1940 closer look at water-related geologic activity on Mars. Science 317, 1706–1709.
1941 McEwen, A.S., Ojha, L., Dundas, C.M., Mattson, S.S., Byrne, S., Wray, J.J., Cull, S.C., Murchie, S.L.,
1942 Thomas, N., Gulick, V.C., 2011. Seasonal Flows on Warm Martian Slopes. Science 333, 740–
1943 743. https://doi.org/10.1126/science.1204816
1944 McKay, C.P., Davis, W.L., 1991. Duration of liquid water habitats on early Mars. Icarus 90, 214–221.
1945 https://doi.org/10.1016/0019-1035(91)90102-Y
1946 Mellon, M.T., Arvidson, R.E., Sizemore, H.G., Searls, M.L., Blaney, D.L., Cull, S., Hecht, M.H., Heet,
1947 T.L., Keller, H.U., Lemmon, M.T., Markiewicz, W.J., Ming, D.W., Morris, R.V., Pike, W.T., Zent,
1948 A.P., 2009. Ground ice at the Phoenix Landing Site: Stability state and origin. J. Geophys. Res.
1949 Planets 114, E00E07. https://doi.org/10.1029/2009JE003417
1950 Mellon, M.T., Phillips, R.J., 2001. Recent gullies on Mars and the source of liquid water. J. Geophys.
1951 Res. 106, 23165–23179. https://doi.org/10.1029/2000JE001424
1952 Mellors, R.A., Waitt, R.B., Swanson, D.A., 1988. Generation of pyroclastic flows and surges by hot-
1953 rock avalanches from the dome of Mount St. Helens volcano, USA. Bull. Volcanol. 50, 14–25.
1954 https://doi.org/10.1007/BF01047505
1955 Mergili, M., Jan-Thomas, F., Krenn, J., Pudasaini, S.P., 2017. r. avaflow v1, an advanced open-source
1956 computational framework for the propagation and interaction of two-phase mass flows.
1957 Geosci. Model Dev. 10, 553.

1958 Milliken, R.E., Mustard, J.F., Goldsby, D.L., 2003. Viscous flow features on the surface of Mars:
1959 Observations from high-resolution Mars Orbiter Camera (MOC) images. J Geophys Res 108,
1960 doi:10.1029/2002JE002005.
1961 Miyamoto, H., Dohm, J.M., Baker, V.R., Beyer, R.A., Bourke, M., 2004. Dynamics of unusual debris
1962 flows on Martian sand dunes. Geophys Res Lett 31, doi:10.1029/2004GL020313.
1963 Morgan, A.M., Howard, A.D., Hobley, D.E.J., Moore, J.M., Dietrich, W.E., Williams, R.M.E., Burr, D.M.,
1964 Grant, J.A., Wilson, S.A., Matsubara, Y., 2014. Sedimentology and climatic environment of
1965 alluvial fans in the martian Saheki crater and a comparison with terrestrial fans in the
1966 Atacama Desert. Icarus 229, 131–156. https://doi.org/10.1016/j.icarus.2013.11.007
1967 Morgan, G.A., Head III, J.W., Marchant, D.R., 2009. Lineated valley fill (LVF) and lobate debris aprons
1968 (LDA) in the Deuteronilus Mensae northern dichotomy boundary region, Mars: Constraints
1969 on the extent, age and episodicity of Amazonian glacial events. Icarus 202, 22–38.
1970 https://doi.org/10.1016/j.icarus.2009.02.017
1971 Morgan, G.A., Head, J.W., Forget, F., Madeleine, J.-B., Spiga, A., 2010. Gully formation on Mars: Two
1972 recent phases of formation suggested by links between morphology, slope orientation and
1973 insolation history. Icarus 208, 658–666. https://doi.org/10.1016/j.icarus.2010.02.019
1974 Morgan, G.A., Head, J.W., Marchant, D.R., Dickson, J.L., Levy, J.S., 2007. Gully Formation on Mars:
1975 Testing the Snowpack Hypothesis from Analysis of Analogs in the Antarctic Dry Valleys. Lunar
1976 Planet. Sci. Conf. 38, no. 1656.
1977 Morishige, K., Kawano, K., 2000. Freezing and melting of methanol in a single cylindrical pore:
1978 Dynamical supercooling and vitrification of methanol. J. Chem. Phys. 112, 11023–11029.
1979 https://doi.org/10.1063/1.481742
1980 Musselwhite, D.S., Swindle, T.D., Lunine, J.I., 2001. Liquid CO2 breakout and the formation of recent
1981 small gullies on Mars. Geophys. Res. Lett. 28, 1283–1285.
1982 Mustard, J.F., Cooper, C.D., Rifkin, M.K., 2001. Evidence for recent climate change on Mars from the
1983 identification of youthful near-surface ground ice. Nature 412, 411–414.
1984 https://doi.org/10.1038/35086515
1985 Mutch, T.A., 1979. Planetary surfaces. Rev. Geophys. 17, 1694.
1986 https://doi.org/10.1029/RG017i007p01694
1987 Naaim, M., Faug, T., Naaim-Bouvet, F., 2003. Dry granular flow modelling including erosion and
1988 deposition. Surv. Geophys. 24, 569–585.
1989 https://doi.org/10.1023/B:GEOP.0000006083.47240.4c
1990 Nunes, D.C., Smrekar, S.E., Safaeinili, A., Holt, J., Phillips, R.J., Seu, R., Campbell, B., 2010.
1991 Examination of gully sites on Mars with the shallow radar. J Geophys Res 115,
1992 doi:10.1029/2009JE003509. https://doi.org/10.1029/2009je003509
1993 Núñez, J.I., Barnouin, O.S., Murchie, S.L., Seelos, F.P., McGovern, J.A., Seelos, K.D., Buczkowski, D.L.,
1994 2016a. New insights into gully formation on Mars: Constraints from composition as seen by
1995 MRO/CRISM: Gully Formation on Mars as Seen by CRISM. Geophys. Res. Lett.
1996 https://doi.org/10.1002/2016GL068956
1997 Núñez, J.I., Barnouin, O.S., Seelos, F.P., Murchie, S.L., 2016b. Compositional constraints on martian
1998 gully formation as seen by CRISM on MRO. 47th Lunar Planet. Sci. Conf. abstract 3034.
1999 Nyberg, R., 1989. Observations of Slushflows and Their Geomorphological Effects in the Swedish
2000 Mountain Area. Geogr. Ann. Ser. Phys. Geogr. 71, 185–198.
2001 O'Brien, J.S., Julien, P.Y., Fullerton, W.T., 1993. Two-dimensional water flood and mudflow
2002 simulation. J. Hydraul. Eng. - ASCE 119, 244–261.
2003 Ojha, L., Chojnacki, M., McDonald, G.D., Shumway, A., Wolff, M.J., Smith, M.D., McEwen, A.S.,
2004 Ferrier, K., Huber, C., Wray, J.J., Toigo, A., 2017. Seasonal Slumps in Juventae Chasma, Mars:
2005 Seasonal Slumps in Juventae Chasma, Mars. J. Geophys. Res. Planets.
2006 https://doi.org/10.1002/2017JE005375

2007 Ojha, L., McEwen, A., Dundas, C., Byrne, S., Mattson, S., Wray, J., Masse, M., Schaefer, E., 2014.
2008 HiRISE observations of Recurring Slope Lineae (RSL) during southern summer on Mars. Icarus
2009 231, 365–376. https://doi.org/10.1016/j.icarus.2013.12.021
2010 Ojha, L., Wilhelm, M.B., Murchie, S.L., McEwen, A.S., Wray, J.J., Hanley, J., Masse, M., Chojnacki, M.,
2011 2015. Spectral evidence for hydrated salts in recurring slope lineae on Mars. Nat. Geosci 8,
2012 829–832.
2013 Okubo, C.H., Tornabene, L.L., Lanza, N.L., 2011. Constraints on mechanisms for the growth of gully
2014 alcoves in Gasa crater, Mars, from two-dimensional stability assessments of rock slopes.
2015 Icarus 211, 207–221.
2016 Osinski, G.R., Léveillé, R., Berinstain, A., Lebeuf, M., Bamsey, M., 2006. Terrestrial Analogues to Mars
2017 and the Moon: Canada's Role. Geosci. Can. Vol. 33 Number 4 2006.
2018 Oyarzun, R., Viedma, C., Marquez, A., Lillo, J., 2003. Freezing-resistant liquid water in porous media,
2019 a possible mechanism to account for the fluidized transport of sediments on Mars: an
2020 example from East Gorgonum crater. Terr Nova 15, 238–242.
2021 Pacifici, A., 2009. The Argentinean Patagonia and the Martian landscape. Planet. Space Sci. 57, 571–
2022 578.
2023 Paola, C., Straub, K., Mohrig, D., Reinhardt, L., 2009. The "unreasonable effectiveness" of
2024 stratigraphic and geomorphic experiments. Earth-Sci. Rev. 97, 1–43.
2025 https://doi.org/10.1016/j.earscirev.2009.05.003
2026 Parsons, R.A., Nimmo, F., 2010. Numerical modeling of Martian gully sediment transport: Testing the
2027 fluvial hypothesis. J Geophys Res 115, doi:10.1029/2009JE003517.
2028 https://doi.org/10.1029/2009je003517
2029 Pasquon, K., Gargani, J., Massé, M., Conway, S.J., 2016. Present-day formation and seasonal
2030 evolution of linear dune gullies on Mars. Icarus 274, 195–210.
2031 https://doi.org/10.1016/j.icarus.2016.03.024
2032 Pasquon, K., Gargani, J., Nachon, M., Conway, S.J., Massé, M., Jouannic, G., Balme, M.R., Costard, F.,
2033 Vincendon, M., 2017. Are the different gully morphologies due to different formation
2034 processes on the Kaiser dune field? Geol. Soc. Lond. Spec. Publ. 467, in press, doi:
2035 10.1144/SP467.13
2036 Pearce, G., Osinski, G.R., Soare, R.J., 2011. Intra-crater glacial processes in central Utopia Planitia,
2037 Mars. Icarus 212, 86–95. https://doi.org/doi: DOI: 10.1016/j.icarus.2010.12.001
2038 Pelletier, J.D., Kolb, K.J., McEwen, A.S., Kirk, R.L., 2008. Recent bright gully deposits on Mars: Wet or
2039 dry flow? Geology 36, 211–214.
2040 Phillips, J.D., 2005. Weathering instability and landscape evolution. Weather. Landsc. Evol. 67, 255–
2041 272. https://doi.org/10.1016/j.geomorph.2004.06.012
2042 Pierson, T.C., 2005. Distinguishing between debris flows and floods from field evidence in small
2043 watersheds (Report No. 2004–3142), Fact Sheet.
2044 Pilorget, C., Forget, F., 2016. Formation of gullies on Mars by debris flows triggered by CO2
2045 sublimation. Nat. Geosci. 9, 65–69. https://doi.org/10.1038/ngeo2619
2046 Piqueux, S., Byrne, S., Richardson, M.I., 2003a. Sublimation of Mars's southern seasonal CO_2 ice cap
2047 and the formation of spiders. J. Geophys. Res. 108. https://doi.org/10.1029/2002JE002007
2048 Piqueux, S., Byrne, S., Richardson, M.I., 2003b. Sublimation of Mars's southern seasonal CO2 ice cap
2049 and the formation of spiders. J. Geophys. Res. 108, 5084.
2050 https://doi.org/10.1029/2002JE002007
2051 Piqueux, S., Kleinböhl, A., Hayne, P.O., Heavens, N.G., Kass, D.M., McCleese, D.J., Schofield, J.T.,
2052 Shirley, J.H., 2016. Discovery of a widespread low-latitude diurnal CO_2 frost cycle on Mars:
2053 Low-Latitude CO_2 Frost on Mars. J. Geophys. Res. Planets.
2054 https://doi.org/10.1002/2016JE005034
2055 Piqueux, S., Kleinböhl, A., Hayne, P.O., Kass, D.M., Schofield, J.T., McCleese, D.J., 2015. Variability of
2056 the martian seasonal CO2 cap extent over eight Mars Years. Dyn. Mars 251, 164–180.
2057 https://doi.org/10.1016/j.icarus.2014.10.045

2058 Platzer, K., Bartelt, P., Jaedicke, C., 2007. Basal shear and normal stresses of dry and wet snow
2059 avalanches after a slope deviation. Cold Reg. Sci. Technol. 49, 11–25.
2060 https://doi.org/10.1016/j.coldregions.2007.04.003
2061 Plaut, J.J., Safaeinili, A., Holt, J.W., Phillips, R.J., Head, J.W., Seu, R., Putzig, N.E., Frigeri, A., 2009.
2062 Radar evidence for ice in lobate debris aprons in the mid-northern latitudes of Mars.
2063 Geophys. Res. Lett. 36, 02203. https://doi.org/10.1029/2008GL036379
2064 Pollard, W., Omelon, C., Andersen, D., McKay, C., 1999. Perennial spring occurrence in the
2065 Expedition Fiord area of western Axel Heiberg Island, Canadian High Arctic. Can. J. Earth Sci.
2066 36, 105–120. https://doi.org/10.1139/e98-097
2067 Portyankina, G., Markiewicz, W.J., Thomas, N., Hansen, C.J., Milazzo, M., 2010. HiRISE observations
2068 of gas sublimation-driven activity in Mars' southern polar regions: III. Models of processes
2069 involving translucent ice. MROHiRISE Stud. Mars 205, 311–320.
2070 https://doi.org/10.1016/j.icarus.2009.08.029
2071 Pouliquen, O., 1999. Scaling laws in granular flows down rough inclined planes. Phys. Fluids 11, 542–
2072 548. https://doi.org/10.1063/1.869928
2073 Putzig, N.E., Mellon, M.T., Kretke, K.A., Arvidson, R.E., 2005. Global thermal inertia and surface
2074 properties of Mars from the MGS mapping mission. Icarus 173, 325–341.
2075 https://doi.org/10.1016/j.icarus.2004.08.017
2076 Raack, J., Conway, S.J., Herny, C., Balme, M.R., Carpy, S., Patel, M.R., 2017. Water induced sediment
2077 levitation enhances down-slope transport on Mars. Nat. Commun. 8, 1151.
2078 https://doi.org/10.1038/s41467-017-01213-z
2079 Raack, J., Reiss, D., Appéré, T., Vincendon, M., Ruesch, O., Hiesinger, H., 2015. Present-Day Seasonal
2080 Gully Activity in a South Polar Pit (Sisyphi Cavi) on Mars. Icarus 251, 226–243.
2081 https://doi.org/j.icarus.2014.03.040
2082 Raack, J., Reiss, D., Hiesinger, H., 2012. Gullies and their relationships to the dust-ice mantle in the
2083 northwestern Argyre Basin, Mars. Icarus 219, 129–141.
2084 https://doi.org/10.1016/j.icarus.2012.02.025
2085 Rapp, A., 1986. Slope processes in high latitude mountains. Prog. Phys. Geogr. 10, 53–68.
2086 https://doi.org/10.1177/030913338601000103
2087 Rapp, A., 1960. Recent Development of Mountain Slopes in Kärkevagge and Surroundings, Northern
2088 Scandinavia. Geogr. Ann. Ser. Phys. Geogr. 42, 65–200.
2089 Reiss, D., Erkeling, G., Bauch, K.E., Hiesinger, H., 2010a. Evidence for present day gully activity on the
2090 Russell crater dune field, Mars. Geophys. Res. Lett. 37, L06203.
2091 https://doi.org/10.1029/2009gl042192
2092 Reiss, D., Hauber, E., Hiesinger, H., Jaumann, R., Trauthan, F., Preusker, F., Zanetti, M., Ulrich, M.,
2093 Johnsson, A., Johansson, L., Olvmo, M., Carlsson, E., Johansson, H.A.B., McDaniel, S., 2011.
2094 Terrestrial gullies and debris-flow tracks on Svalbard as planetary analogs for Mars. Geol.
2095 Soc. Am. Spec. Pap. 483, 165–175. https://doi.org/10.1130/2011.2483(11)
2096 Reiss, D., Hauber, E., Hiesinger, H., Jaumann, R., Trauthan, F., Preusker, F., Zanetti, M., Ulrich, M.,
2097 Johnsson, A., Johansson, L., Olvmo, M., Carlsson, E., Johansson, H.A.B., McDaniel, S., 2010b.
2098 Terrestrial Gullies on Svalbard as Planetary Anologs for Mars. Lunar Planet. Sci. Conf. 41,
2099 1665.
2100 Reiss, D., Hiesinger, H., Hauber, E., Gwinner, K., 2009a. Regional differences in gully occurrence on
2101 Mars: A comparison between the Hale and Bond craters. Planet. Space Sci. 57, 958–974.
2102 Reiss, D., Hiesinger, H., Hauber, E., Zanetti, M., Preusker, F., Trauthan, F., Reimann, G.M., Raack, J.,
2103 Carlsson, A.E., Johnsson, A., Olvmo, M., Jaumann, R., Johansson, H.A.B., Johansson, L.,
2104 McDaniel, S., 2009b. Morphologic and Morphometric Comparision of Gullies on Svalbard
2105 and Mars. Lunar Planet. Sci. Conf. 40, 2362.
2106 Reiss, D., Jaumann, R., 2003. Recent debris flows on Mars: Seasonal observations of the Russell
2107 Crater dune field. Geophys Res Lett 30, doi:10.1029/2002GL016704.

2108 Reiss, D., van Gasselt, S., Neukum, G., Jaumann, R., 2004. Absolute dune ages and implications for
2109 the time of formation of gullies in Nirgal Vallis, Mars. J Geophys Res-Planets 109,
2110 doi:10.1029/2004JE002251.
2111 Richardson, M.I., Mischna, M.A., 2005. Long-term evolution of transient liquid water on Mars. J.
2112 Geophys. Res. Planets 110, 03003. https://doi.org/10.1029/2004JE002367
2113 Rummel, J.D., Beaty, D.W., Jones, M.A., Bakermans, C., Barlow, N.G., Boston, P.J., Chevrier, V.F.,
2114 Clark, B.C., de Vera, J.-P.P., Gough, R.V., Hallsworth, J.E., Head, J.W., Hipkin, V.J., Kieft, T.L.,
2115 McEwen, A.S., Mellon, M.T., Mikucki, J.A., Nicholson, W.L., Omelon, C.R., Peterson, R.,
2116 Roden, E.E., Sherwood Lollar, B., Tanaka, K.L., Viola, D., Wray, J.J., 2014. A New Analysis of
2117 Mars "Special Regions": Findings of the Second MEPAG Special Regions Science Analysis
2118 Group (SR-SAG2). Astrobiology 14, 887–968. https://doi.org/10.1089/ast.2014.1227
2119 Russell, P., Thomas, N., Byrne, S., Herkenhoff, K., Fishbaugh, K., Bridges, N., Okubo, C., Milazzo, M.,
2120 Daubar, I., Hansen, C., McEwen, A., 2008. Seasonally active frost-dust avalanches on a north
2121 polar scarp of Mars captured by HiRISE. Geophys. Res. Lett. 35, 1–5.
2122 https://doi.org/10.1029/2008GL035790
2123 Saunders, R.S., Zurek, R.W., 2000. Ideas about the surface runoff features on Mars. Science 290,
2124 712–713.
2125 Schon, S.C., Head, J.W., 2012. Gasa impact crater, Mars: Very young gullies formed from impact into
2126 latitude-dependent mantle and debris-covered glacier deposits? Icarus 218, 459–477.
2127 https://doi.org/10.1016/j.icarus.2012.01.002
2128 Schon, S.C., Head, J.W., 2011. Keys to gully formation processes on Mars: Relation to climate cycles
2129 and sources of meltwater. Icarus 213, 428–432.
2130 https://doi.org/10.1016/j.icarus.2011.02.020
2131 Schon, S.C., Head, J.W., 2009. Terraced Cutbanks and Longitudinal Bars in Gully Channels on Mars:
2132 Evidence for Multiple Episodes of Fluvial Transport. Lunar Planet. Sci. Conf. 40, # 1691.
2133 Schon, S.C., Head, J.W., Fassett, C.I., 2009a. Unique chronostratigraphic marker in depositional fan
2134 stratigraphy on Mars: Evidence for ca. 1.25 Ma gully activity and surficial meltwater origin.
2135 Geology 37, 207–210. https://doi.org/10.1130/g25398a.1
2136 Schon, S.C., Head, J.W., Milliken, R.E., 2009b. A recent ice age on Mars: Evidence for climate
2137 oscillations from regional layering in mid-latitude mantling deposits. Geophys Res Lett 36.
2138 https://doi.org/10.1029/2009GL038554
2139 Schorghofer, N., Edgett, K.S., 2006. Seasonal surface frost at low latitudes on Mars. Icarus 180, 321–
2140 334. https://doi.org/10.1016/j.icarus.2005.08.022
2141 Senthil Kumar, P., Keerthi, V., Senthil Kumar, A., Mustard, J., Gopala Krishna, B., Amitabh, Ostrach,
2142 L.R., Kring, D.A., Kiran Kumar, A.S., Goswami, J.N., 2013. Gullies and landslides on the Moon:
2143 Evidence for dry-granular flows. J. Geophys. Res. Planets 118, 206–223.
2144 https://doi.org/10.1002/jgre.20043
2145 Sharpton, V.L., 2014. Outcrops on lunar crater rims: Implications for rim construction mechanisms,
2146 ejecta volumes and excavation depths: Outcrops constrain crater rim components. J.
2147 Geophys. Res. Planets 119, 154–168. https://doi.org/10.1002/2013JE004523
2148 Shelef, E., Hilley, G.E., 2016. A Unified Framework for Modeling Landscape Evolution by Discrete
2149 Flows: LANDSCAPE FORMATION BY DISCRETE FLOWS. J. Geophys. Res. Earth Surf.
2150 https://doi.org/10.1002/2015JF003693
2151 Shinbrot, T., 2007. Delayed transitions between fluid-like and solid-like granular states. Eur Phys J E
2152 22, 209–217.
2153 Shinbrot, T., Duong, N.-H., Kwan, L., Alvarez, M.M., 2004. Dry granular flows can generate surface
2154 features resembling those seen in Martian gullies. Proc. Natl. Acad. Sci. U. S. A. 101, 8542–
2155 8546. https://doi.org/10.1073/pnas.0308251101
2156 Siebert, L., Glicken, H., Ui, T., 1987. Volcanic hazards from Bezymianny- and Bandai-type eruptions.
2157 Bull. Volcanol. 49, 435–459. https://doi.org/10.1007/BF01046635

Sinha, R.K., Sivaprahasam, V., Shukla, A.D., Das, P., Bhattacharya, F., 2018. Gullies and Debris-flows in Ladakh Himalaya, India: a potential Martian analogue. Geol. Soc. Lond. Spec. Publ. 467, in press, doi: 10.1144/SP467.9.

Sklar, L., Dietrich, W.E., 1998. River longitudinal profiles and bedrock incision models: stream power and the influence of sediment supply, in: Tinkler, K.J., Wohl, E.E. (Eds.), Rivers over Rock: Fluvial Processes in Bedrock Channels, Am. Geoph. Union Geophysical Monograph. pp. 237–260.

Soare, R.J., Conway, S.J., Dohm, J.M., 2014a. Possible ice-wedge polygons and recent landscape modification by "wet" periglacial processes in and around the Argyre impact basin, Mars. Icarus 233, 214–228. https://doi.org/10.1016/j.icarus.2014.01.034

Soare, R.J., Conway, S.J., Dohm, J.M., El-Maarry, M.R., 2014b. Possible open-system (hydraulic) pingos in and around the Argyre impact region of Mars. Earth Planet. Sci. Lett. 398, 25–36. https://doi.org/10.1016/j.epsl.2014.04.044

Soare, R.J., Conway, S.J., Gallagher, C., Dohm, J.M., 2017. Ice-rich (periglacial) vs icy (glacial) depressions in the Argyre region, Mars: a proposed cold-climate dichotomy of landforms. Icarus 282, 70–83. https://doi.org/10.1016/j.icarus.2016.09.009

Soare, R.J., Conway, S.J., Gallagher, C., Dohm, J.M., Reiss, D., 2018. Periglacial complexes and the deductive evidence of "wet"-flows at the Hale impact-crater, Mars. Geol. Soc. Lond. Spec. Publ. 467, in press, doi: 10.1144/SP467.7

Soare, R.J., Horgan, B., Conway, S.J., Souness, C., El-Maarry, M.R., 2015. Volcanic terrain and the possible periglacial formation of "excess ice" at the mid-latitudes of Utopia Planitia, Mars. Earth Planet. Sci. Lett. 423, 182–192. https://doi.org/10.1016/j.epsl.2015.04.033

Soare, R.J., Kargel, J.S., Osinski, G.R., Costard, F., 2007. Thermokarst processes and the origin of crater-rim gullies in Utopia and western Elysium Planitia. Icarus 191, 95–112.

Souness, C., Hubbard, B., 2012. Mid-latitude glaciation on Mars. Prog. Phys. Geogr. 36, 238–261. https://doi.org/10.1177/0309133312436570

Souness, C., Hubbard, B., Milliken, R.E., Quincey, D., 2012. An inventory and population-scale analysis of Martian glacier-like forms. Icarus 217, 243–255. https://doi.org/10.1016/j.icarus.2011.10.020

Sparks, R.S.J., Wilson, L., 1976. A model for the formation of ignimbrite by gravitational column collapse. J. Geol. Soc. 132, 441. https://doi.org/10.1144/gsjgs.132.4.0441

Squyres, S.W., 1979. The distribution of lobate debris aprons and similar flows on Mars. J. Geophys. Res. Solid Earth 84, 8087–8096. https://doi.org/10.1029/JB084iB14p08087

Squyres, S.W., 1978. Martian fretted terrain: Flow of erosional debris. Icarus 34, 600–613. https://doi.org/10.1016/0019-1035(78)90048-9

Squyres, S.W., Knoll, A.H., Arvidson, R.E., Clark, B.C., Grotzinger, J.P., Joliff, B.L., McLennan, S.M., Tosca, N.J., Bell III, J.F., Calvin, W.M., Farrand, W.H., Glotch, T.D., Golombek, M.P., Herkenhoff, K.E., Johnson, J.R., Klingelhöfer, G., McSween, H.Y., Yen, A.S., 2006. Two years at Meridiani Planum: Results from the Opportunity Rover. Science 313, 1403–1407. https://doi.org/10.1126/science.1130890

Steele, L.J., Balme, M.R., Lewis, S.R., Spiga, A., 2017. The water cycle and regolith–atmosphere interaction at Gale crater, Mars. Icarus 289, 56–79. https://doi.org/10.1016/j.icarus.2017.02.010

Stewart, S.T., Nimmo, F., 2002. Surface runoff features on Mars: Testing the carbon dioxide formation hypothesis. J Geophys Res-Planets 107, doi:10.1029/2000JE001465.

Stillman, D.E., Grimm, R.E., 2018. Two pulses of seasonal activity in martian southern mid-latitude recurring slope lineae (RSL). Icarus 302, 126–133. https://doi.org/10.1016/j.icarus.2017.10.026

Stillman, D.E., Michaels, T.I., Grimm, R.E., 2017. Characteristics of the numerous and widespread recurring slope lineae (RSL) in Valles Marineris, Mars. Icarus 285, 195–210. https://doi.org/10.1016/j.icarus.2016.10.025

Stillman, D.E., Michaels, T.I., Grimm, R.E., Hanley, J., 2016. Observations and modeling of northern mid-latitude recurring slope lineae (RSL) suggest recharge by a present-day martian briny aquifer. Icarus 265, 125–138. https://doi.org/10.1016/j.icarus.2015.10.007

Stillman, D.E., Michaels, T.I., Grimm, R.E., Harrison, K.P., 2014. New observations of martian southern mid-latitude recurring slope lineae (RSL) imply formation by freshwater subsurface flows. Icarus 233, 328–341. https://doi.org/10.1016/j.icarus.2014.01.017

Stoffel, M., Bollschweiler, M., Hassler, G.-R., 2006. Differentiating past events on a cone influenced by debris-flow and snow avalanche activity – a dendrogeomorphological approach. Earth Surf. Process. Landf. 31, 1424–1437. https://doi.org/10.1002/esp.1363

Sutton, S.L.F., McKenna Neuman, C., Nickling, W., 2013a. Lee slope sediment processes leading to avalanche initiation on an aeolian dune. J. Geophys. Res. Earth Surf. 118, 1754–1766. https://doi.org/10.1002/jgrf.20131

Sutton, S.L.F., McKenna Neuman, C., Nickling, W., 2013b. Avalanche grainflow on a simulated aeolian dune. J. Geophys. Res. Earth Surf. 118, 1767–1776. https://doi.org/10.1002/jgrf.20130

Sylvest, M.E., Conway, S.J., Patel, M.R., Dixon, J.C., Barnes, A., 2016. Mass wasting triggered by seasonal CO_2 sublimation under Martian atmospheric conditions: Laboratory experiments. Geophys. Res. Lett. 43, 12,363–12,370. https://doi.org/10.1002/2016GL071022

Sylvest, M.E., Dixon, J.C., Conway, S.J., Patel, M.R., McElwaine, J.N., Hagermann, A., Barnes, A., 2018. CO_2sublimation in martian gullies: laboratory experiments at varied slope angle and regolith grain sizes. Geol. Soc. Lond. Spec. Publ. Martian Gullies and their Earth Analogues. 467, in press, doi: 10.1144/SP467.11

Tamppari, L.K., Lemmon, M.T., 2014. Vertical water vapor distribution at Phoenix, in: 8th International Conference on Mars. The Woodlands, TX, p. abstract 1092. https://doi.org/10.1029/2009JE003415

Tornabene, L.L., Watters, W.A., Osinski, G.R., Boyce, J.M., Harrison, T.N., Ling, V., McEwen, A.S., 2018. A depth versus diameter scaling relationship for the best-preserved melt-bearing complex craters on Mars. Icarus 299, 68–83. https://doi.org/10.1016/j.icarus.2017.07.003

Treiman, A. H., 2003. Geologic settings of Martian gullies: Implications for their origins. J. Geophys. Res. Planets 108, doi:10.1029/2002JE001900. https://doi.org/10.1029/2002JE001900

Treiman, Allan H., 2003. Geologic settings of Martian gullies: Implications for their origins. J. Geophys. Res. 108, 8031. https://doi.org/10.1029/2002JE001900

van Gasselt, S., 2007. Cold-Climate Landforms on Mars. der Freien Universität Berlin, Berlin.

Védie, E., Costard, F., Font, M., Lagarde, J.L., 2008. Laboratory simulations of Martian gullies on sand dunes. Geophys. Res. Lett. 35, doi:10.1029/2008GL035638.

Vincendon, M., 2015. Identification of Mars gully activity types associated with ice composition. J. Geophys. Res. Planets 120, 1859–1879. https://doi.org/10.1002/2015JE004909

Vincendon, M., Forget, F., Mustard, J., 2010a. Water ice at low to midlatitudes on Mars. J. Geophys. Res. E Planets 115, 1–13. https://doi.org/10.1029/2010JE003584

Vincendon, M., Mustard, J., Forget, F., Kreslavsky, M., Spiga, A., Murchie, S., Bibring, J.P., 2010b. Near-tropical subsurface ice on Mars. Geophys. Res. Lett. 37, 1–8. https://doi.org/10.1029/2009GL041426

Wang, X., Luo, L., Guo, H., Mu, L., Li, C., Ji, W., Cai, H., 2013. Cratering process and morphological features of the Xiuyan impact crater in Northeast China. Sci. China Earth Sci. 56, 1629–1638. https://doi.org/10.1007/s11430-013-4695-1

Whipple, K.X., Tucker, G.E., 1999. Dynamics of the stream-power river incision model: Implications for height limits of mountain ranges, landscape response timescales, and research needs. J. Geophys. Res. B Solid Earth 104, 17661–17674.

Williams, K.E., Toon, O.B., Heldmann, J.L., Mellon, M.T., 2009. Ancient melting of mid-latitude snowpacks on Mars as a water source for gullies. Icarus 200, 418–425. https://doi.org/10.1016/j.icarus.2008.12.013

Xiao, L., Wang, J., Dang, Y., Cheng, Z., Huang, T., Zhao, J., Xu, Y., Huang, J., Xiao, Z., Komatsu, G., 2017. A new terrestrial analogue site for Mars research: The Qaidam Basin, Tibetan Plateau (NW China). Earth-Sci. Rev. 164, 84–101. https://doi.org/10.1016/j.earscirev.2016.11.003

Yue, Z., Hu, W., Liu, B., Liu, Y., Sun, X., Zhao, Q., Di, K., 2014. Quantitative analysis of the morphology of martian gullies and insights into their formation. Icarus 243, 208–221. https://doi.org/10.1016/j.icarus.2014.08.028

Zimbelman, J.R., 2001. Image resolution and evaluation of genetic hypotheses for planetary landscapes. Geomorphology 37, 179–199. https://doi.org/10.1016/S0169-555X(00)00082-9

Figure Captions

Figure 1: Example images of gullies on Mars with context images. North is up unless indicated otherwise. The scales in images b-d and o-s are the same as indicated in a. For images e-n all scale bars are 200 m. (a) Southern part of Kaiser Crater dunefield in CTX image D07_030133_1330, black boxes indicate locations of panels e and f. (b) Part of the wall of one of the polar pits in Sisyphi Cavi in CTX image B10_013598_1092 with black box indicating the location of panel g. (c) Part of Nirgil Vallis in CTX image F08_038957_1517 with black box indicating the location of panel h. (d) 12-km-diameter crater in Acidalia Planitia, CTX image F21_043861_2326 with black box indicating the location of panel i. (e) Linear dune gullies on a dune in Kaiser crater with frost visible in upper-left corner, HiRISE image ESP_028788_1325 at Ls 173°. (f) A classic gully also on Kaiser Crater dunefield with a new deposit outlined by a bright halo, HiRISE image ESP_027944_1325 at Ls 139°. (g) Gullies on the wall of a polar pit in Sisyphi Cavi, HiRISE image ESP_049531_1090. (h) Gullies on the wall of Nirgil Vallis, HiRISE image ESP_038957_1515. (i) Gullies originating at bedrock layer on the inner wall of an impact crater, HiRISE image ESP_045193_2325. (j) A gully system spanning ~4 km in length with large tributary catchment in HiRISE image ESP_013894_1410. (k) Gully which does not extend up to the slope crest in HiRISE image ESP_014312_1320. (l) Gullies extending into alcoves incised into the bedrock of Galap crater in HiRISE image PSP_003939_1420. (m) Gullies entirely contained within deposits of the LDM in HiRISE image PSP_002514_1420. (n) Gullies surrounded by pitted ground in the LDM in HiRISE image ESP_026097_2310. (o) Part of the wall of a 19-km-diameter crater in Terra Sirenum in CTX image B11_013894_1412 with black box indicating the location of panel j. (p) Mesa in Nereidum Montes in CTX image B12_014312_1323 with black box indicating the location of panel k. (q) Galap Crater in Terra Sirenum in CTX image B09_012971_1421 with black box indicating the location of panel l. (r) Inner wall of Bunnik Crater in Terra Sirenum in CTX image P04_002659_1418 with black box indicating the location of panel m. (s) Inner wall of Lyot Crater in CTX image D19_034800_2310 with black box indicating the location of panel n. HiRISE image credit: NASA/JPL/University of Arizona. CTX image credit: NASA/JPL-Caltech/MSSS.

Figure 2: Alcove zones of gullies on Mars. (a) An individual gully located within LDM inside an impact crater on a south-facing slope in the rim materials of the Argyre Impact Basin. The alcove of this gully is comprised of a single incision or chute. HiRISE image ESP_013850_1415. (b) Gasa crater whose rim hosts numerous gully alcoves incised into the bedrock. Location of panel c is given by the black box. HiRISE image ESP_014081_1440. (c) Detail of chutes and channels emerging from the alcoves in Gasa Crater onto the fans below. Discontinuous secondary channels can be identified on the fan as well as primary channels which are still connected to the chutes and alcoves. (d) A gully incised into LDM, where the channels are located within a chute. The chute walls have mass wasting scars. HiRISE image PSP_005616_1440. (e) A gully-system where the alcoves are poorly defined topographically, but instead comprise many coalescing rills which come together to form the primary channels midslope. HiRISE image ESP_022685_1400. (f) Gullies on a crater wall which appear to originate at bedrock outcrops, yet on closer inspection rills can be seen above the outcrops upslope of their parent gullies. HiRISE image PSP_006261_1410. (g-i) context images for panels d-f using the same HiRISE images. HiRISE image credit: NASA/JPL/University of Arizona.

Figure 3: Spur and gully morphology on Mars and the Moon. (a) Inner wall of Dawes crater on the Moon, with spur and gully features identified by Kumar et al. (2013) in LROC NA image M175104387. (b) Wall of Noctis Labyrinthus on Mars, showing extensive evidence of aeolian activity in the form of ripples on the talus slope, HiRISE image ESP_028805_1725. (c) Inner wall of a ~6 km impact crater at 2°S in Libya Montes, showing tongues of granular material extending downslope, HiRISE image ESP_014412_1780. (d) Inner wall of a 21-km-diameter central pit crater, mentioned in the pristine crater catalogue of Tornabene et al. (2018), where the dark slope streaks originating at the top of the talus slope are thought to be triggered by a recent rockfall. HiRISE image PSP_010037_1965. HiRISE image credit: NASA/JPL/University of Arizona. LROC image credit: NASA/GSFC/Arizona State University.

Figure 4: Gully-like landforms at equatorial latitudes (a-c) and adjacent to mid-latitude gully-systems (d-f) on Mars. (a) Alcove into an interior layered deposit in Ganges Chasma with associated fan of dark sediments, HiRISE image ESP_032324_1715. (b) Inner wall of a 5-km-diameter crater at 14°S, with linear incisions (channels) and associated fans on the crater wall, HiRISE image ESP_046433_1655. (c) An isolated alcove-channel-fan system within an 800-m-diameter crater superposed on an ancient valley leading northwards into the Isidis Basin at 2°S, HiRISE image ESP_036987_1825. (d) Alcove-channel-fan systems on the west-facing wall of Istok Crater adjacent to a series of well-developed gullies (Johnsson et al., 2014), HiRISE image PSP_006837_1345. (e) Alcove-channel-fan systems on a north-facing wall within Asimov Crater, where south-facing gullies are abundant (Morgan et al., 2010), HiRISE image ESP_016657_1330. (f) Alcove-channel-fan systems on a west-facing portion of Hale Crater's rim adjacent to large well-developed gully systems (Kolb et al., 2010), HiRISE image ESP_012597_1435. HiRISE image credit: NASA/JPL/University of Arizona.

Figure 5: Martian gully channel features. (a) Highly-sinuous gully channels highlighted by black arrows in HiRISE image PSP_003464_1380. (b) Channels with well-developed lateral levees in Istok crater highlighted by black and white arrows in HiRISE image PSP_006837_1345. (c) Terraces in a gully-fan channel in Gasa crater highlighted by black arrows in HiRISE image ESP_014081_1440. (d) Braided channel pattern on a gully-fan surface in Gasa crater in HiRISE image ESP_014081_1440. (e-g) context images for panels a-d. HiRISE image credit: NASA/JPL/University of Arizona.

Figure 6: Depositional features and cross-cutting relationships, indicating martian gully formation over multiple flow events. (a-b) Multiple superposed channels with lateral levees ending in well-defined lobate deposits on gully-fans in Hale crater (after Reiss et al., 2011) and Istok crater (after Johnsson et al., 2014), respectively. Panel a: HiRISE image PSP_006822_1440, panel b: HiRISE image PSP_006837_1345. (c) Cross-cutting channels and gully-fan sectors of different ages on a gully-fan in Artik crater (after de Haas et al., 2013 and; Schon and Head, 2011) (HiRISE image ESP_012314_1450). (d) Gully-fan deposits predating and postdating fractured washboard terrain (after Dickson et al., 2015) (HiRISE image PSP_005943_1380). HiRISE image credit: NASA/JPL/University of Arizona.

Figure 7: The relationship between arcuate ridges and martian gullies. (a) Overview of a ridge in Nereidum Montes with arcuate ridges downslope of gullies on its eastern flank. HiRISE image ESP_022685_1400 overlain on CTX image G11_022685_1402. (b) Overview of a 9-km-diameter crater in Terra Sirenum, containing a "Viscous Flow Feature", with gullies upslope of arcuate ridges on its pole-facing wall. HiRISE image ESP_022108_1410 overlain on CTX image B07_012337_1408. (c) Detailed view of gullies upslope of a complex of arcuate ridges, whose fans superpose the terrain hosting the ridges. Location of panel d is indicated by the black box. (d) Small gully-like landforms on the scarps of the arcuate ridges. (e) Detailed view of the gullies upslope of the arcuate ridges, where the gully fans appear to be backfilling the spatulate depression behind the ridges. HiRISE image credit: NASA/JPL/University of Arizona. CTX image credit: NASA/JPL-Caltech/MSSS.

Figure 8: The relationship between gullies and scalloped depressions and pingo-like-mounds. The scale indicated in panel a is the same in b, idem for c and d. North is up in all panels. (a) A 9-km-diameter crater in Utopia Planitia reported by Soare et al. (2007) containing gullies and scalloped depressions. HiRISE image ESP_016113_2305. (b) Pingo-like mounds and gullies on a massif in the Nereidum Montes reported by Soare et al. (2014b). HiRISE image ESP_020720_1410. (c) Detailed view of scalloped depression located downslope of the gullies, with polygonised floor and steep, cuspate margins particularly on the pole-facing slope. (d) Detailed view of the pingo-like mounds, where the right-hand example has a collapsed summit and both have fissures at their summits. HiRISE image credit: NASA/JPL/University of Arizona.

Figure 9: Relation between gullies and LDM deposits. (a) Gullies with and without LDM cover in Domoni crater (HiRISE image ESP_016213_2315) (after de Haas et al., 2018). (b) Polygonal ground in gully-alcoves in Langtang crater (HiRISE image ESP_023809_1415) (after de Haas et al., 2018). (c) Polygons on an inactive gully-fan lobe (HiRISE image PSP_002368_1275) (after Levy et al., 2009). (d) Washboard terrain superposing old gully-fan deposits, while being covered by younger gully-fan deposits (HiRISE image PSP_005943_1380 see also Figure 6d) (after Dickson et al., 2015). HiRISE image credit: NASA/JPL/University of Arizona.

Figure 10: The relationship between gullies and lobes, patterned ground and RSL. (a) Gullies in Ruhea Crater in HiRISE image ESP_023679_1365, black box marks location of d. (b) Gullies in a 20-km-diameter crater in Acidalia Planitia, HiRISE image ESP_045997_2520 overlain on CTX image B01_010077_2520, where black box marks the location of e. (c) Gullies on the central mounds of Lohse crater in HiRISE image PSP_006162_1365, where black box marks the location of f. (d) Lobes on the terraces in the chute walls of gullies and on the surrounding terrains as first reported in Johnsson et al. (2018). (e) Stripes between the gully fans first reported in Fig. 12 Gallagher et al. (2011). Inset box shows that clasts make up the lower albedo parts of the stripes. (f) RSL in the alcoves of gullies, first reported in Fig. 14 of Ojha et al. (2014). HiRISE image credit: NASA/JPL/University of Arizona. CTX image credit: NASA/JPL-Caltech/MSSS.

Figure 11: Global gully trends on Mars. (a) Map showing the orientation of gullies and their relation to the occurrence of steep slopes, data from Conway et al. (2017). Red colour indicates gullies are 100% pole-facing, blue 100% equator-facing and yellow 50-50%. Darker shades are the locations where there are more steep slopes and lighter shades, fewer. In detail the number of pixels with 20° slopes derived from projection-corrected MOLA data was counted inside a 250 km moving window, which was then normalised by the true area of that moving window. The cutoff between the two shades is 3×10^{-3} steep pixels per km^2. MOLA hillshaded relief is in the background for context. (b) Comparison between the location of gullies (black-white), large glacier like forms (blue) and the roughness boundary of Kreslavsky and Head (2000) as an orange dashed line, thought to represent the equatorward limit of the LDM. Number of gully sites per km^2 of steep slope are given in black and white, where black is >250 and white is <250. The glacier like forms are compiled from the catalogues of Souness et al. (2012), van Gasselt (2007) and Levy et al. (2014). MOLA hillshaded relief is in the background for context. (c) Histograms showing the latitudinal distribution of glacier like forms (Lineated Valley Fill – LVF, Concentric Crater Fill – CCF, Lobate Debris Aprons – LDA all from Levy et al., 2014), dissected Latitude Dependant Mantle (LDM) from Milliken et al. (2003), slope-normalised gully density from Conway et al. (2018b) and raw counts of gullies from Harrison et al. (2015). LVF, CCF and LDA are given as number of landforms per 1° latitude bin. Dissected LDM is given as the percentage of MOC images per 2.5° latitude bin. Gullies are given as the mean number of sites per steep slope and counts in 5° latitude bins.

Figure 12: Frost visible in equator-facing and pole-facing alcoves of gullies in a 12-km-diameter crater located in the northern hemisphere in Acidalia Planitia. (a) Overview in HiRISE image ESP_052090_2450 overlain on CTX image P18_007995_2448. (b) Frost in the equator-facing alcove (black arrows), but on the facets of the alcove that do not face directly south. (c) Frost in the pole-facing alcove (black arrows), located at the most sheltered positions. HiRISE image credit: NASA/JPL/University of Arizona. CTX image credit: NASA/JPL-Caltech/MSSS.

Figure 13: Present-day activity in martian gullies. Images have been selected to best highlight the new morphology so are not necessarily the closest in time. For each row the leftmost image is the "before" image. The middle image is the "after" image, which is the same image used in the overview panel located on the far right. (a) A new dark flow, which is superposed on seasonal frost on the crater wall making it particularly visible even though the slope is in shadow. HiRISE images ESP_022688_1425 (before) and ESP_027567_1425 (after and overview). (b) New relatively light toned deposits on a gully-fan, highlighted by black arrows in the middle panel. HiRISE images ESP_014368_1435 (before) and ESP_031919_1435 (after and overview). (c) New massive deposit on the fan of a gully in Galap Crater, outlined in middle pane by arrows, this new deposit is lobate and contains boulders. HiRISE images PSP_003939_1420 (before) and ESP_032078_1420 (after and overview). (d) A newly incised channel branching off a pre-existing gully, highlighted by black arrow. HiRISE images ESP_013115_1420 (before) and ESP_032011_1425 (after and overview). HiRISE image credit: NASA/JPL/University of Arizona.

Figure 14: Dry mass wasting features. (a) Dry powder avalanches in the European Alps taken from the European Avalanche Warning Services (http://www.avalanches.org/eaws/en/includes/glossary/glossary_en_all.html). Hillslope length is approximately several hundred metres. (b) Deposits from 17th October (light grey) and 7th August pyroclastic flows at Mount Saint Helens, Figure 294 from Lipman and Mullineaux (1981). Lobe widths on the order of several tens of metres. (c) Experimental granular flows, where numbers across the top denote percentage of fines (white 150–250 μm ballotini) in natural sand (300–355 μm quartz). Adapted from Figure 4 of Kokelaar et al. (2014). Top-down photos of a 29° inclined plane where the mixture was dropped to give initial velocity. (d) Deposits of experimental granular flow of microbeads released onto an inclined plane at 25° as described in Félix and Thomas (2004), photo credit Nathalie Thomas. Lobe width ~8 cm. (e-f) Two views of a leveed channel created by an experimental granular flow of microbeads released onto an inclined plane at 25°, experiments described in Félix and Thomas (2004). In panel e the distance between the levees is ~17cm and in panel f there is a 10 cm interval between the lines. Photos courtesy of Nathalie Thomas. (g) Granular flow deposits at the foot of the scree slope on the western face of Hafnarfjall in Iceland. The channel width is approximately 2 m. Photo taken by S.J. Conway . (h) Dune slip face avalanche on a dune in the Namib desert near Walvis Bay, avalanche is approximately 50cm long. Photo taken by S.J. Conway. (i) Experimental slip face avalanche on a slope of 34° with a mean sand of diameter of 277 μm. Taken from Figure 2 of Sutton et al. (2013b). Avalanche is approximately 2 m long. (j) Granular flow under simulated low gravity conditions (spinning disk), taken from Figure 1 of Shinbrot et al. (2004). Copyright (2004) National Academy of Sciences.

Figure 15: Terraces and braided morphology in gullies on Earth. (a-d) Fluvial fans in the periglacial environment of Svalbard, showing braided channel morphology, terraces and cut banks. Panels a and c show a fan in Adventdalen, panels b and d show a fan in Bjørndalen (see also de Haas et al., 2015c). Source: HRSC-AX orthoimages from DLR (German Aerospace Centre), see Hauber et al. (2011a) for details. (e-f) Hillshaded images of debris-flow and fluvial fan in the arid Saline Valley (Mojave Desert, USA). Panels e and h show terraces and cut banks on a debris-flow fan, panel f shows braided channel morphology on an adjacent fluvial fan. Source: EarthScope Southern & Eastern California Lidar Project (www.opentopography.org).

Figure 16: Debris-flow deposits on Earth. (a) Debris-flow lobe deposit on a fan surface in periglacial environment of Svalbard. (b) Debris-flow lobe deposit in the Chilean hyperarid Atacama Desert (from Figure 2 of de Haas et al., 2015d). (c) Debris-flow channel with clearly-defined lateral levees on Svalbard. This channel is connected to the lobe shown in panel a. (d) Debris-flow channel with well-defined levees on the Dolomite Fan in the Mojave Desert (USA).

Figure 17: Secondary, post-depositional, modification of fan surfaces on Earth, masking the original depositional morphology. (a) Debris-flow fan surfaces covered by aeolian sand, in the Atacama Desert, Chile (from Figure 11 of de Haas et al., 2015d). (b) Polygonal ground on top of a debris-flow fan surface in Svalbard (from Figure 15 of de Haas et al., 2015c). (c) Hummocks on top of a fluvial fan surface in Svalbard (from Figure 15 of de Haas et al., 2015c). (d) Detail of the fan shown in panel a. (e) Detail of polygonal ground on fan in panel b (from Figure 15 of de Haas et al., 2015c). (f) Detail of hummocky ground on fan in panel c (from Figure 15 of de Haas et al., 2015c). (g) Desert pavement on top of a debris flow fan surface in Nevada (USA) (from Blair and McPherson, 1994). (h) Fluvial channels on a debris-flow fan surface in the Atacama Desert, Chile, as a result of secondary runoff; person for scale is 1.85 m tall (from Figure 11 of de Haas et al., 2015d). (i) Broken down clast on the surface of a debris-flow fan as a result of salt weathering in the Atacama Desert, Chile (from Figure 7 of de Haas et al., 2014).

Figure 18: Geophysical flows involving ice on Earth. (a) Low gradient slushflow cutting across Snøheim road in Norway taken from https://reccoprofessionals.files.wordpress.com/2011/05/slush_flow_no.jpg (b) Gully dominated by slushflow processes on the northwest flank of Mount Saint-Pierre, Québec (Canada) studied by Hétu et al. (2017) and taken from Figure 15 of the same paper – person for scale. (c) Cirque at McCarthy Creek, Wrangell St. Elias National Park, Alaska studied by Kochel and Trop (2008), right fan is dominated by avalanche processes and the left one by icy debris flows, taken from Figure 2A of Kochel and Trop (2008). (d) Icy debris flow on the left fan shown in panel c, where its length is approximately 50m taken from Figure 13A of Kochel and Trop (2008). (e) The fan on the right of panel c with a fresh wet snow avalanche deposit showing lateral levees and lobate snout. The avalanche deposit is approximately 200 m in length. Taken from Figure 8B of Kochel and Trop (2008). (f) Wet snow avalanche deposit Vallée de la Sionne in Switzerland showing complex morphologies, including lateral levees and overbank deposits, taken from Figure 1 of Bartelt et al. (2012). House in top right for scale. (g) Snow avalanche dominated debris fans in in Longyeardalen, Svalbard after Figure 7c of de Haas et al. (2015c). (h) Isolated boulders deposited by snow avalanches in Erdalen, Norway, taken by A. Decaulne on 27 August 2010. The largest rocks in the foreground are approximately 30 cm across.

Figure 19: Physical scale models of martian gullies. (a) Sediment transport engendered by liquid water over fine sand at 14° slope under low pressure (~7mbar) and low sediment temperature (-25°C) reported in Conway et al. (2011a). Water at the base of the flow has frozen solid and the flow propagated over a lens of frozen, saturated sediment. Bubbles formed by boiling were frozen into this mixture as the flow progressed. Tray is 1 m in length. Photo taken by S.J. Conway. (b) Sediment transport engendered by liquid water over an active-layer of several millimetres deep formed in saturated frozen fine sand at 14° slope under low pressure (~7mbar) reported in Jouannic et al. (2015). Bubbles visible across the surface are formed by gas produced within the sediment by boiling. Tray is 1 m in length. Photo taken by G. Jouannic. (c) Figure 4 from Védie et al. (2008) showing channels on a sloping active-layer formed in a frozen bed of silt caused by pulses of water from a perched aquifer. Top of the slope is 55 cm across and the experiments were performed under terrestrial pressure. (d) Sediment transport engendered by liquid water over fine sand at 20° slope under low pressure (~9mbar) and elevated sediment temperature (~25°C) reported in Raack et al. (2017) and Herny et al. (2018). White arrow points to sediment displaced by dry avalanches triggered by grain saltation at the flow front and black arrow saturated pellets levitated on cushions of gas released by boiling. Tray is 1 m in length. Photo taken by C. Herny.

Figure 20: Martian and terrestrial obliquity during the past 10 Ma (Laskar et al., 2004), along with estimated maximum gully ages. Maximum gully ages based on crater impact ages: Istok crater (Johnsson et al., 2014), Gasa crater (Schon et al., 2009a), Roseau crater (de Haas et al., 2018), Galap crater (de Haas et al., 2015a). Maximum gully age based on superposition relationship with Nirgal Vallis dune field from Reiss et al. (2004).

Figure 21: Gullies as a result of aquifer seepage at Ice River, Nunavut, Canadian High Arctic. (a) Satellite image overview of the zone containing the gullies with box indicating the location of panel b. Image credit Quickbird-2 © 2011 DigitalGlobe, Inc. (b) Detail of the gullies. Image credit Quickbird-2 © 2011 DigitalGlobe, Inc. (c) Oblique aerial view taken from Figure 4A of Grasby et al. (2014).

Figure 22: Active-layer detachment on Earth and potentially on Mars. (a) Gullies and candidate active-layer detachments (indicated by white arrows and boxes) in Yaren crater as seen in HiRISE image ESP_024086_1360 (after Johnsson et al., 2018). (b) Detail of shallow landslides from possible active-layer detachments in the lower gully-alcove. (c) Possible active-layer detachment scars in the upper alcove. (d) Active-layer detachment slides in Hanaskogdalen, Svalbard (from Hauber et al., 2011a). (e) Photograph of two active-layer detachment slides in panel d (from Figure 12 of de Haas et al., 2015c). (f) Active-layer detachment on a steep slope near Svea, Svalbard (from de Haas et al., 2015c). HiRISE image credit: NASA/JPL/University of Arizona.

Figure 23: Periglacial landform assemblage in northern Canada. (a) High centred polygonally patterned ground, Tuktoyaktuk Coastlands, with meltwater visible in polygon troughs, taken from Figure 14 of Soare et al. (2014a), polygons are ~20-50 m across. (b) Alases or thermokarstic depressions (Tuktoyaktuk Coastlands) surrounded by polygonally patterned ground, taken from Figure 2 of Soare et al. (2015). The thermokarst lake in the background is ~100 m across. (c) Cross section though a polygon margin revealing the ice-wedge (~2.5 m across at the top), Tuktoyaktuk Coastlands, taken from Figure 13 of Soare et al. (2014a). (d) Ibyuk Pingo with Split Pingo in the background, Northwest Territories, Canada, taken from Figure 7 of Soare et al. (2014b).

Figure 24: Gullies on Earth generated by snowmelt. (a) Satellite images of the gullies shown in panel b. Image credit GeoEye-1 © 2013 DigitalGlobe, Inc. (b) Debris flows in Jameson Land, Greenland, which occurred by the infiltration of melting snow during the summer season, taken from Figure 10.4 in Costard et al. (2007a). (c) Debris flow on the slopes above Ísafjörður in NW Iceland triggered by rapid snowmelt in 1999 (Track #1 of Decaulne et al., 2005), photo taken by John Murray in 2007. (d) Gullies studied by Levy et al. (2009) in Wright Valley, Antarctica. Polygonal patterned ground visible on the plateau and the depositional fans. Image credit GoogleEarth, DigitalGlobe.

Figure 25: Sliding sublimating CO_2-ice blocks down dunes as analogues for martian linear gullies, frames captured from the video included as Supplementary video 4 in Diniega et al. (2013), where block is released over a 20° slope on Kelso Dunes, California, person at dune brink for scale. Black arrows point to block at each time-step labelled t1 to t4.

Figure 26: Hillslopes with frosted granular flow in the St. Pierre river valley in Québec, investigated initially by Hétu and Vandelac (1989) and Hétu et al. (1994) and reported as a terrestrial analogue by Hughenholtz (2008a). (a) Overview of the hillslopes with debris flows and talus slope with frosted granular flow and (b) zoom showing the talus slope. (c) Photo from of the talus slope taken by taken by Maxime Chevalier. Panels a and b modified from Harrison et al. (2015) with image credit: Google Earth/CNES/Spot and c taken by Maxime Chevalier from Harrison (2016).

Figure 27: CO_2 gas-lubricated flow model from Figure 6 of Hoffman (2002). (A) Sunlight (black arrows) penetrates through the surface CO_2 frost and warms the underlying regolith. This causes the frost layer to sublimate at its base, destabilizing the slope and generating an avalanche. (B) A mixture of the CO_2 frost, gas, and entrained debris move downslope, with the frost continuing to degas and generating a vapour-lubricated flow.

Figure 28: Submarine gullies and canyons. Data from the USGS showing the bathymetry of the Los Angeles, California Margin surveyed between 1996 and 1999 and detailed in Gardner and Dartnell (2002).

Figure 29: Channelized deposits from different processes on different planetary surfaces, scale bars are 50 m in all cases. (a) Debris flow deposits in Svalbard, image credit DLR HRSC-AX campaign. (b) Lava flows on Tenerife, aerial image courtesy of IGN, Plan Nacional de Ortofotografía Aérea de España. (c) Self-channelling pyroclastic deposits at Lascar volcano, Chile, Pléiades image. (d) Depositional lobes in Istok crater on Mars, where channels (likely from debris flows) are formed as part of the depositional fans, HiRISE image PSP_007127_1345. (e) Fingering granular flows on the Moon, likely self-channelling dry granular flows (Shinbrot, 2007), LROC image M167036896. (f) Lobate deposit and associated channel on the Moon, perhaps from impact melt or ejecta processes, LROC image M143676946. HiRISE image credit: NASA/JPL/University of Arizona. LROC image credit: NASA/GSFC/Arizona State University.

Table 1: Summary of Earth analogues used for comparison to martian gullies, including the climate and which gully formation model they have been used to support. The analogues are listed by continent and then by site (in descending latitude) and grouped by team where appropriate.

Continent	Authors	Location(s)	Climate type	Ground conditions	Process	Trigger	In support of:
Antarctica	Marchant and Head (2007), Dickson and Head (2009), Levy et al. (2009, 2007), Dickson et al. (2018, 2007), Morgan et al. (2007)	McMurdo Dry Valleys	hyper-arid cold polar desert	permafrost at 35-45 cm	pure water flow	insolation	surface melt, influence of brines, no rain, snow drifting
Antarctica	Harris et al. (2007)	McMurdo Dry Valleys			groundwater and surface flow of brines	meltwater	shallow groundwater
	Lyons et al. (2005)				groundwater seep	melting of subsurface ice	shallow groundwater
Antarctica	Hauber et al. (2018)	Northern Victoria Land	hyper-arid cold polar desert	permafrost	debris flows, percolation	meltwater	meltwater from ice and/or snow, highlight as analogue
S. America	Heldmann et al. (2010)	Atacama desert, Chile	arid desert	dry	debris flows	rare rain event	fluvial processes
S. America	Oyarzun et al. (2003)	Atacama, Chile, Road from Copiapo´ to Maricunga	arid desert	dry	mudflow		water in gullies from the surface or groundwater
S. America	de Haas et al. (2015d, 2014)	Atacama Desert coast, northern Chile	arid desert	dry	debris flow	rare rain events	role of secondary modification on fan morphology
S. America	Conway and Balme (2016)	Quebrada de Camarones, Atacama, Chile	arid desert	dry	dry rockfalls	unknown	counter-example for water hypotheses from morphometrics
S. America	Pacifici (2009)	Santa Cruz region, Argentinean Patagonia	arid steppe highlands	progalcial deposit, unknown if ice			highlight as an analogue
S. America	Pilorget and Forget (2016)	Lascar, Chile	desert	dry	pyroclastic	volcanic eruption	CO_2
S. America	Stewart and Nimmo (2002)						Counter-example, support instead water hypotheses
N. America	Costard et al. (2007a, 2002)	Jameson Land, E. Greenland	dry periglacial	thick permafrost, active-layer 1 m	debris flows	melting permafrost	melting in the near surface
N. America	Lee et al. (2006, 2004, 2002, 2001)	Devon Island, High Arctic; valleys and Haughton impact	polar desert climate	talus	debris flows	all temperature triggered (very transient)	surface snowmelt
				talus	snow gullies	snow gullies, surface snowmelt	
N. America	Oskinski et al. (2006)	Arctic Canada		permafrost			highlight as an analogue
N. America	Andersen at al. (2002)	Axel Heiberg Island, Canada	polar desert climate	permafrost 600 m thick	brine flow from groundwater		groundwater
N. America	Heldmann et al. (2005)	Axel Heiberg Island, Canada		permafrost	brine flow from groundwater		brines

Continent	Authors	Location(s)	Climate type	Ground conditions	Process	Trigger	In support of:
N. America	Grasby et al. (2014)	Ellesmere Island, Nunavut, Canadian High Arctic	polar desert	permafrost	fluvial	spring	groundwater
N. America	Soare et al. (2018, 2014a, 2014b, 2007)	Tuktoyaktuk, NWP, Canada	thermokarst - degraded permafrost areas	permafrost and substantial segregated ice lenses	long term temperature increase and thaw	possibly insolation triggered snowmelt, or permafrost melting	melting near surface
N. America	Hugenholtz et al. (2007)	Bigstick Sand Hills - southwestern Saskatchewan, Canada	continental	permafrost	debris flow	snowmelt and niveo-aeolian	melt
N. America	Hugenholtz (2008b)	St. Pierre valley, Gaspé region, Québec	continental, humid	talus, possible permafrost	frosted granular flow	temperature oscillations around freezing	frosted granular flow
N. America	Kochel and Trop (2008)	Wrangell Mountains, Alaska	supraglacial	substantial snow and ground ice on debris fans	icy debris flow snow avalanche	rainfall solar heating	generic process analogue
N. America	Conway et al. (2011b) Conway and Balme (2016)	St Elias Mountains, Alaska	Periglacial	talus, discontinuous permafrost	rockfalls	unknown	counter-example for water hypotheses from morphometrics
N. America	Hooper and Dinwiddie (2014)	Great Kobuk Sand Dunes, Alaska	subarctic		debris flow, fluvial	snowmelt and niveo-aeolian	near surface melt
N. America	Conway et al. (2015b, 2011b) Conway and Balme (2016)	Front Range, Colarado	mountainous periglacial	talus	debris flow	unknown	water hypotheses from morphometrics
N. America	de Haas et al., (2015d)	Panamint Valley, Death Valley, California	desert		Debris flow, secondary aeolian modification		role of secondary modification on fan morphology
N. America	Conway et al. (2015b, 2011b) Conway and Balme (2016)	San Jacinto Fault, Death Valley, Lucerne Valley and Anderson Dry Lake, California	desert	dry	fluvial	precipitation	water hypotheses from morphometrics
N. America	Eyles and Daurio (2015)	Ubehebe Crater, Death Valley, California	desert	dry porous volcanic products	fluvial gullies assocated with protalus ramparts		highlight as an analogue in terms of snow-driven processes
N. America	Kumar et al. (2010), Yue et al. (2014) Conway and Balme (2016)	Meteor Crater, Arizona	arid, wetter in past	dry	fluvial and debris flow	rainfall, snowmelt and springs	water hypotheses, debris flow
Europe & N. America	Treiman (2003)	Adventdalen, Svalbard; Ashcroft, Colorado			snow avalanches		dry granular flow
Europe	Reiss et al. (2011, 2010b, 2009b), Hauber et al. (2011a, 2011b, 2009), Johnsson et al. (2014, 2012), Conway and Balme (2016)	Svalbard, Norway	arctic desert	permafrost	fluvial and debris flow		water hypotheses, meltwater, snowmelt fluvial, debris flow, influence of freeze-thaw cycles, landscape assemblage in periglacial environment

Continent	Authors	Location(s)	Climate type	Ground conditions	Process	Trigger	In support of:
Europe	Hartmann et al. (2003)	Esja Plateau, Iceland	periglacial	ground sometimes frozen	debris flow	snowmelt, connected to drainage,	water hypotheses
Europe	Conway et al. (2015b, 2011b) Conway and Balme (2016)	Westfjords & Tindastóll, Iceland	fjordlands, periglacial	talus	debris flow	Snowmelt, heavy precipitation	water hypotheses from morphometrics
Europe	Mangold et al. (2003b) 2003	Southern French Alps	alpine	talus	debris flows		debris flow
Europe	Marquez et al. (2005) Conway et al. (2015b)	La Gomera, Canary Islands	warm and wet	no ice, dry talus with calcrete	fluvial	aquifer outflow	groundwater water hypotheses from morphometrics
Oceania	Hobbs et al. (2014)	Island Lagoon near Woomera, Australia	semi-arid		fluvial	overland flow	water and dry
		Pasture Hill, New Zealand	periglacial		fluvial	frost processes, rain, snowmelt	
	Hobbs et al. (2013)	Lake George escarpment, Australia	arid		surficial runoff		water and LDM melt
	Hobbs et al (2015)	all three of the above					water and melt
	Hobbs et al. (2016)	Cooma, Australia	arid		runoff	rainfall	
Asia	Komatsu et al. (2014)	Lonar Crater, India	tropical savanna	humid soils	debris flow, fluvial	groundwater and overland flow	highlight as an analogue
Asia	Xiao et al. (2017)	Qaidam Basin, Tibetan Plateau (NW China)	high elevation desert		fluvial	rainfall	highlight as an analogue
Asia	Anglés and Li (2017)	Qaidam Basin, Tibetan Plateau (NW China)	high elevation desert				overland flow or melt
Asia	Sinha et al. (2018)	Ladakh Himalaya	high elevation desert	talus and alluvial fans	debris flow	snowmelt	debris flow from snowmelt
Asia	Yue et al. (2014) Wang et al. (2013)	Xiuyan Crater, NE China	humid, continental	humid soils	fluvial	precipitation	water hypotheses and dry processes
Several	Hugenholtz and Tseung 2007	Escuer fan in central Spanish Pyrenees, intense thawing of frozen sand Canada, New Zealand, beach sand fans triggered by groundwater, Spain base of cliffs with ephemeral groundwater.			debris flow dominated alluvial fans		debris flow

figure 1

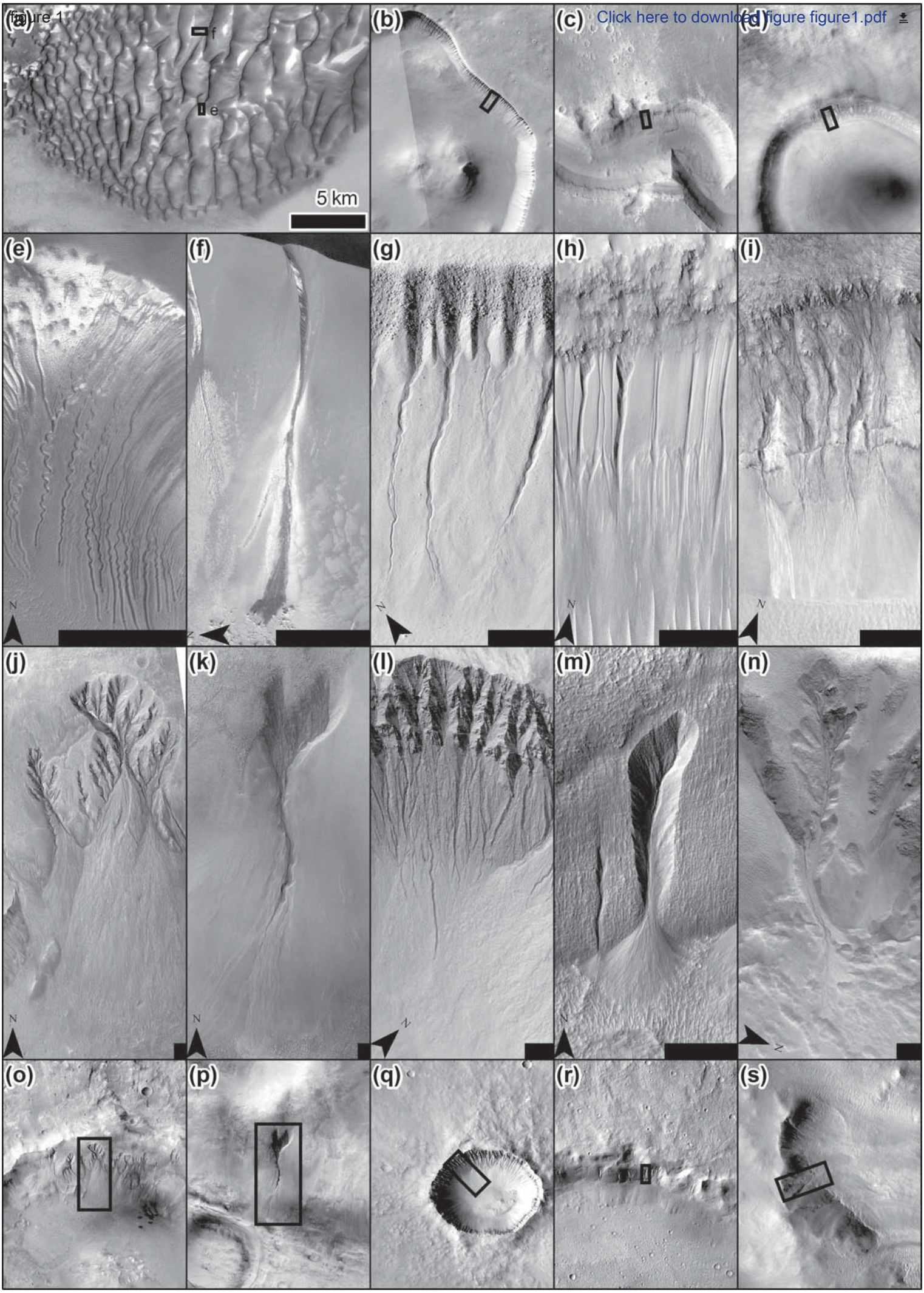

figure 2

Click here to download figure figure2.pdf

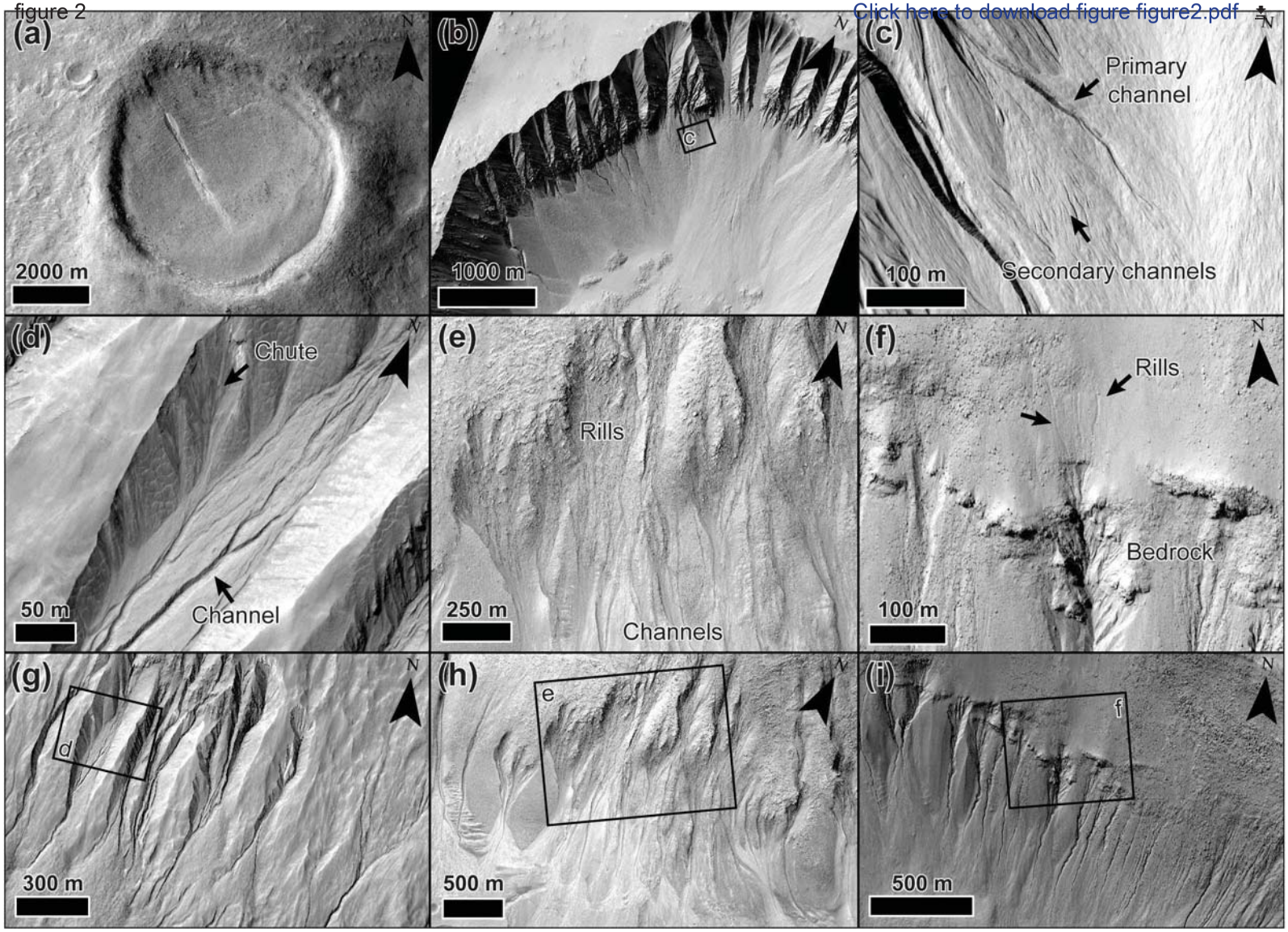

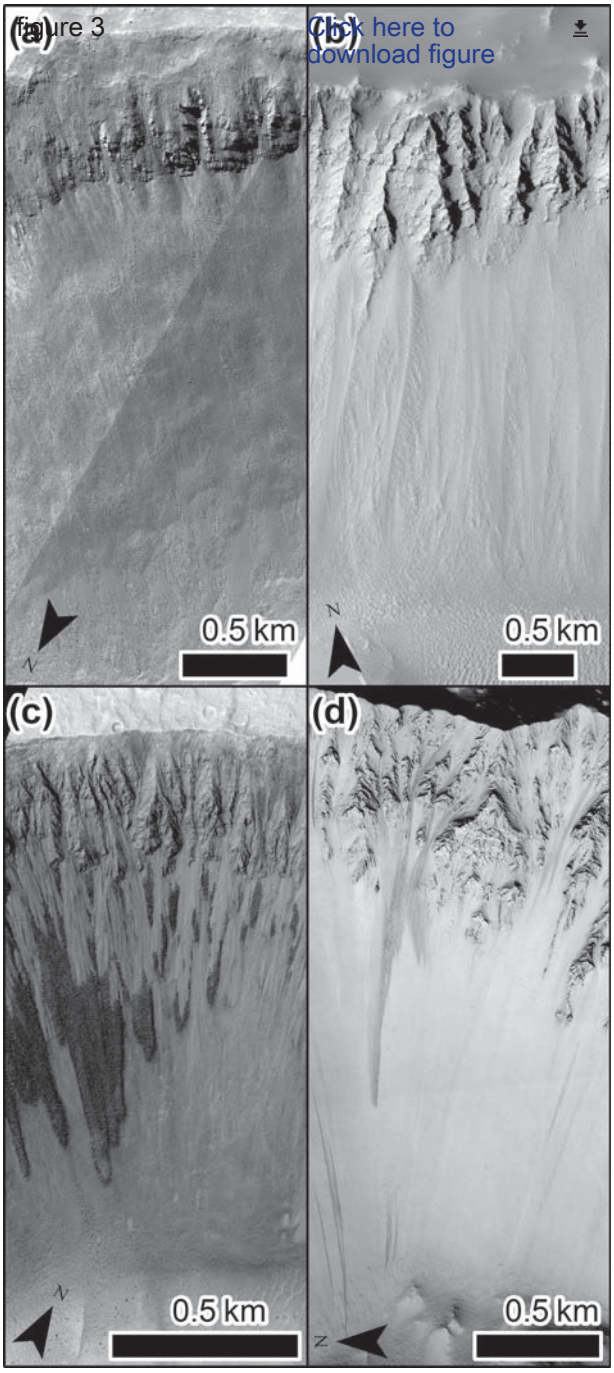

Figure 4

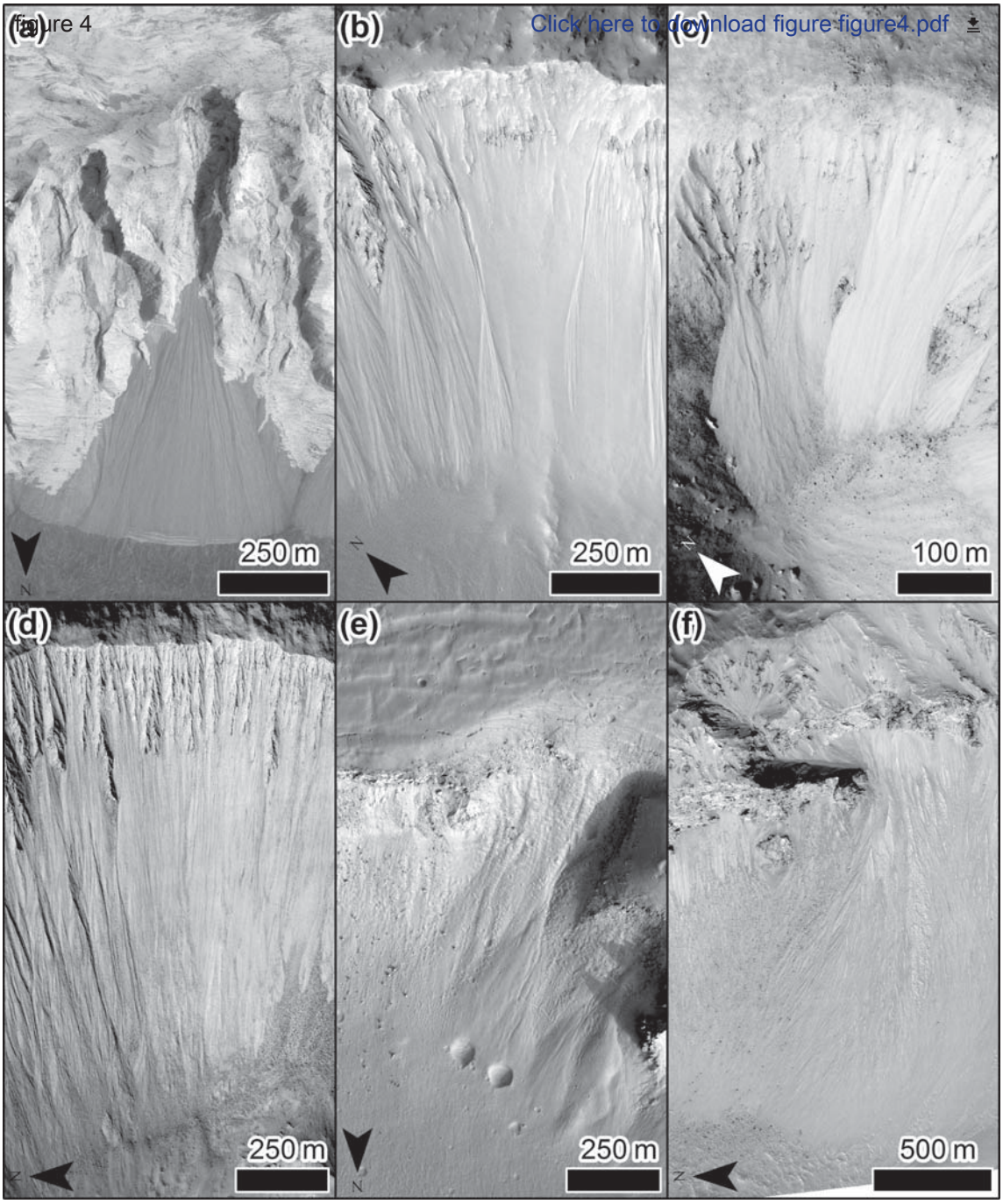

figure 5

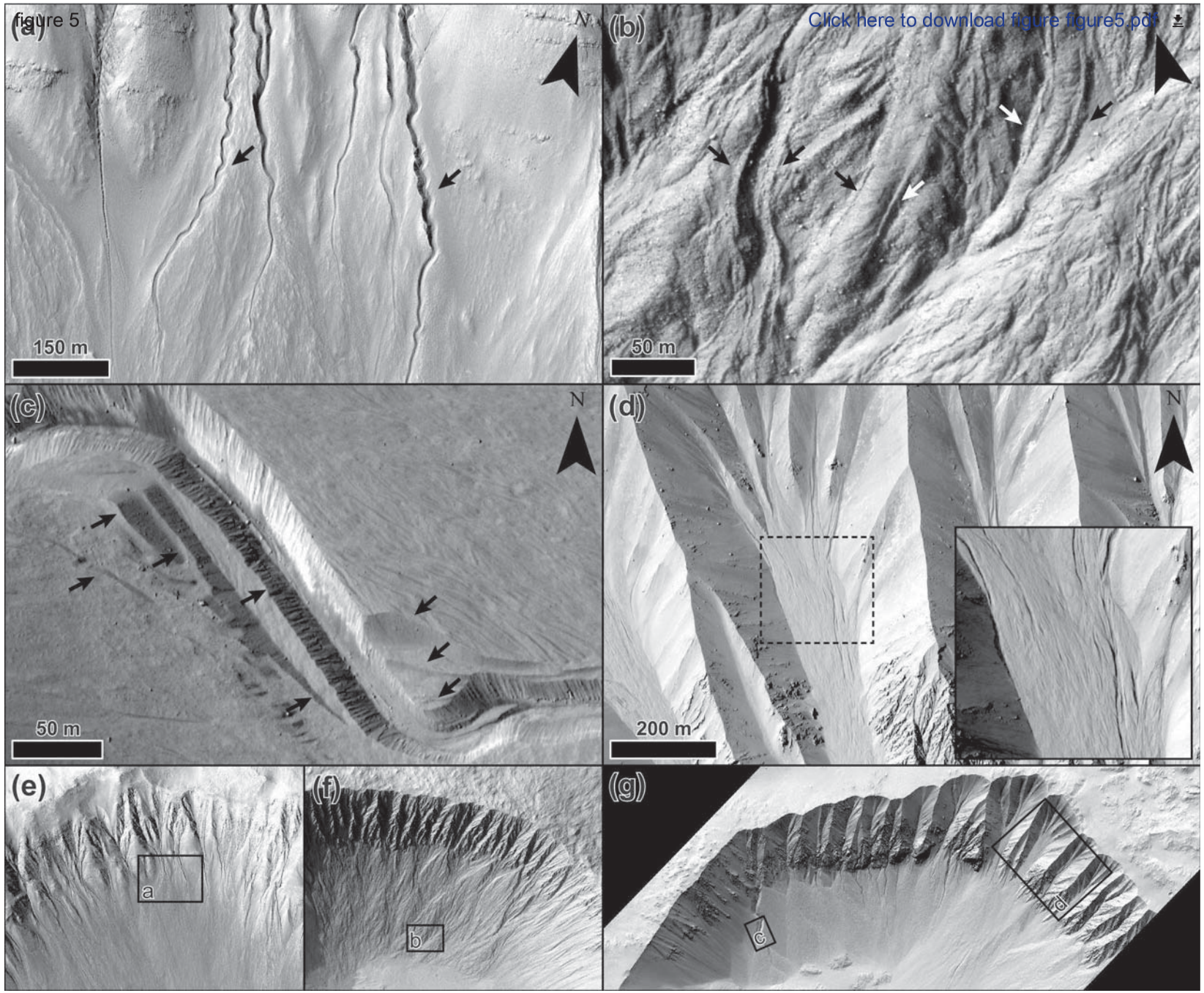

figure 6

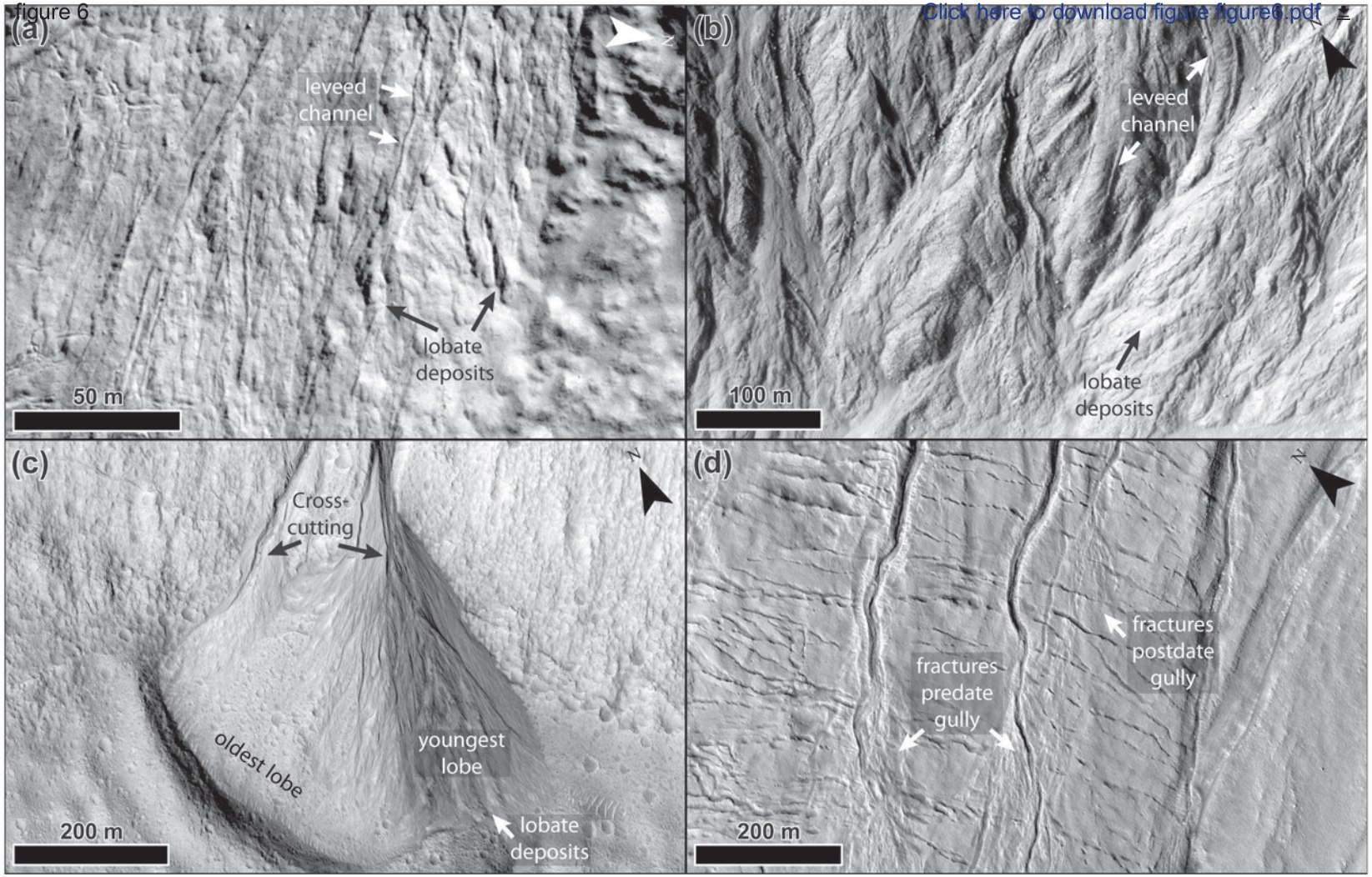

Figure 7

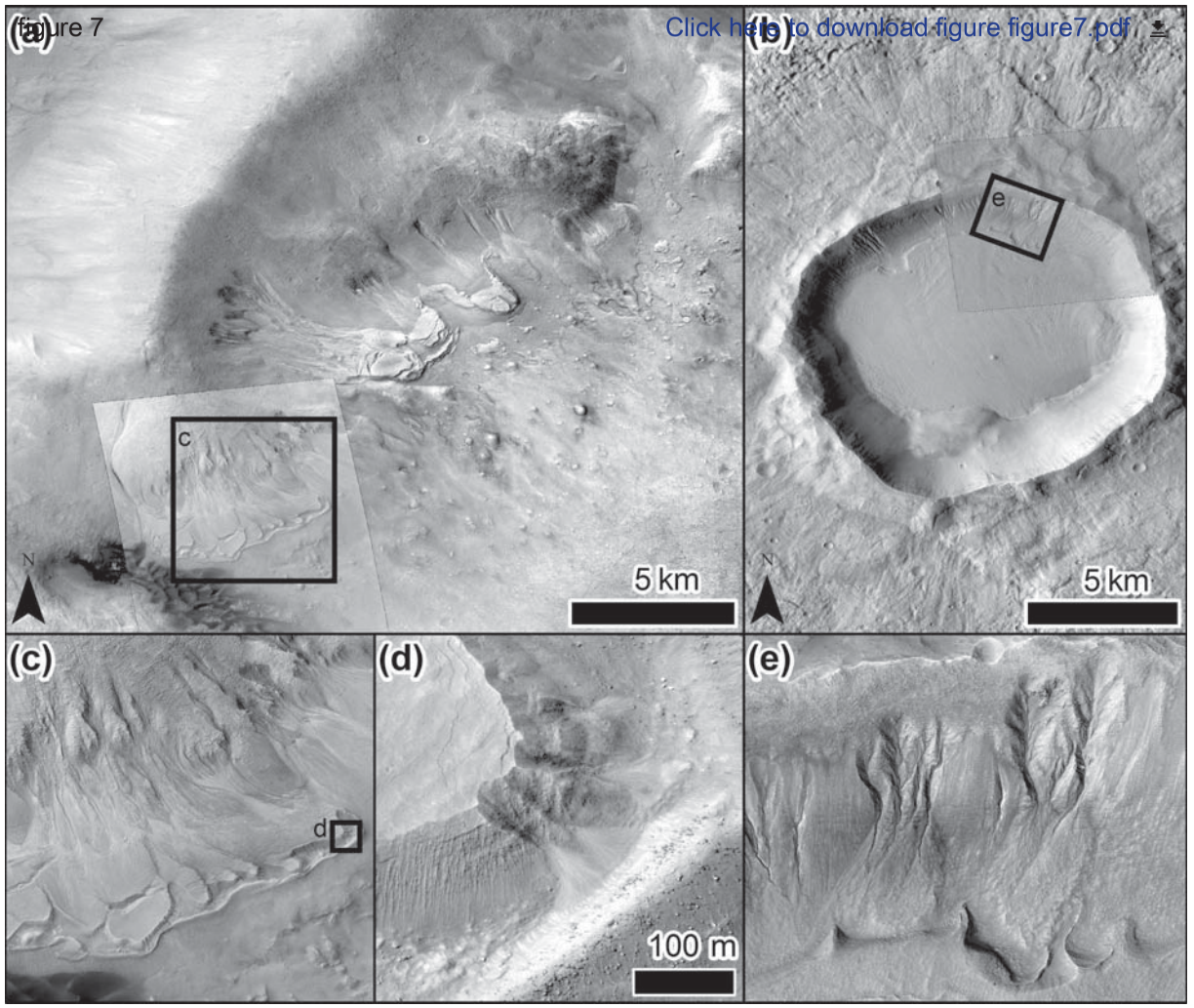

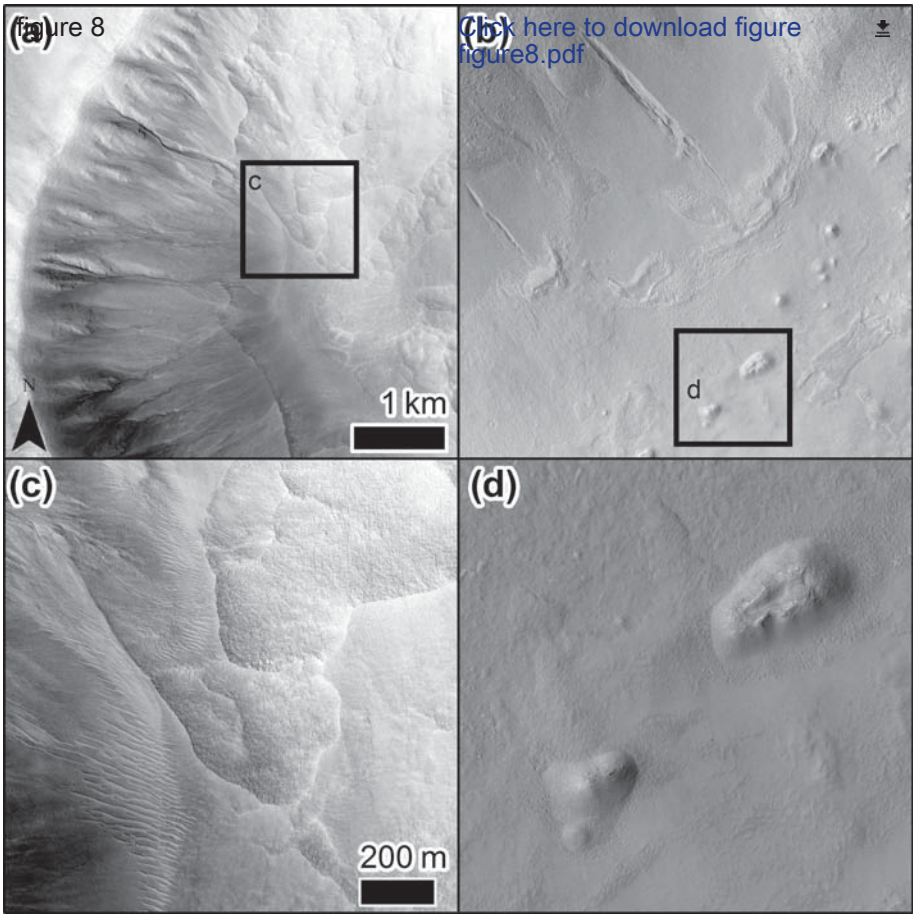

figure 9

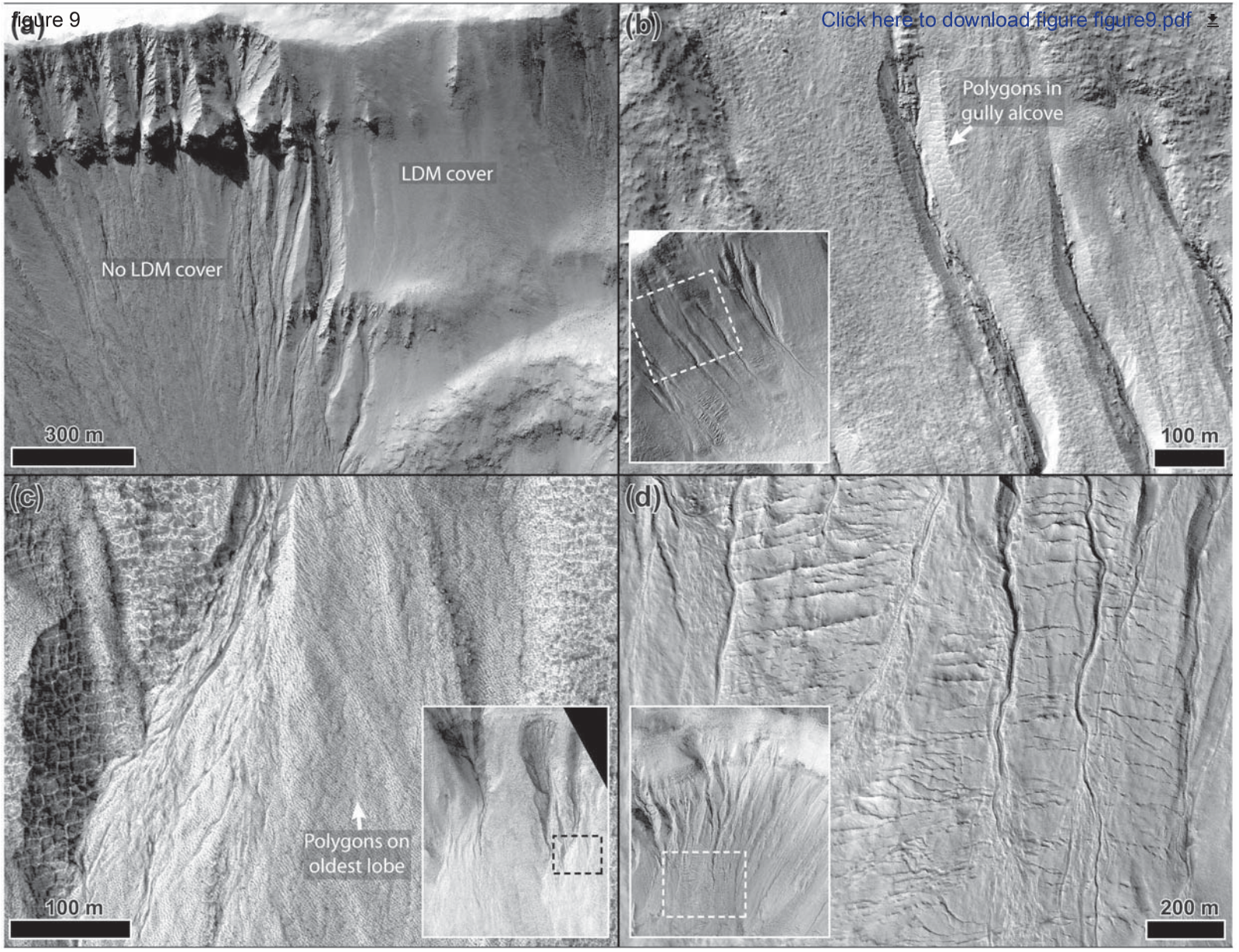

Figure 10

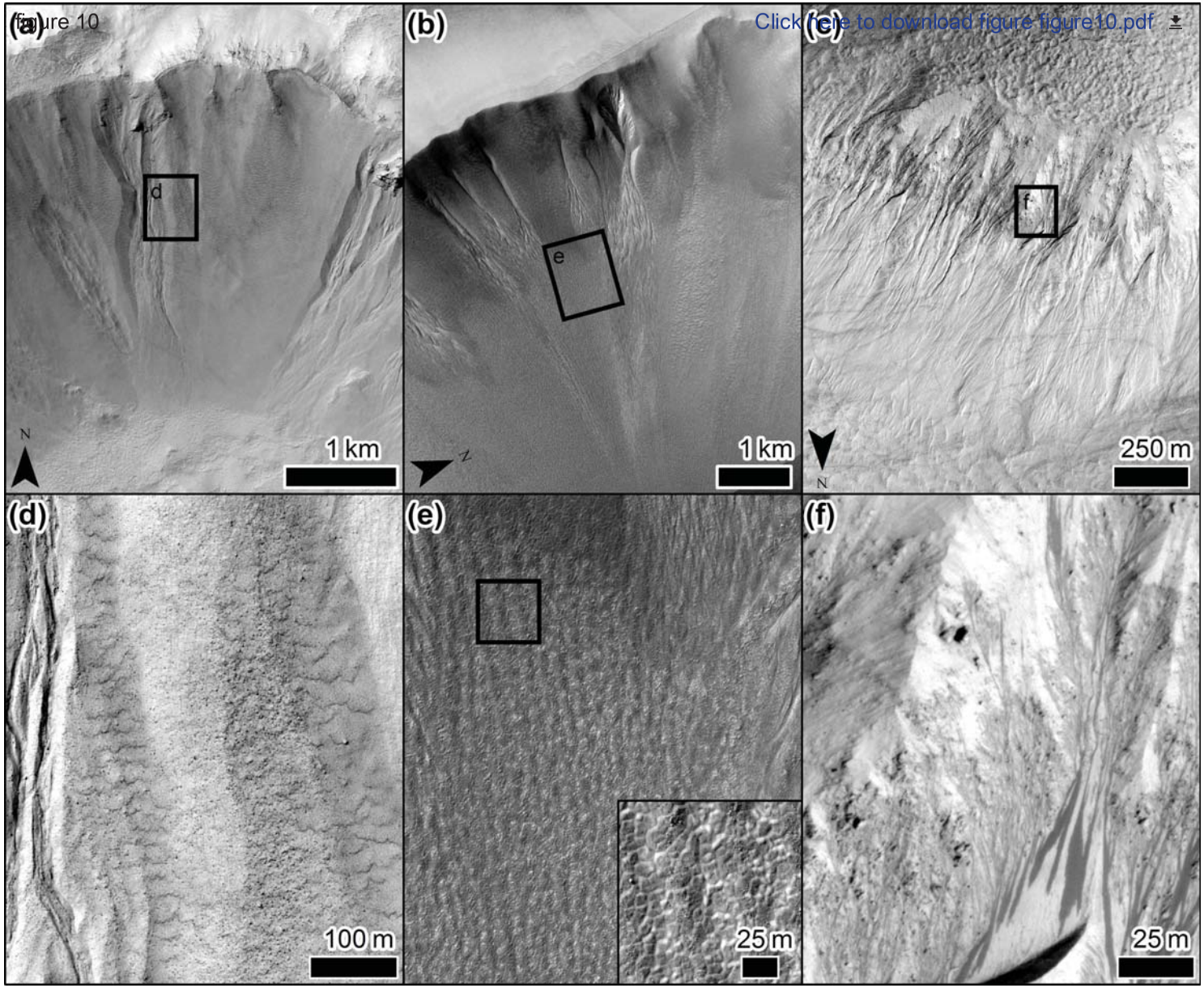

figure 11

Click here to download figure figure11.pdf

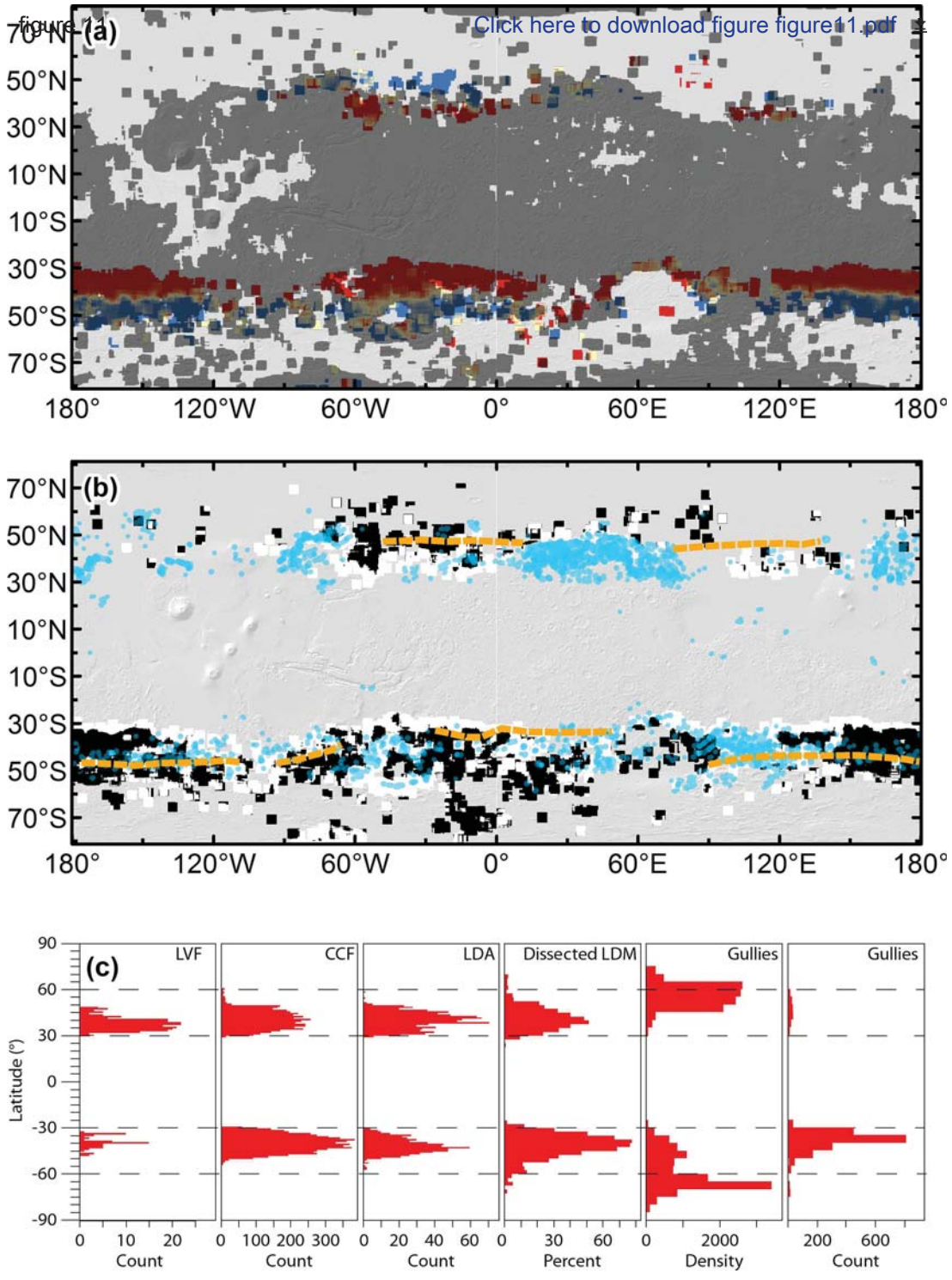

figure 12

Click here to download figure figure12.pdf

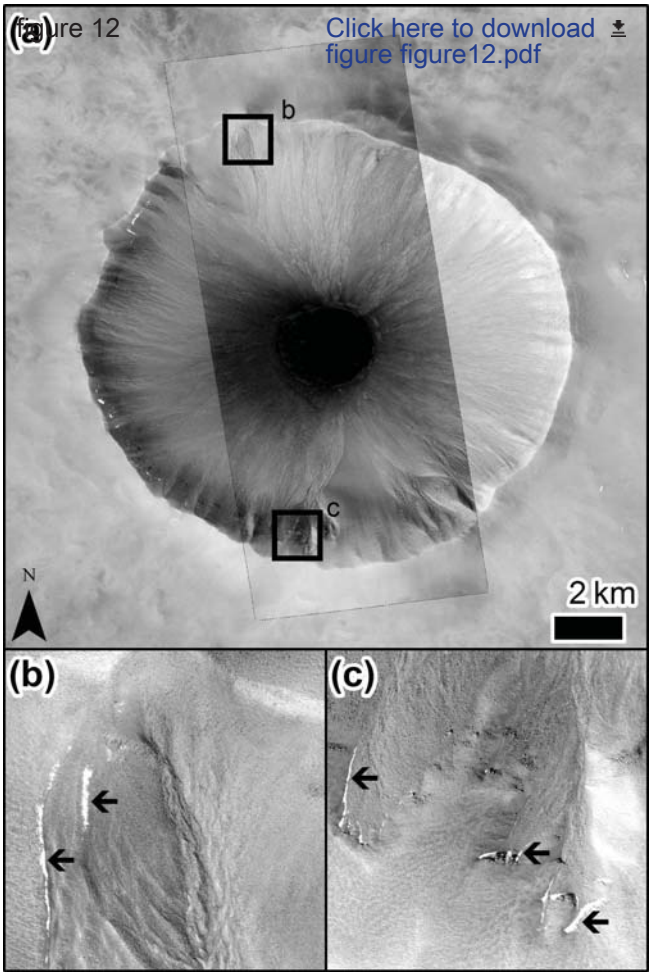

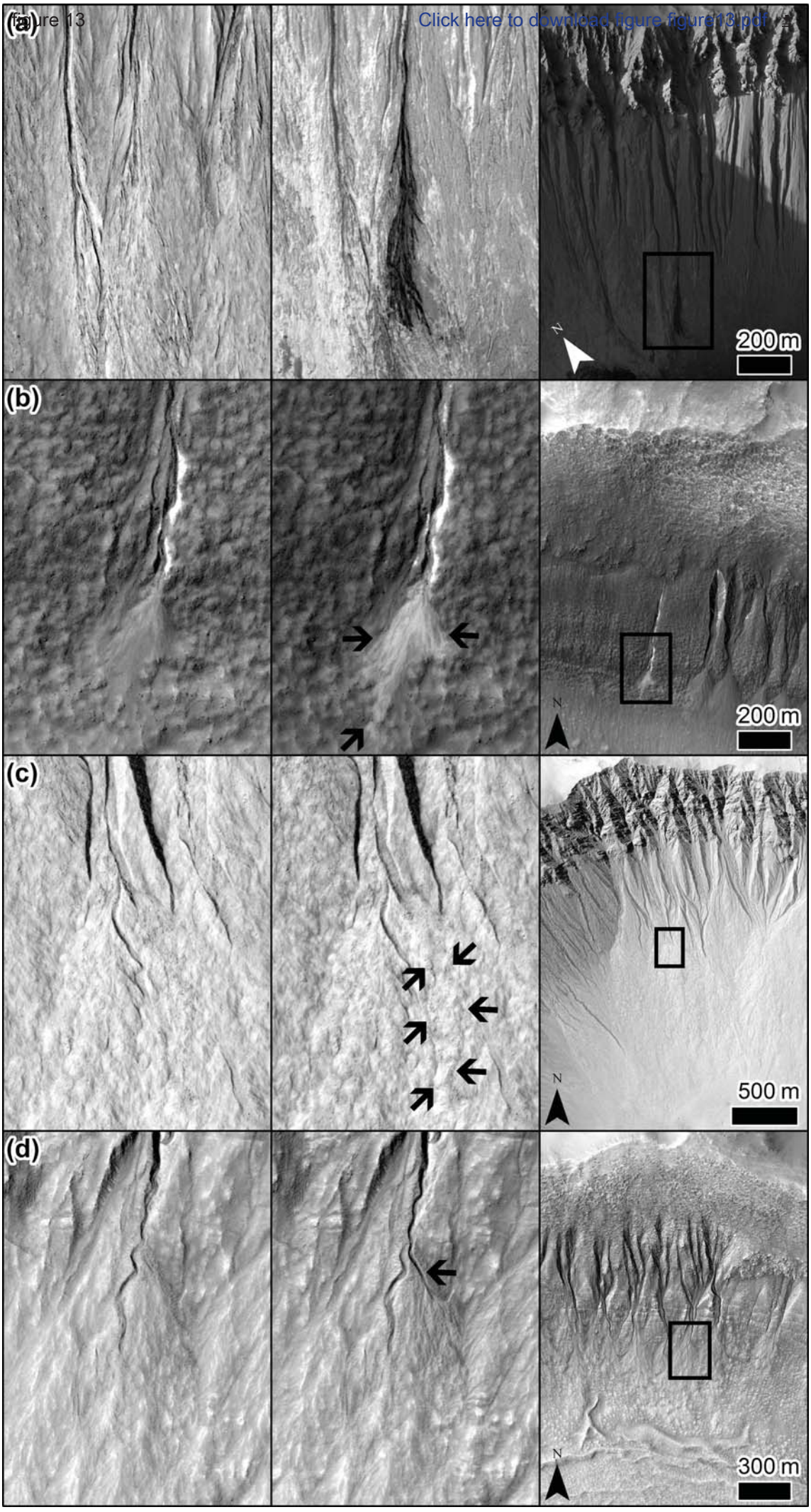

Figure 14

Click here to download figure: figure14.pdf

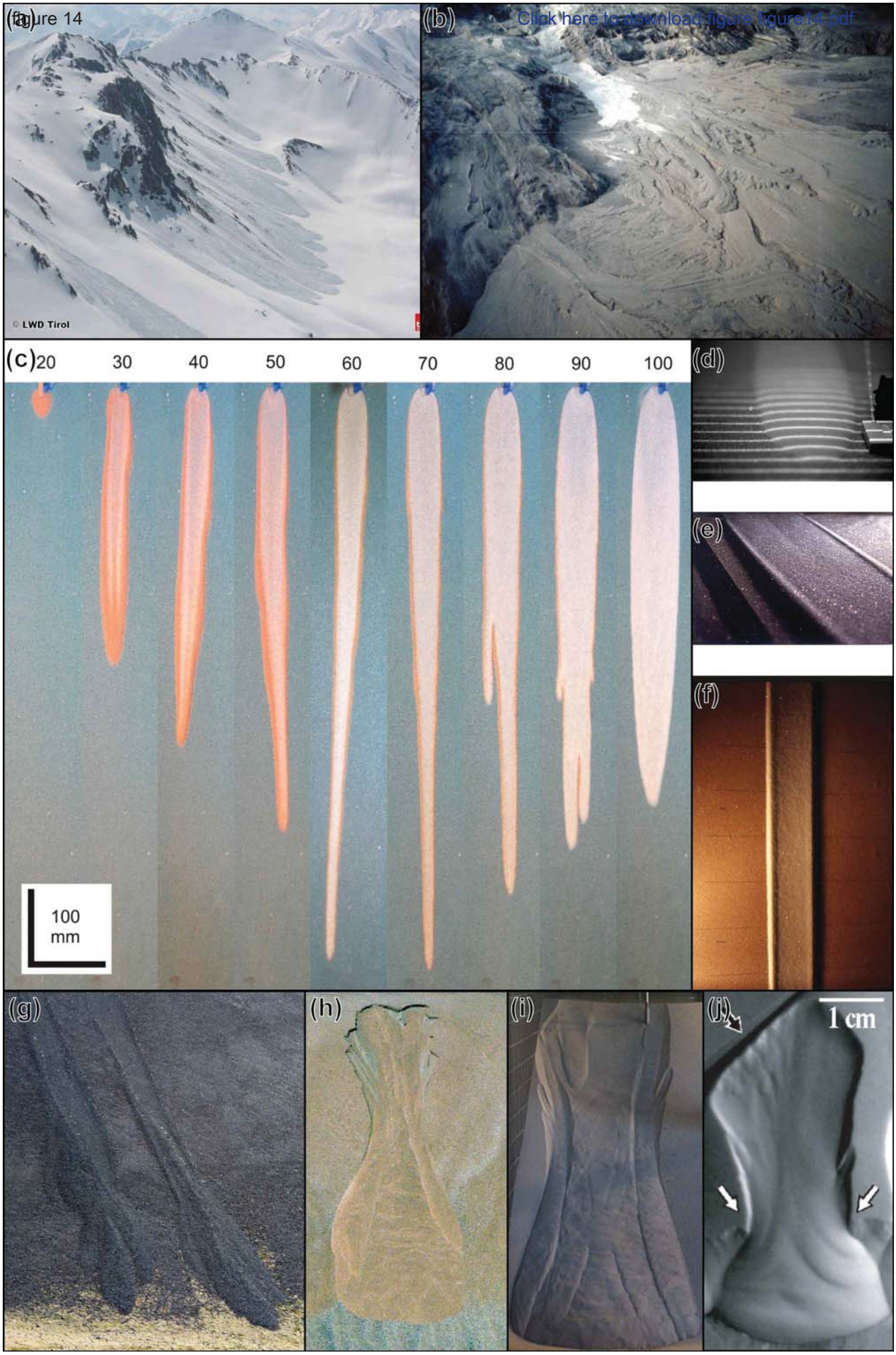

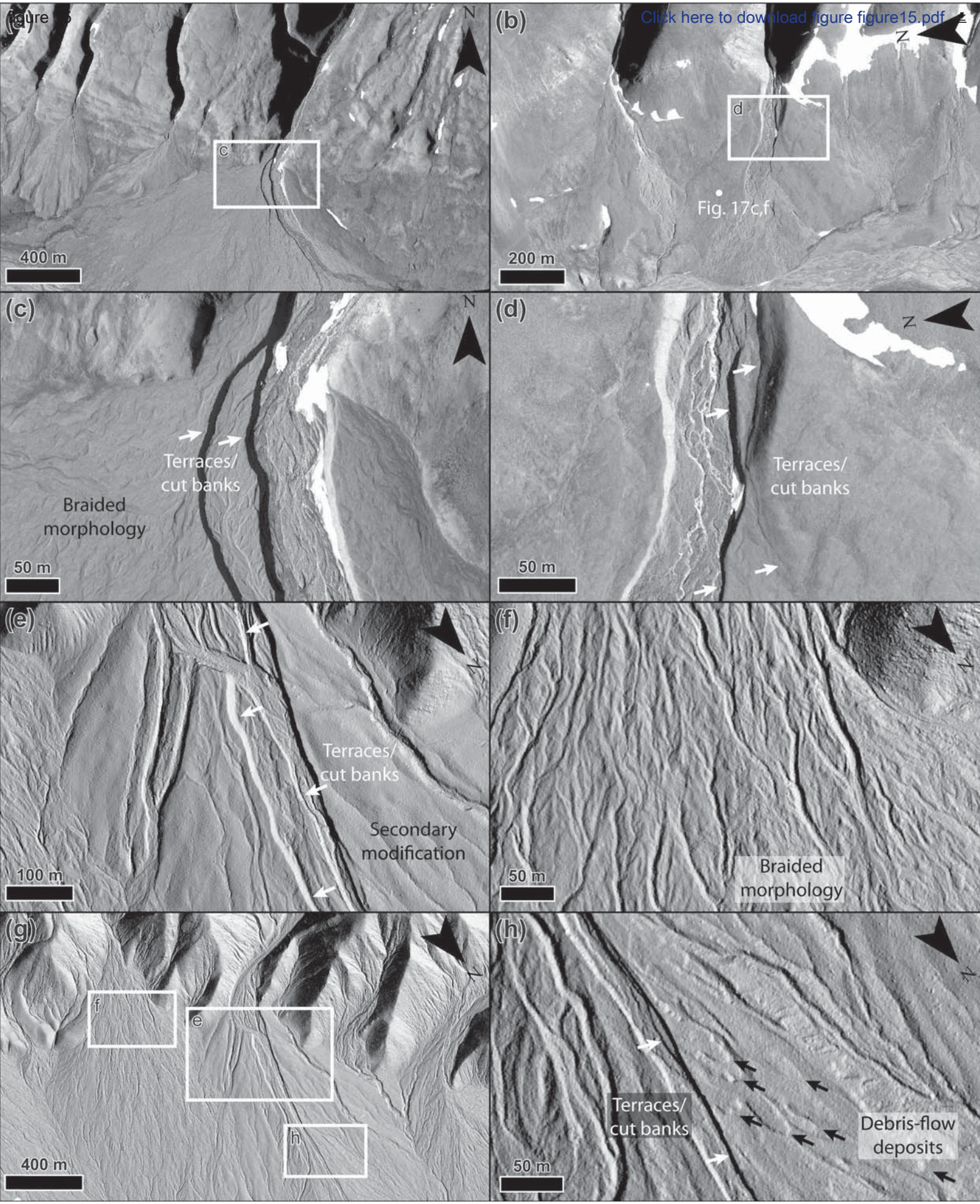

figure 16

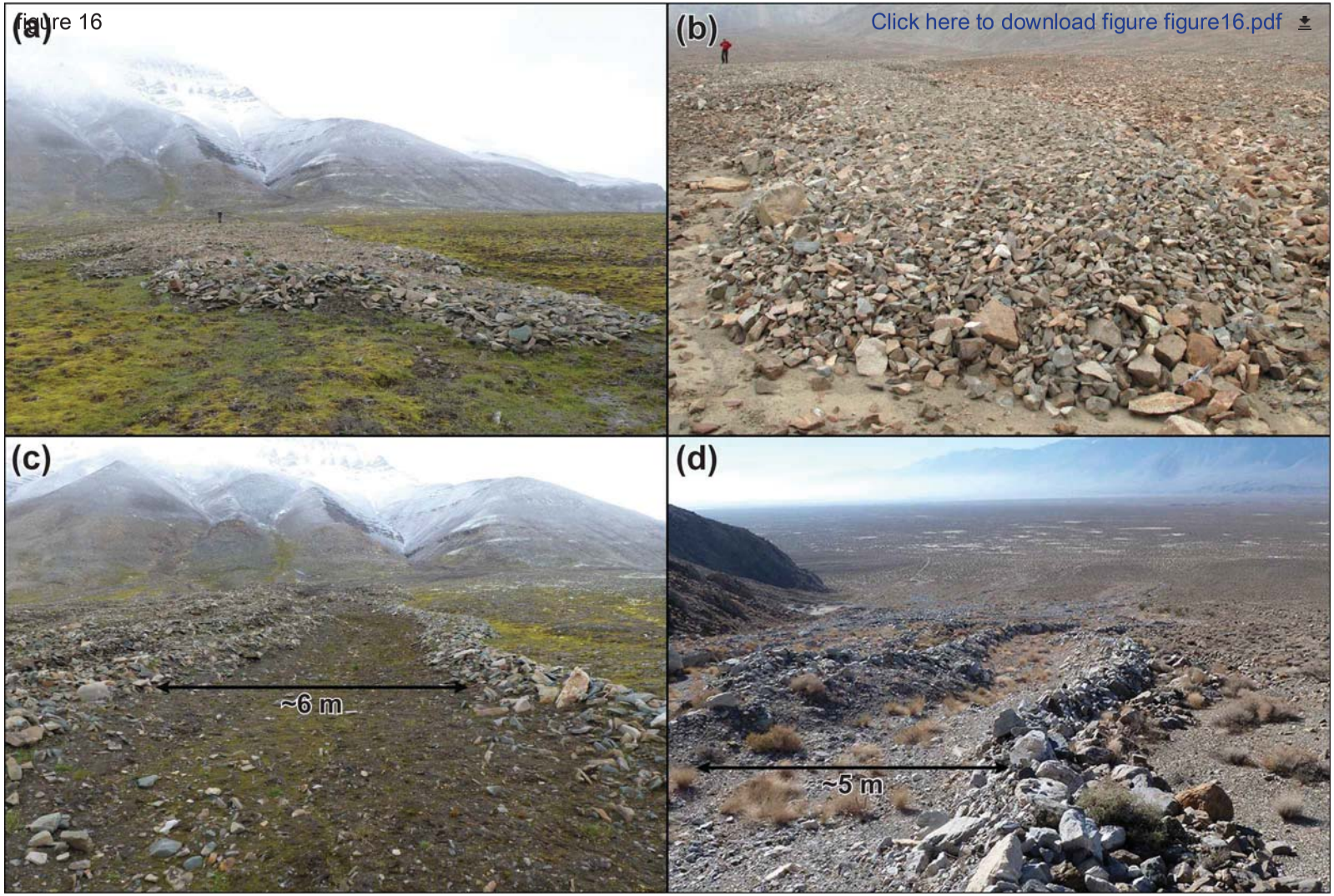

Figure 17

Click here to download figure figure17.pdf

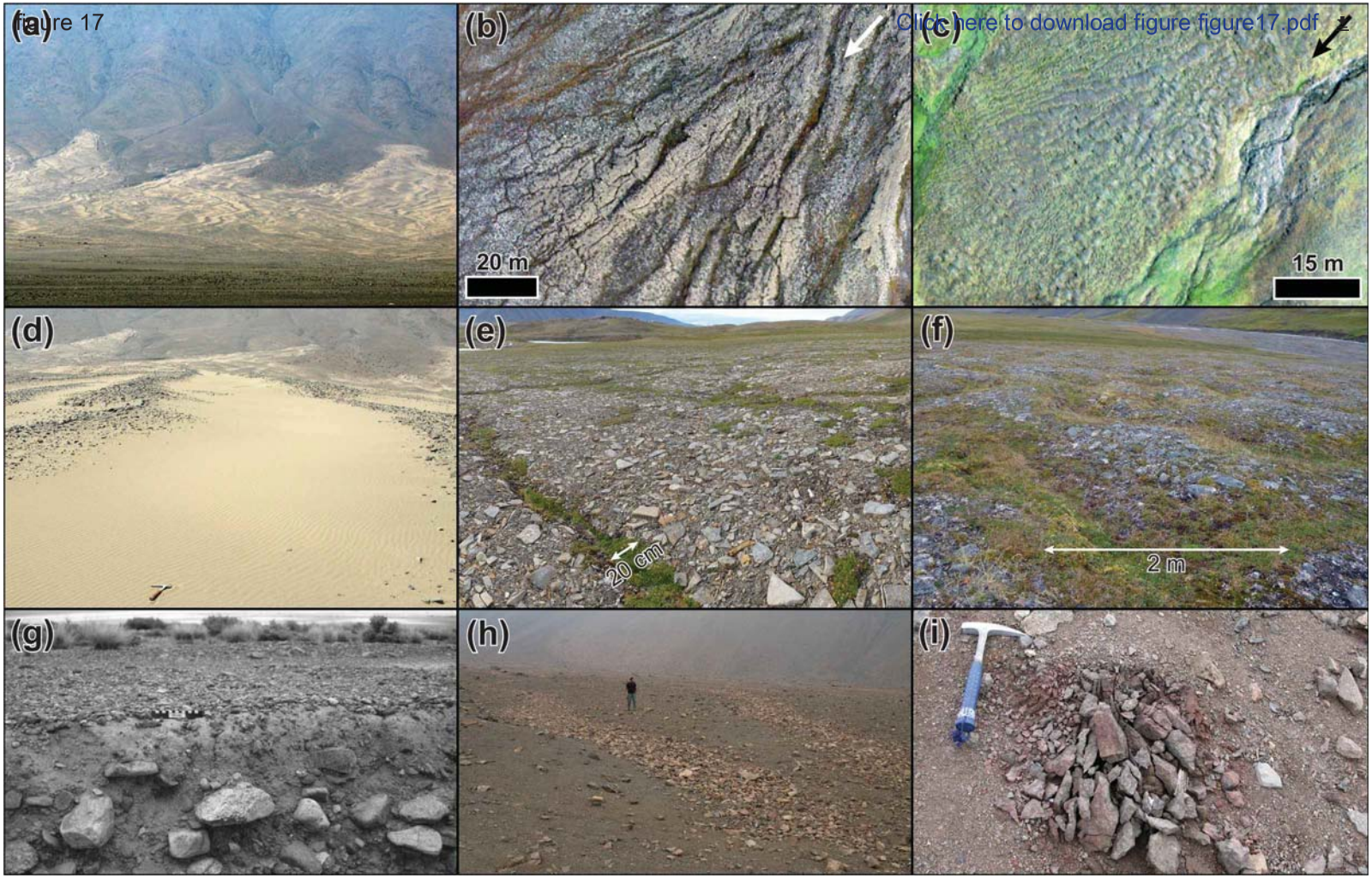

Figure 18

Click here to download figure
figure18.pdf

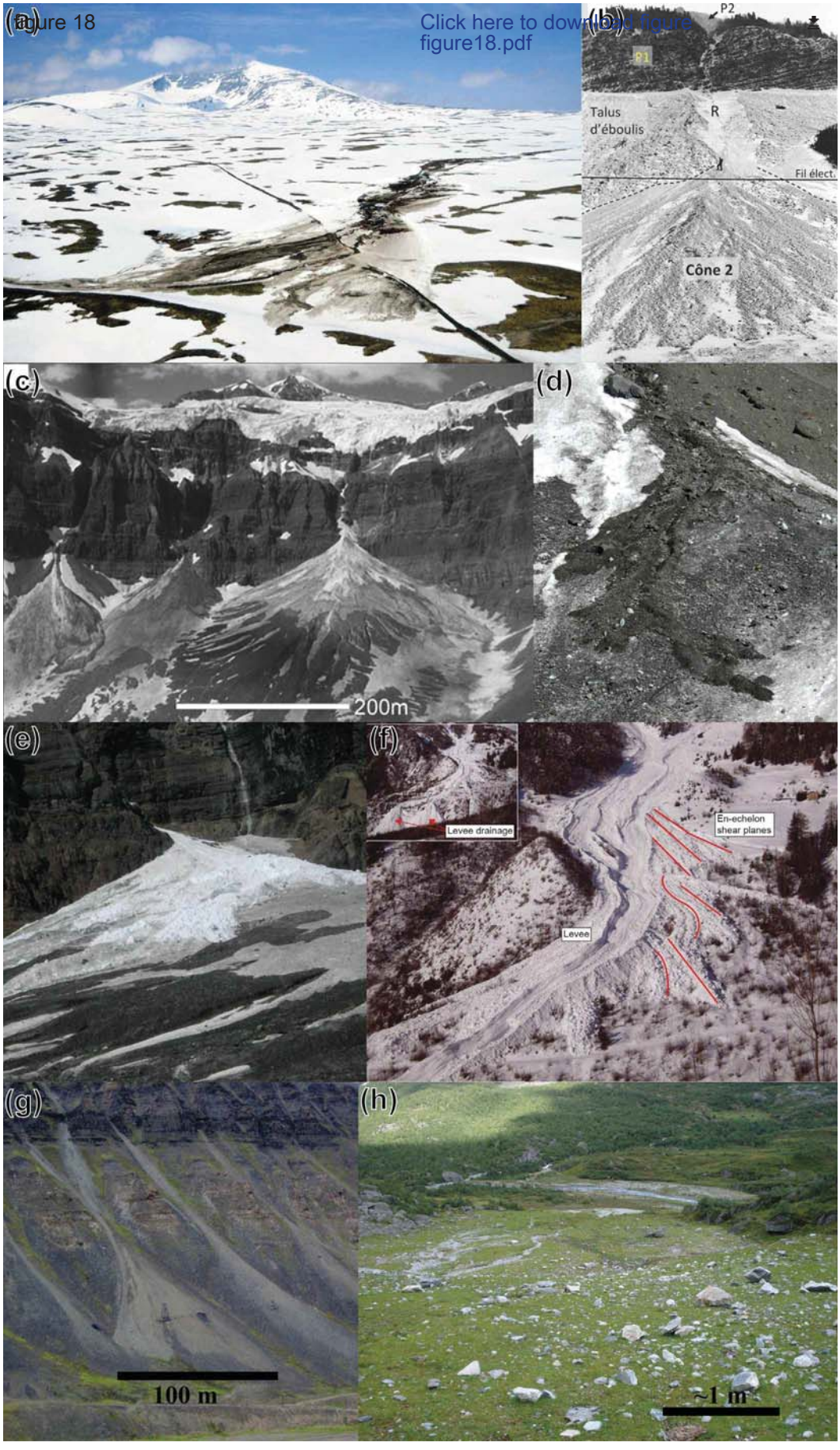

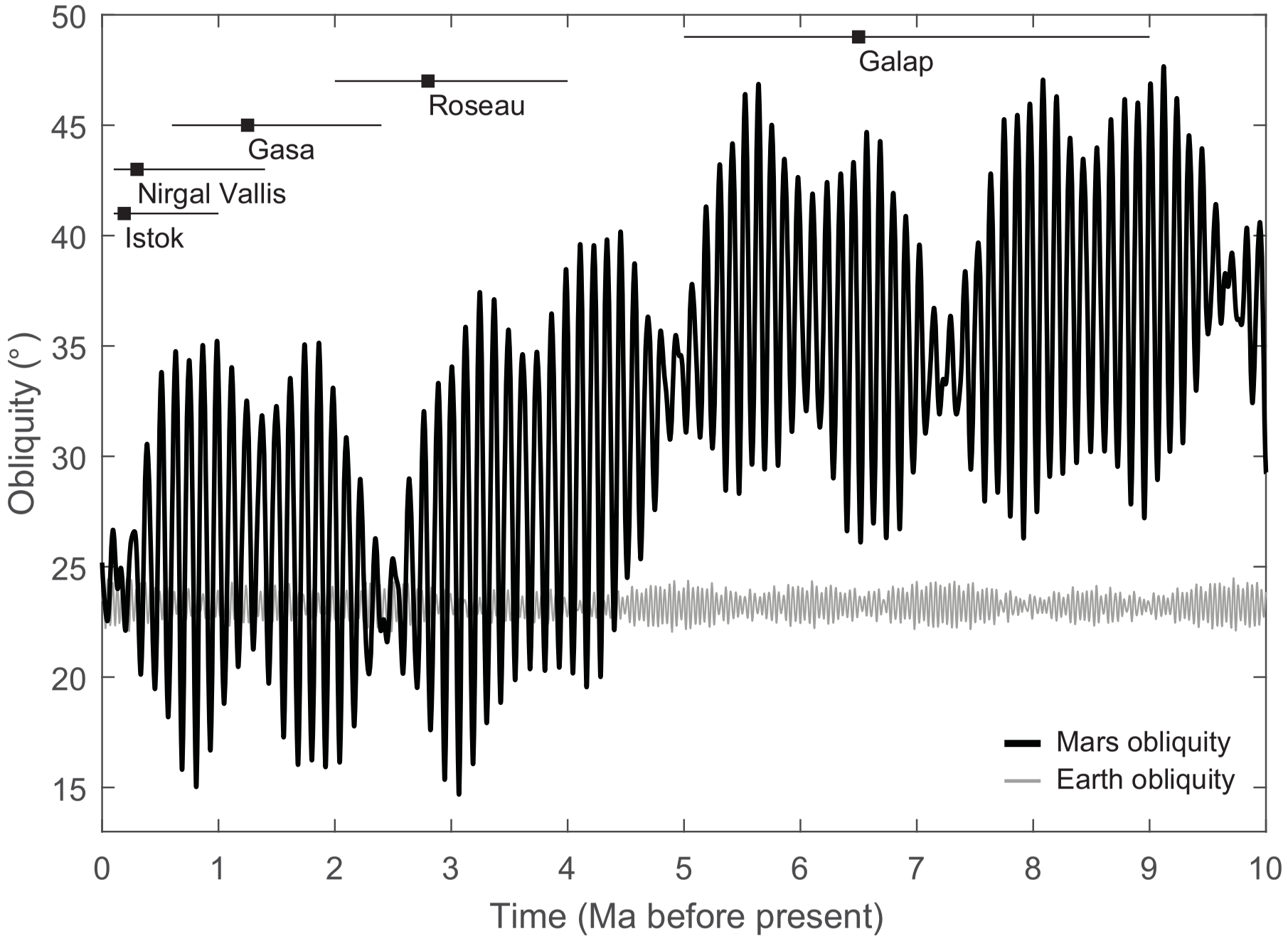

Figure 21

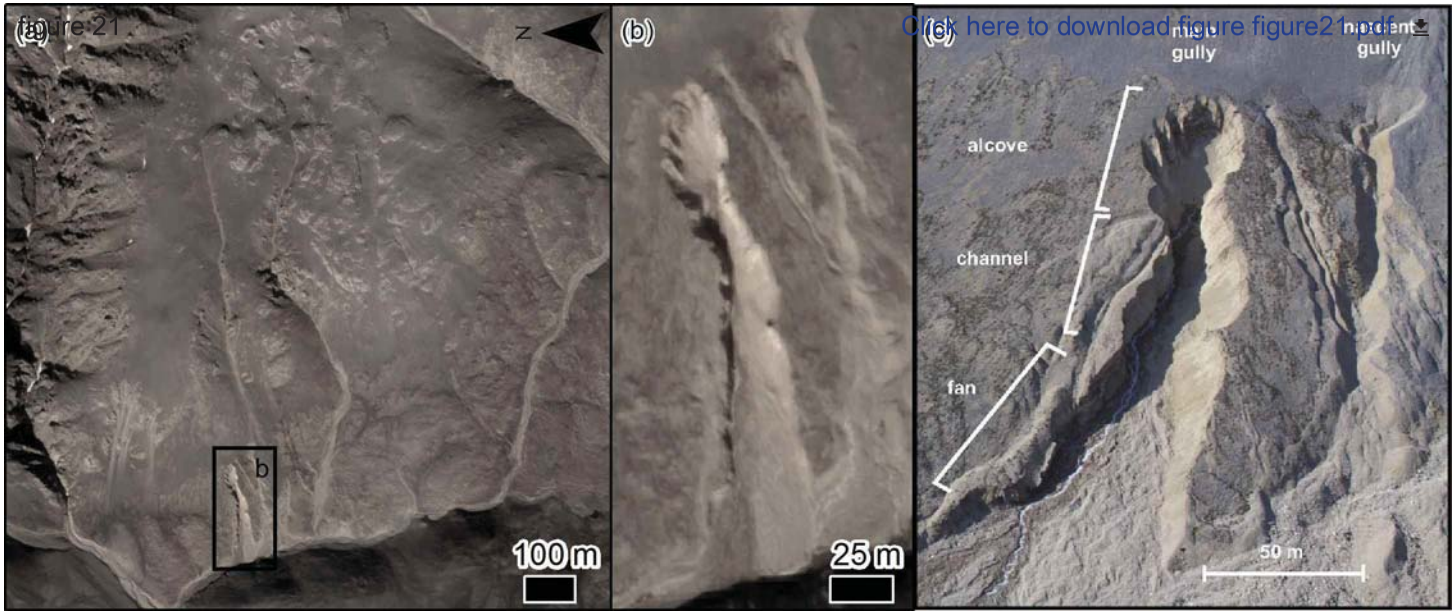

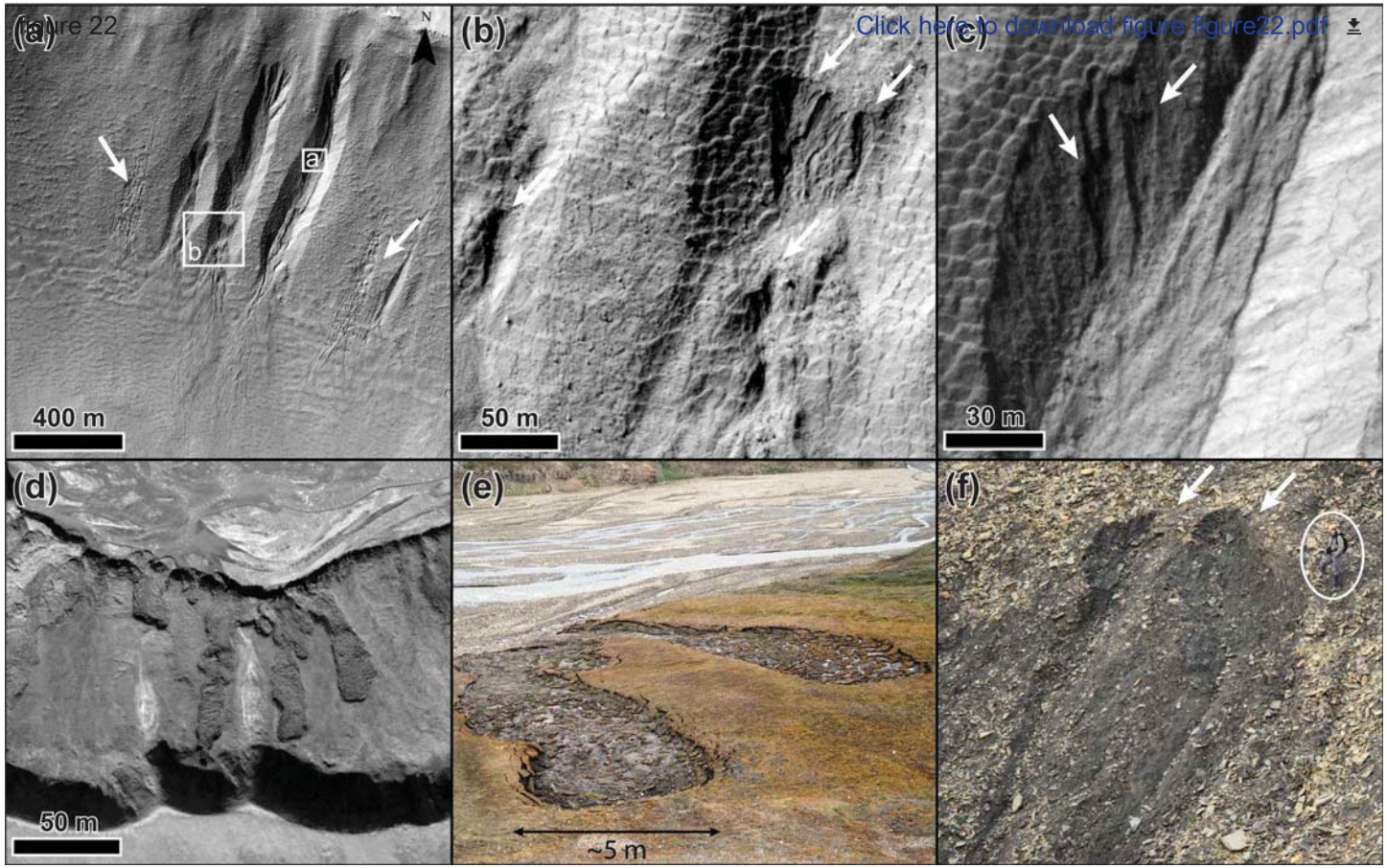

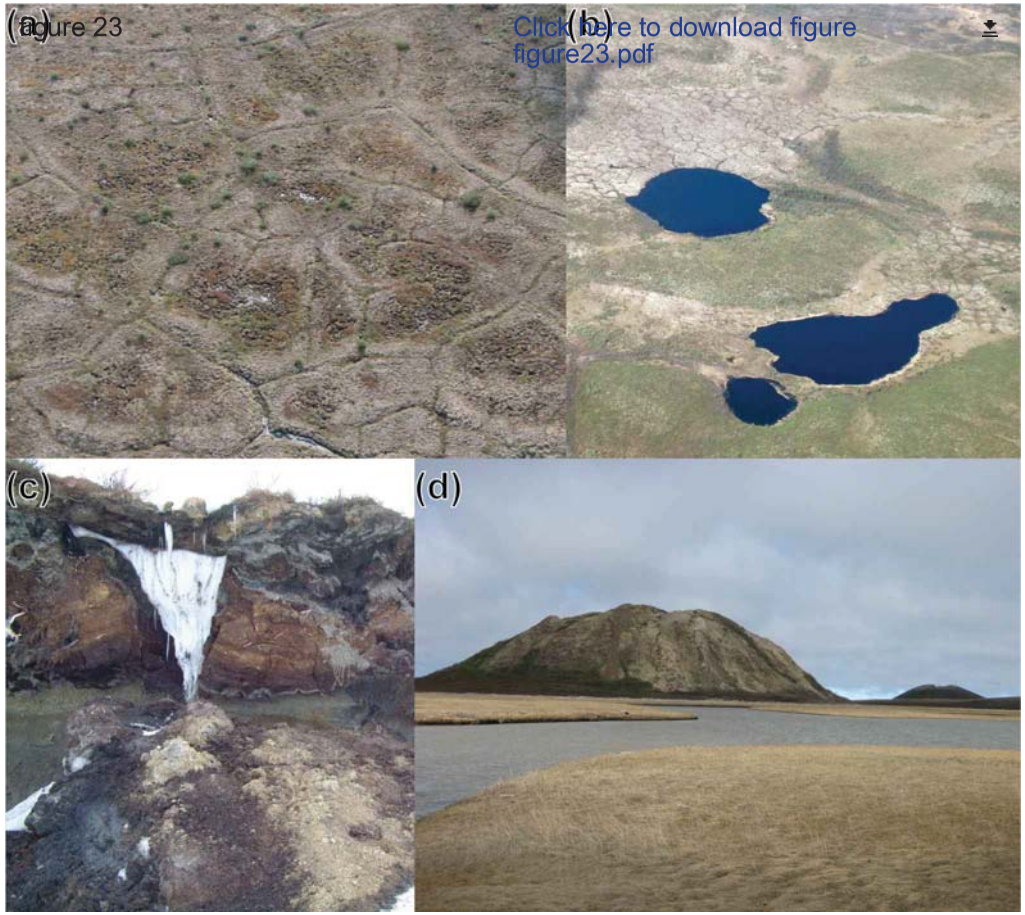

Figure 23

Click here to download figure
figure23.pdf

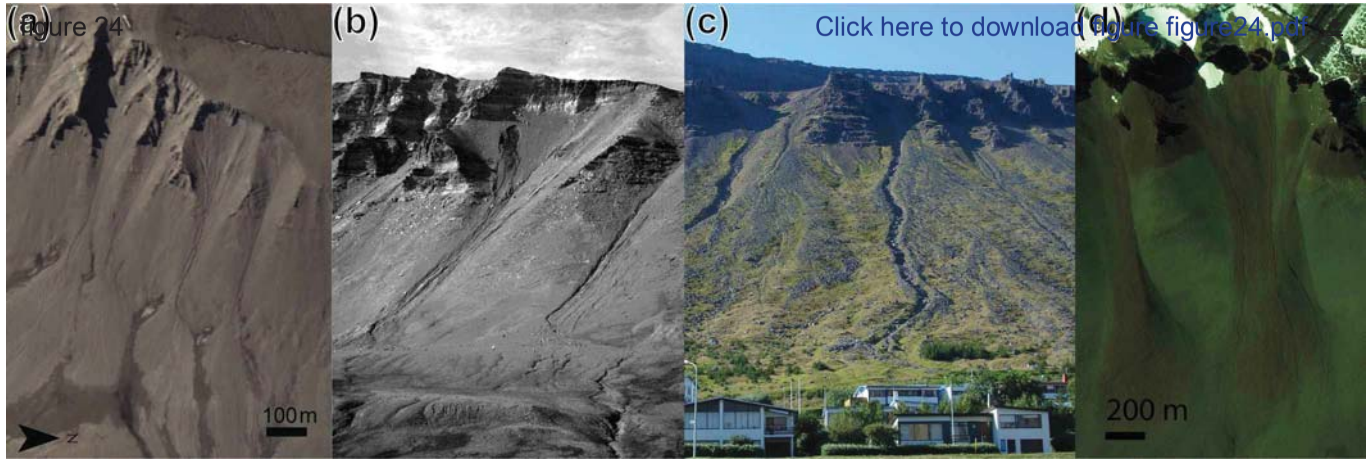

figure 25

Click here to download figure figure25.pdf

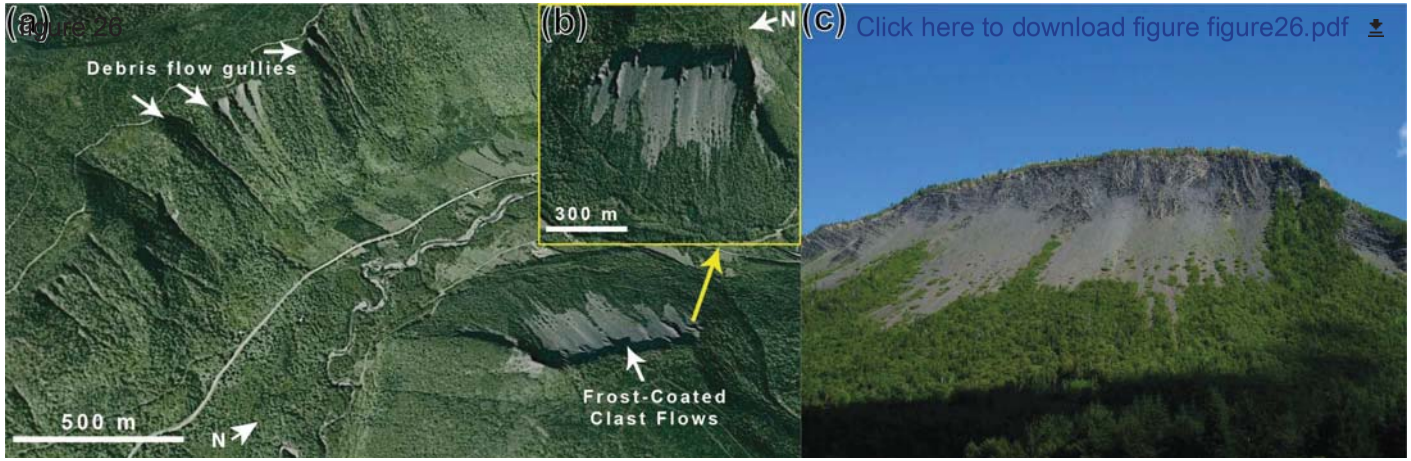

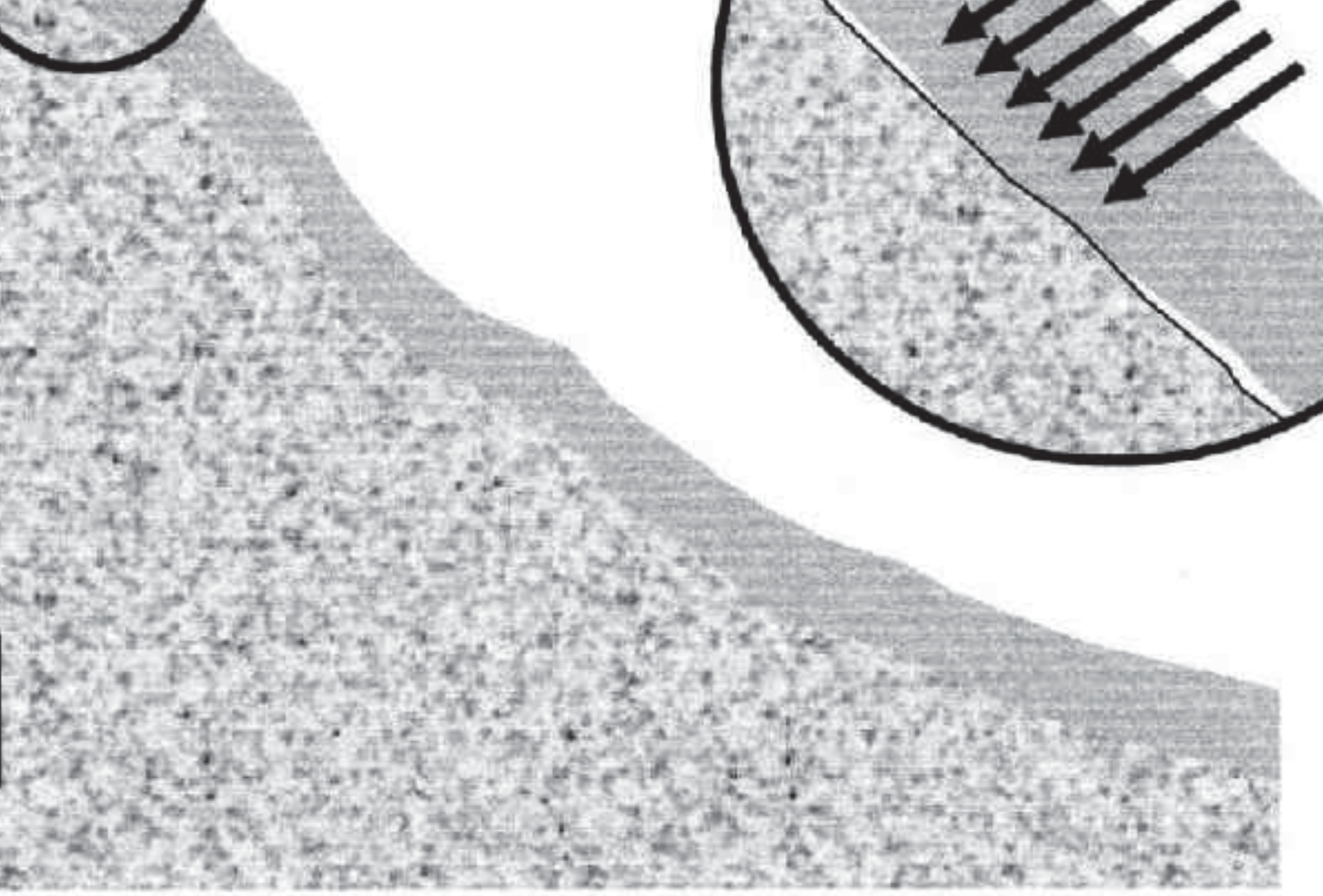

figure 28

Click here to download figure figure28.pdf

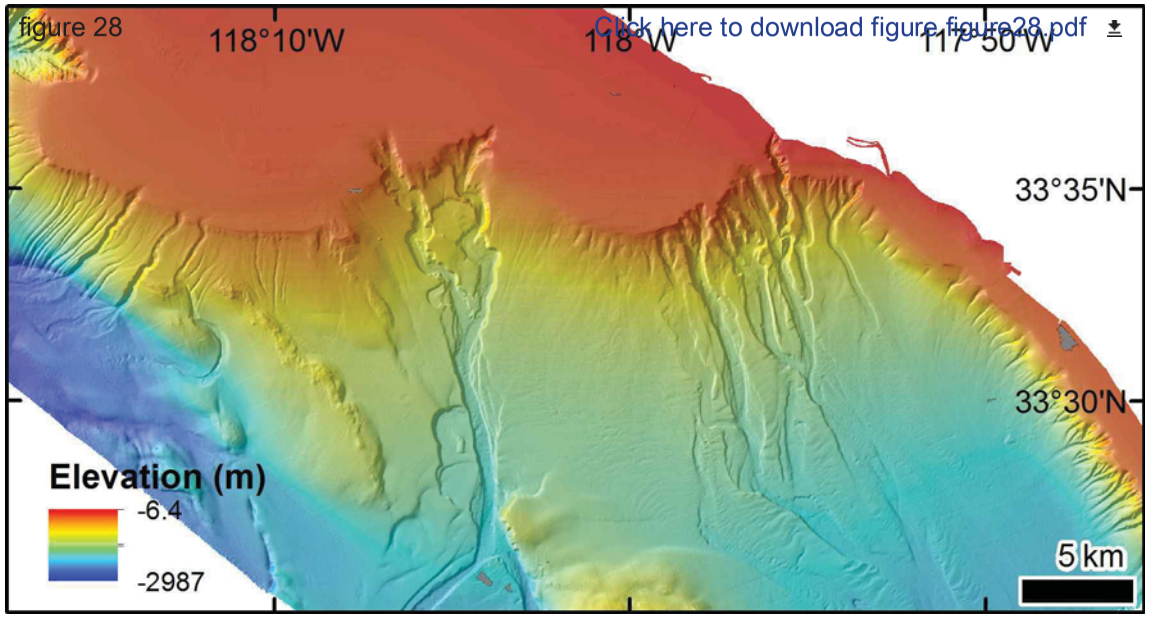

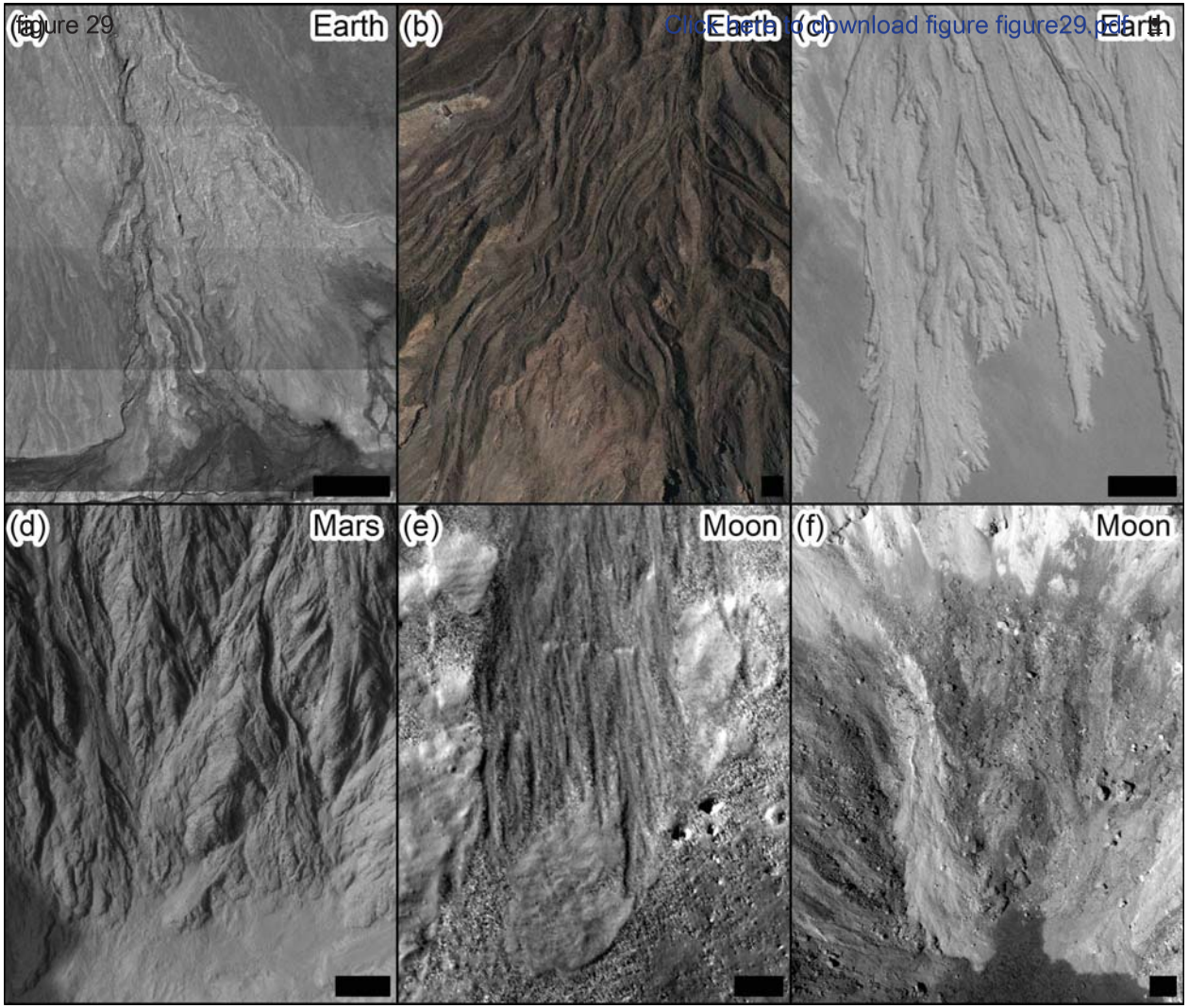

Figure 29